# Resilient Control in Long-Range Sensor and Actuator Networks

**Jose Manuel Linares**

Cert Web Apps (Open), BSc Open (Open), BSc Computing (Hons) (Sund)
School of Computing and Communications

Lancaster University

This dissertation is submitted for the degree of
*Master of Philosophy*

Graduate College                                      April 2017

# Dedication

I would like to start this dedication in memory of four of my family relatives who have passed away since I have been here conducting my research in Lancaster from 2012 to 2017.

**In memory of:**

- Concepción (Puri) Viagas

- Francisca Rumbo

- Dr. Bernard Linares

- Amalia Rumbo Martinez

Two of my family members succumbed to Cancer (Amalia and Bernard) and a sum of £612 was raised for Cancer Research UK in 2015 and cycled Wrynose or Bust 115 mile cyclo-sportive challenge and a 65 mile reliability ride The Coal Road Challenge run by The Lune Road Cycle Club. Thank you to the Lancaster Rotary Club for organizing the Wrynose Or Bust annual event.

**I would like to thank the following as they have supported me in my success either directly or indirectly**

My pet dog Frank the Pug, who has always kept me company on my long nights typing away, a dog is really a man's best friend.

Lastly, I would like to dedicate this to Georgina Garcia, she is always supportive of me and without her, I doubt this work would have been completed - I love you.

I would like to end this dedication with a quote which is fitting to this body of research as there were many unforeseen challenges along the way. I hope it will serve as an inspiration for those considering doing a research degree. Doing research is akin like running a marathon or participating in an arduous cyclo-sportive; there will be many challenges and obstacles ahead and you have to pace yourself to reach the finishing line. Perseverance and resilience will pay dividends.

*"After climbing a great hill, one only finds that there are many more hills to climb"*

-Nelson Mandela

# Declaration

I hereby declare that except where specific reference is made to the work of others, the contents of this dissertation are original and have not been submitted in whole or in part for consideration for any other degree or qualification in this, or any other university. This dissertation is my own work and contains nothing which is the outcome of work done in collaboration with others, except as specified in the text and Acknowledgements. This dissertation contains fewer than 65,000 words including appendices, bibliography, footnotes, tables and equations and has fewer than 150 figures.

<div align="right">

Jose Manuel Linares

April 2017

</div>

# Acknowledgements

# Abbreviations

[4B] Four Bit

[ACK] Acknowledgement

[AHP] Analytical Hierarchy Process

[AI] Artificial Intelligence

[AT] Attention

[ARQ] Automatic Repeat Request

[ATEX] Appareils destinés à être utilisés en ATmosphères EXplosives

[CMOS] Complimentary Metal Oxide Semiconductor

[CSI] Channel State Information

[CSO] Combined Sewage Overflows

[DTU] Disruption Tolerant Networking

[DUCHY] Double Cost Field Hybrid Link

[EWMA] Estimated Window Moving Average

[ETX] Expected Transmission Count

[FFEWMA] Flip-Flop Estimated Window Moving Average

[FFPLSI] Flip-Flop Packet Loss and Success Interval

[FIS] Fuzzy Inference System

[FISPI] Fuzzy Inference System Pi

[FISCOM] Fuzzy Inference System Communication

[FISIO] Fuzzy Inference System Input/Output

[FISCORE] Fuzzy Inference System Core

[FISAI] Fuzzy Inference System Artificial Intelligence

[FRB] Fuzzy Rule Base

[GLONASS] Global Navigation Satellite System

[GPS] Global Positioning System

[GSM] Global System for Mobile Communications

[ISM] Industrial, Scientific and Medical Band

[KLE] Kalman Link Estimator

[LAN] Local Area Network

[LI] Link Inefficiency

[LQE] Link Quality Estimator

[LQI] Link Quality Indicator

[LUSTER] Light Under Shrub Thicket for Environmental Research

[MADM] Multiple Attribute Decision Making

[MANET] Mobile and Adhoc Networks

[OFCOM] Office of Communications

[PDR] Packet Data Reception

[PRR] Packet Reception Rate

[PSR] Packet Success Rate

[RH] Relative Humidity

[RNP] Required Number of Packets

[RSSI] Received Signal Strength Indicator

[RTU] Remote Terminal Unit

[SCADA] Supervisory Control and Data Acquisition

[SSA] Signal Stability Based Adaptive

[SNR] Signal to Noise Ratio

[TCP] Transmission Control Protocol

[TWMA] Time Weighted Moving Average

[UHF] Ultra High Frequency

[VHF] Very High Frequency

[WiFi] Wireless Fidelity

[WMEWMA] Window Mean Exponential Weighted Moving Average

[WPAN] Wireless Personal Access Networks

[WSN] Wireless Sensor Network

# Abstract

This thesis will provide an insight on how weather factors such as temperature, humidity and air pressure affects radio links and use this body of knowledge to better understand how to mitigate unnecessary radio switching to take place and then use this knowledge to suggest ways of developing a Link Quality Estimator that utilize online weather data to be able to conduct smart link switching. In the context of this thesis, we focus on the case study of a water utility company as these entities are under increasing economic and environmental pressures to optimise their infrastructure, in order to save energy, mitigate extreme weather events, and prevent water pollution. One promising approach consists in using smart systems. However, a smart infrastructure requires reliable communication links which are difficult to provide. In particular, communication links that are distributed and geographically located in rural areas are highly affected by changing weather conditions, hence efficient control of these distributed hosts requires robust communications. Multiple communication transceivers are used to mitigate this issue and to enable nodes to switch to reliable links. Short-term link quality estimators are used to decide which link to use which often leads to the situation where a link switch is initiated which does not prove helpful in the long term. It is not beneficial to switch a link and associated routing for only a brief duration hence we conduct test bed experiments to better understand the relationships between the radio links and weather factors and use this body of data to devise a LQE that can use this data and then make a smart choice based on this data which reduces switching costs.

# Table of contents

# List of figures

# List of tables

# Chapter 1

# Introduction

In most developed countries, water infrastructures and services play a critical role in protecting the public health, and preventing damages to human and natural environments. Water infrastructures are well known for delivering drink-water, but they also play a key role in providing irrigation to agriculture, limiting water-based pollution, and mitigating extreme weather events such as floods and droughts. Managing, maintaining, and updating these infrastructures is, however, costly and complex. Water infrastructures are heavily distributed (over several 10,000 $km^2$ in some instances), include a large range of equipment (pipes, pumps, sewers, vanes, treatment plants, controllers), and have often been constructed over several decades, sometimes going back as far as Victorian times (1837 - 1901).

As environmental regulations are developed, water consumption surges (mainly due to population growth), and energy costs rise, water companies are under increasing pressure to update and improve the management of their infrastructure. One promising plan is in using better control systems ("smart" systems) to reduce operational costs and improve services. Such systems rely on control theory (fuzzy logic, decision trees), wireless sensors and actuators networks (WSANs), and better models to achieve their aims. Unfortunately, in spite of some promising starts [18, 42], few of these systems are deployed in production today. One reason, we argue, is the lack of an appropriate integration platform (a "middleware")

tailored towards the water industry where each wet well can handle communications between other pumping stations and control its own pumps to prevent localised flooding.

## 1.1   Chapter Overview

In this chapter, the motivations for this project will be highlighted with the contributions made, then proceed in outlining how this document is structured. We then give a background of how waste water industries generally work but specific to one company who we co-operated with. We give examples of such control algorithm to control inputs and outputs that can be applied to a Remote Terminal Unit (RTU), and lastly, describe present and future wireless communications within the waste water industry. We then give a brief summary of what was discussed in this chapter.

## 1.2   Motivation

It is limiting to work with Remote Terminal Unit's (RTU's) that utilize closed architecture systems due to their closed nature in terms of gaining access to the source code used for specific hardware. Most of these systems work at high voltages of 12V in order to make switches to actuators possible. Hence it is desirable for researchers in this field to build an open architecture that can be easily replicated and can be easily replaced with ubiquitous off-the-shelf components that are available in specialized electronic stores making it easy to build, maintain, cheap to build and less demanding in terms of voltage use than the proprietary 12V RTU. Hence we will outline how to build an RTU that is an open architecture, inexpensive to build and utilizing software that has a vibrant community of developers.

Therefore, a possible solution would be to integrate a communication platform that can address these difficulties that current systems have at the moment. We can address this issue by utilizing GSM radio, but this would prove costly on the long term. Another

solution would be to use cheaper long range radio transceivers (for e.g. 868 Mhz range) to communicate with sensor nodes. Unfortunately this too faces challenges as meteorological environments do impact radio quality. A possible way of building a communication platform is by integrating different existing technologies together. In brief, we need the following to make a communication platform:

1) A control algorithm (fuzzy logic as an example) to decide when actuator switches should take place and react on sensed data from sensors, in our case, it will be water levels.

2) A hardware open platform to be able to integrate our code and test it appropriately for our evaluation.

3) An understanding of how weather affects radio communications and explore ways of how transceiver switches can be done.

## 1.3 Contribution

The contribution in this thesis is explained as follows on the three points below:

1) To better understand how meteorological aspects affect radio link quality, explore how it is possible to reduce radio interface switching and suggest how a new Link Quality Estimator can be built utilizing online meteorological data. This contribution would provide a better understanding on the relationships that meteorological factors play when carrying out switching.

2) Design a Link Quality Estimator (LQE) based on the data provided from the first contribution to reduce costly switching (Evil Switching).

3) Using the LQE developed to make smart link switching.

To carry out these contributions, we therefore need to have a test bed that collects RSSI data, packet drops and weather data to better understand the relationship between radio links and weather factors.

## 1.4    Structure of Document

The structure of this thesis is divided into 6 chapters. The first chapter gives an introduction to the problem that this thesis addresses and its motivation, it describes how this thesis contributes to a unique body of knowledge giving a brief introduction of Link Quality Estimators. In chapter 2, we give an overview and discussion on related work on link quality estimators, link selection algorithms and meteorological effects on wireless propagation. In chapter 3, we give a introduction on the meteorological factors and data we collect, explain how these factors are related to each other and show our observations on how these have affected our test bed. In chapter 4, we discuss the strengths and weaknesses of current Link Quality Estimators and explain why we need a new link quality estimator that relies on externally available weather data. In chapter 5, we describe the prototype RTU that was developed for our case scenario and give an overview of the test bed used, ending with an evaluation of communication performance and a conclusion in chapter 6.

## 1.5    Background

In this section, we give an overview of how waste water infrastructures operate, how are such infrastructures controlled, why do these infrastructures require communications and the need for an open platform Remote Terminal Unit (RTU) to operate a bespoke control system as described by our industrial partners in Anglia Waters Ltd. An RTU may be locally present within a sub station, but its control algorithms may reside on another host located remotely as there is a desire to move from a centralised topology into a hybrid distributed topology in case there is a fault.

Waste water networks are complex infrastructures that combine civil engineering works (sewers, basins, reservoirs), hydraulic actuators (pumps, gates, valves), sensors (water levels and flows, toxins, gasses), and control devices (Programmable Logic Controllers). The

control logic usage in waste water networks is very simple, often relying on fixed threshold values to trigger behaviours (e.g. switching a pump on or off), but more advanced control techniques are now being considered, with fuzzy logic proposing to be a promising candidate [35]. In the context of Anglian Waters, they employed Fuzzy Logic in their system, we would emphasise here that there are many types of control algorithms that can do the same task of controlling actuators and sensing data although efficiencies will vary between algorithms which require separate analysis. In the following, we describe in detail the structure and constituents of a waste water network (Section 1.5.1). We then provide a quick introduction to fuzzy logic, and explain how it applies to the control of waste water networks (Section 1.5.2).

## 1.5.1  Wastewater Systems

A waste water infrastructure is usually organised in catchments. Each sewer catchment consists of a connected network of sewer pipes that collect sewage in an area and bring it to a treatment plant or a discharge point. The number of catchments managed by a water company can be substantial and, taken together, can cover an extensive area. Anglian Water for instance collects waste water from about 6 million customers through 1,100 waste water catchments over an area of 27,500 km$^2$ in the East of England.

Many sewer catchments use a *combined sewer system* which collects both waste water from households and storm water during rainfall. A combined sewer system must have enough capacity to process a large range of water inflows. This large capacity is needed to prevent toxic flooding in case of heavy waters (wet weather conditions), but also to avoid high concentrations of toxic substances if the rainwater is insufficient (dry weather conditions).

Mere gravity is usually insufficient to transport water in a sewer catchment. A catchment is therefore often equipped with a set of pumping stations that transport waste water over an elevation, so that it can continue to flow under the effect of gravity.

Ground level

Wet well

High sewage water level

Storm pump

Assist pump

Duty pump

Discharge line

Low sewage water level
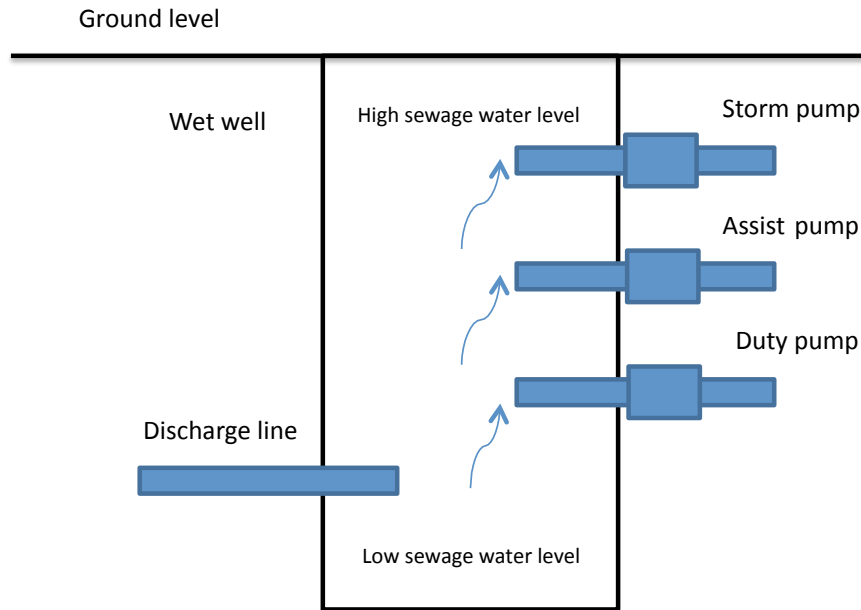
Fig. 1.1 Schematic of a wet well

A pumping station is built around a wet well (Figure 1.1), an underground reservoir that acts as a buffer for incoming water from a main sewer pipe. A wet well is usually equipped with 2 to 3 pumps: a *duty pump*, an *assist pump* and, in some critical wet wells, a *storm pump* (see [35] for more details of pumps).

The pumps of a wet well can be switched on and off, and must be controlled to process the incoming water, while minimising energy consumption, and optimising the pumps' lifetime. The opportunities for energy consumption are substantial, as energy costs constitute a substantial part of the operational budget of most water companies [35]. Anglian Water for instance spends about £60 million pounds in energy costs annually, with £32 million being spent on waste water operations, of which £9 million allocated for waste water networks (Figure 1.2). Similarly, unexpected pump failures can have drastic consequences, possibly leading to the flooding of pollutants. Finally, although this is rarely implemented at the moment, an advanced control of pumps holds the promise of minimising adverse events
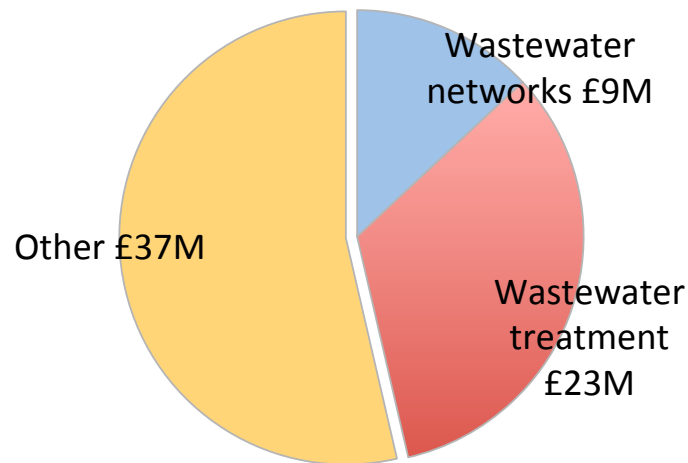
Fig. 1.2 Anglian Water's energy costs (£60m)

known as *Combined Sewer Overflows* (CSO for short), which are tightly regulated, and can carry heavy financial and environmental consequences.

A Combined Sewer Outage occurs when the capacity of a combined sewer system is exceeded, usually as a result of heavy rainfall. Sewer networks are in this case, designed to discharge some the excess water directly into the environment (river, lake or sea) without treatment. A better management of pumps during (short) heavy rainfall could in principle mitigate CSO by better utilising the buffer capacity of wet wells.

### 1.5.2   Fuzzy Logic Control

In this subsection, we describe one of many possible types of control algorithms that may be implemented into an RTU. A control algorithm is needed to carry out actuator controls of pumps and receive inputs on water levels so that the RTU can react to constant changes in levels. This particular method of using fuzzy logic was researched by Dr.Ostojin from Sheffield University who were part of the Anglia Water Ltd research project. Dr.Ostojin et al attempted to improve energy savings by reducing pump activations which in turn also

reduces maintenance costs [35]. Other methods of control algorithms exist, but this was chosen by the sponsor.

In spite of the potential benefits of better control in combined sewer systems, most pumping stations are handled today by a basic logic, embedded in a Programmable Logic Controller (PLC) installed in the station. The PLC uses input from ultrasonic sensors to activate each of the pumps according to hard-coded water levels [35].

Any improvement on this basic approach should fit the needs of the water industry: It should have a low total cost of ownership, due to the large number of pumping stations to be equipped (Anglian Water for instance manages approximately 4,500 pumping stations which have 12,500 pump sets all together); it should be robust for unexpected events and failures; and should be easily portable to different stations with little deployment and tuning efforts.

**Principles Of Fuzzy Logic**

Fuzzy logic meets most of these needs, and is one of the solutions currently researched by Anglian Water [35]. Fuzzy logic extends traditional Boolean logic with continuous truth values between 0 (false) and 1 (true), rather than just 0 and 1. In control, a fuzzy logic approach usually starts by a *fuzzyfication* step, in which the inputs of the control system are processed through a set of fuzzy membership functions [23, 32]. For instance, if one of the inputs is the water level in the wet well, Figure 1.3 shows the truth value of the three fuzzy predicates LOW_LEVEL, MEDIUM_LEVEL, and HIGH_LEVEL. For a water level of 1.25 meters, the truth value of LOW_LEVEL is 0.75, that of MEDIUM_LEVEL is 0.25 and that of HIGH_LEVEL is 0.

The control part of a fuzzy-base control logic typically takes the form of *fuzzy rule-based inference systems*, FRB for short. An FRB uses a set of if-then rules to encode the actions the system should take, depending on its input predicates, for instance:

if LOW_LEVEL and HEAVY_RAIN then ASSIST_PUMP_ON
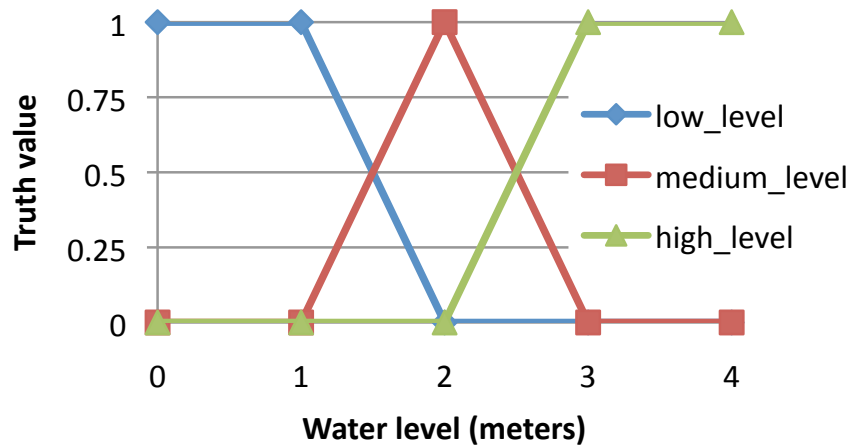
Fig. 1.3 Fuzzy membership functions

The `if` parts (the antecedent) of all rules are evaluated in parallel, using a fuzzy semantic for Boolean operators (e.g. $x$ and $y$ is usually interpreted as $min(x, y)$). The resulting truth values are then used to compute the `then` part (consequent) of each rule, in a way that differs depending on the type of FRBs considered.

In the simplest case (known as Mamdani FRBs), the consequent and antecedents are used to determine a fuzzy membership function for the whole FRB through an *implication* and an *aggregation* step. This function computes how the truth value of the whole system varies with the output variables (in our case the switching states of the pumps) for the observed input (the water level).

The final stage consists then of transforming this system-wide membership functions into actual control values (which pumps to switch on/off), known as the *defuzzyfication* step. This last step usually seeks to maximise the average truth value of the system, while taking into account the many-value logic captured by the FRB.

Although all FRB follow the above steps (*fuzzyfication*, *implication*, *aggregation*, *defuzzyfication*) variations point are numerous. First, Mamdani inference systems are only one type of FRBs, with Tagani-Sugeno FRBs another important alternative. Tagani-Sugeno FRBs use linear combinations of antecedent truth values in the *implication* and *aggregation* steps to

directly provide an output value for control. Within the Mamdani family itself, many variants exists depending on the semantic of the fuzzy operators (*max* being one option only for and for instance), and the detail of the aggregation and defuzzyfication steps.

Besides the above design choices, the quality of control delivered by an FRB strongly depends on the design of its input membership functions. Here again several approaches exist. A basic approach consists in relying on expert knowledge. More advanced strategies are however often taken that use optimisation to search for an optimal set of membership functions maximising particular quantities (energy consumption, pump lifetime, risk of CSOs). This optimisation usually occurs off-line using historical data, but recent works have been proposed to optimise membership functions dynamically based on the system's feedback [41].

**Fuzzy Logic At Anglian Water**

Anglian Water have started experimenting with fuzzy-logic to optimise the energy consumption of one pumping station in dry weather condition [35]. The approach uses a Mamdani FRB to switch the pumps of the wet well on and off depending on the wet well's water level, the flow of water coming in, and the current electricity tariff (night or day). The input membership functions are configured off-line on historical data using a genetic algorithms to optimise the energy consumption, while minimising pump switching (a factor of premature wear).

This early system was shown to deliver energy saving of between 2 and 2.5%, a promising start which is now being refined by Anglian Water (at present, it is over 6% with matlab simulations). Unfortunately the latest development in a real setting has not been able to produce the energy saving envisaged and thus, the company has asked for the advice of Lincoln University on other methods of control which may be less complex (such as IF statements).

### 1.5.3    Wireless Communications for Waste Water Networks

Control algorithms are required to sense data from sensors to detect water levels and send signals to actuators to activate or deactivate pumps. In the previous section, we described the fuzzy logic that was employed within Anglia Water's test bed. We re-iterate here that fuzzy logic is one of several types of control algorithms and this is an active research area that is being conducted at other Universities (Sheffield and Lincoln). Anglia Waters Ltd is one of the largest water companies in the UK, part of their problem was due to utilizing GSM radio during periods of stormy weather. Their implementation was to have a contract GSM SIM card where each pumping station can send data wirelessly. This means that data needs to be transported through the network provider's infrastructure which may have some latency. This can be costly to the company but also depends on which contract plan there are available specifically for industrial purposes.

One solution they found was to implement an OFCOM licensed 150Mhz (VHF) point to point system which can carry a signal to a range of over 20 miles. This solved the company's initial problem, but at an annual cost of over £8000 per year to have that band protected.

An envisaged wireless future is to use similar radio implementations but at a higher frequency such as 433 Mhz or 868 Mhz radio frequencies. We selected the 868 Mhz frequency as it is currently available and free to use radio band and some hardware devices were available at the time. The hardware implementation used is Xbee series 5 which has its own proprietary mesh protocol, but it is possible not to use it and have a generic or specialised protocol programmed in the host instead.

In our scenario, a future of decentralised sub stations would be able to communicate with each other running a middleware platform where software modules may be remotely located and not necessarily present locally should failure occur. Instead of control being sent over a SCADA centralised network, we would have a hybrid decentralised system, capable of automating the activation of pumps in wet wells, by sensing levels and data being either a)

transmitted to another wet well for decisions to be taken or b) locally managed by the wet well host.

## 1.6   Chapter Summary

We have given an overview as to why resilient communications is needed within waste water networks and given an overview of how these systems operate. We have also given an idea of one possible way of controlling inputs and outputs via a control algorithm. We give an overview of what fuzzy logic is and why it was used in this context. We ended the chapter by giving an overview of how present and future communication infrastructures would look like within the waste water industry either by utilizing licensed radio frequencies, or utilize hybrid radio systems with smart LQE algorithms.

# Chapter 2

# Related Work

In this chapter, we discuss the related work that is based on Link Quality Estimators that have been surveyed and tested in a real outdoor environment setting similar to our test bed, Link Quality Selection and the impact that meteorological factors have, such as air temperature, relative humidity and air pressure has on links and link quality estimators.

## 2.1   Link Quality Estimators

In this subsection, we will cover the different types of related work that encompasses Link Quality Estimators. Fundamentally, a Link Quality Estimator provides a service to higher communication protocols that would mitigate link unreliability at the physical level, thus ensuring that the routing layer maintains good links and provide a stable topology.

Link Quality Estimators (LQE) can be categorised as either hardware or software based schemes. Software based LQE's are further subdivided into three categories, Packet Reception Rate (PRR) based, Required Number of Packets (RNP) based and Score based. Software LQE's can provide more fine grain control [10] and are able to monitor link quality for certain applications that might involve indoor monitoring applications or outdoor applications that require more resilient links such as monitoring water pumping stations.

## 2.1.1 Hardware Based LQE's

These types of LQE's include the received signal strength (RSSI), Link Quality Indicator (LQI) which is available on certain nodes and Signal to Noise Ratio (SNR). These LQE's are read from the radio transceiver and an advantage of hardware LQE's over software LQE's is that there is no further computations required, thus saving CPU cycles and saves energy which is beneficial to an energy limited node.

**Received Signal Strength Indicator**

In RSSI, the RSSI register is the received power of a connected region of the last received packet and it does not look into the correctness or quality of the signal [3]. The RSSI value is not standardised across the physical hardware to the RSSI reading; for example, 802.11 WiFi standard does not define a relationship between milliwatts (mW) or decibel milli watt (dBm) [2]. Generally, the closer the value is to 0, the better the received signal will be; as an example, -50 dBm has a greater received signal power than -80 dBm. We state that in our work, a value of 0 means a dropped packet and not an excellent RSSI signal strength.

Liu et al noticed in his work that different vendors and even devices from the same vendor will differ in RSSI levels [29], thus RSSI has a limitation to be used to measure distances in Wireless Local Area Networks.

A single reading can determine if the link is within the transitional region according to Baccour [10] although it is not possible to determine an RSSI value if the packet was not received .

Srinivasan et al [28], states that link estimation is important when designing new protocols based on RSSI, as he stated in his work that there is a wide belief in the Wireless Sensor Network community that RSSI is a bad estimator. His motivation for his work was based in the assumption that older generation radio motes such as the MicaZ, Telos and Intel Mote 2 (CC2420 chipset) that operate on the 2.4 Ghz band and Rene Motes (TR1000 chipset) have

asymmetric links; one radio node may have a link but the other radio node does not have enough range. In Srinivasan's work [28], he shows that the CC2420 chipset has a low or insignificant miscalibration due to symmetric link between nodes. The CC2420 chipset has a reliable RSSI indicator when it is above a sensitivity threshold of -87 dBm [28]. When this threshold is broken, it does not have a correlation with Packet Reception Rate (PRR) and it is believed that this is due to local noise variations at different nodes. Srinivasan states that protocol designers looking for cheap and agile link estimators might consider RSSI over Link Quality Indicator (LQI).

**Signal to Noise Ratio (SNR)**

Signal to Noise Ratio is the difference between the pure signal strength and the level of background noise floor at the receiver [10]. According to Srinivasan [44], SNR metrics will be better than RSSI readings as noise floor across different nodes differ. An observation that Aguayo et al [8], Senel et al [43] and Yunqian et al [30], showed that there are difficulties in establishing relationships between SNR and PRR, thus SNR cannot be used alone as an estimator as this depends on the actual hardware sensor as environmental effects like temperature [43] has an effect on the sensor hardware.

**Link Quality Indicator (LQI)**

LQI is a metric that is used to measure signal quality and is an estimate on how a signal can be demodulated (extraction of data from an analogue signal to a digital signal) by acquiring the magnitude of errors between motes that have good links and the received signal over the 64 symbols (a symbol is a waveform such as a tone when transmitting via a modem or a pulse in digital baseband transmission which represents a number of bits) after the sync word [3].

LQI is a proposed standard for IEEE (2003) 802.15.4 but is vendor specific [10]; the CC2420 chipset which is a widely available chip, utilizes LQI in this manner. This metric is measured on the first 8 symbols (a symbol can be conveyed as either a single bit of data or several bits of data) of the received packet as a score which ranges from 50 which is a low quality link to 110 which is good quality link. However, Srinivasan [28] argues that LQI is not a good predictor for intermediate quality links due to its high variance (due to that it is a statistical value) unless it is averaged over some time with several readings, however, it is preferred that LQI is averaged over a larger window of packets (40 to 120 packets) to determine if the link is of good quality but sacrificing agility and responsiveness in changes.

### 2.1.2   Software Based LQE's

In this sub section, we shall give an overview of the popular types of Link Quality Estimators that have been tested in a real smart grid setting for an electric utility company by Gungor et al [21]. These LQE's have also been evaluated in a survey by Baccour et al [10] who has given some results albeit some are indoors whereas we are more concerned on real outdoor environment experiments done by Gungor et al [21] as the application is similar to our test bed and intended application area.

**Packet Reception Rate (PRR)**

Packet Reception Rate or PRR, is a simple metric that was widely used in routing protocols and it is a receiver based LQE that calculates the average rate of packets received on the receiver node [10]. The shorter the window is to calculate the average, the more accurate it can be in predicting failures, but at the cost of network stability as failure could be for a short time caused by external factors such as interference or moving objects. Under the PRR category, we will look into Window Mean Exponential Weighted Moving Average (WMEWMA) and Kalman Link Estimator (KLE).

**Weighted Mean (WMEWMA)**

The Window Mean Exponential Weighted Moving Average is a simple LQE algorithm that is measured as the percentage of packets that have been received on the receiver side intact [46] [10].

In Woo's work [46], he ran a test bed using Berkely motes which use the 916 Mhz band and running over the TinyOS operating system. He used a single sender generating packets which are sequenced over a rate of 8 packets per second. The receiver node then redirects these packets over a serial port to a PC where these are stored. By looking at the sequence numbers, Woo was able to calculate packet losses by using success/loss events over time and packet success rates over time as the fraction of packets that were received over the 30 second interval. The nodes were placed indoors and outdoors but within short distances of 15 feet which is approximately 4.5 metres.

In WMEWMA or Window Mean Exponentially Weighted Moving Average, Woo uses a low pass filtering by taking the average of a time window and adjust the estimation using the latest estimation. The computed average success rate over a time period is smoothed with and exponentially weighted moving average. This LQE takes in two parameters; the first is time and the second is the history size of the estimator. It also takes in two tuning parameters; time and history size of the estimator. The estimator however does require a minimum number of packets before it can make a link quality estimation.

In Woo's experiments [46], there was observable results when an obstruction was placed (a person) in between the two nodes with a distance of 8 feet where packet probability was 0.8 to 0.6 without an obstruction and then dropped down to 0 when the obstruction was present. Packet probability oscillated between 0.5 and 0.8 when there was no obstruction. Therefore, there is a need to address this problem by designing a link estimator that can track these changes in an agile and responsive way which is simple and uses little computational power by tracking discrete changes rapidly and lock into stationary regions despite statistical

variations. In Woo's work, he lays out the different types of agile estimators suited ideally for multi hop routing.

One candidate is Estimated Window Moving Average or EWMA were Woo et al, [46] used this estimator to compare it with other link estimators since it is widely used. In EWMA, the algorithm requires constant storage of the old estimates to be able to do any fine tuning. EWMA uses linear combination of infinite history that are weighted exponentially, thus this makes the algorithm reactive to small shifts and it is considered an agile detector in many statistical process control applications.

In Woos' work, [46], it is suggested that the Flip-Flop EWMA is the best estimator to provide agility and stability by Kim et al [26] since statistical theory is used to select the best estimator. Woo explored the possibility of using Flip Flop-EWMA by setting the agile and stable EWMA tunings to be the same as in the EWMA study [46]. There are two methods in setting this estimator; the agile method can be set as default and make the estimator switch to the stable estimator when there is a 10% difference in noise margin. The other approach is to make the stable estimator as default but as soon as disturbances are detected, it will switch to the agile estimator when estimations deviate by 10%. However, it is shown in Woo's paper [46] that Flip-Flop EWMA does not provide an advantage over the much simpler EWMA in his test bed because fluctuations in the agile estimator are so bad, it will introduce instability and errors and criticises Kim's work [26] as to why Flip-Flop EWMA is better in his test bed as it does not show the dynamics of either estimator in a separate way over time. Other estimators taken into consideration are Moving Average, Time Weighted Moving Average (TWMA) and Flip-Flop Packet Loss and Success Interval with EWMA (FFPLSI) all which underperform WMEWMA.

Woo's conclusion is that WMEWMA outperforms other forms of estimations since it provides stable estimates within a 10% margin that reacts to large steps in approximately

100 packet times. WMEWMA is ideal for resource constrained devices since the storage requirement is constant for all tunings.

### Kalman Filter (KLE)

Software based schemes such as Kalman filter (KLE) [43] estimates PSR (Packet Success Rate) by adjusting PSR-SNR relationships which gives an indication to the link quality although it must be stated that accuracy was not examined in Baccour's survey [10] and the KLE filter was tested in controlled indoor environments which delivered consistent results. This LQE was devised to overcome the poor reactivity of average based LQE's such as PRR. Essentially, it provides link quality estimation based on the received signal strength of one packet. It is unnecessary to wait for several packets in order to compute a value. As soon as it receives a packet, this packet is transferred to the Kalman filter which outputs an estimate of the received signal strength. An output of the Signal to Noise Ratio (SNR) which is the KLE representation is computed by subtracting the noise floor (the sum of all non-man made and man-made interference) estimate from the estimated received signal strength and then using a pre-calibrated PRR-SNR (Packet Reception Ratio - Signal to Noise Ratio) curve at the receiver node, the approximated SNR is mapped to an approximated PRR.

### Required Number Of Packets (RNP)

RNP is a sender-side estimator that takes into account the number of transmissions and retransmissions needed before the node successfully receives it [10]. The RNP is calculated by the window of transmitted or retransmitted packets divided by the number of successfully received packets minus one to exclude the first packet sent. This LQE assumes an automatic repeat request (ARQ) protocol at the link layer which will send retransmissions of a packet until it is correctly received at the other node end. Under the RNP category, we look into ETX, LI and Four bit.

**Expected Transmission Count (ETX)**

The ETX scheme by Couto et al [16] was developed to take into account lossy links and find paths with the highest throughput despite how long the link may be, requiring several hops to reach its destination. In his paper [16], he took measurements from a wireless test bed using 29 nodes consisting of Linux PC with a Cisco/Aironet 340 PCI 802.11b card with a 2.2 dBi dipole antenna and showed that ETX can find routes that yield higher throughputs rather than using a minimum hop count metric. Several improvements have been proposed in the protocol development such as prediction of loss ratios for varying packet sizes, handling of networks that run on different bit rates and making ETX more robust when handling high levels of data traffic. The ETX was developed to be an improvement from the existing minimum hop count metric as it does not take into consideration that longer paths may yield higher throughputs. ETX is an active monitoring LQE scheme on the receiver side which is calculated by computing the loss ratio between the two directions of each link and interference caused from outside sources taking into account link asymmetry (electromagnetic radio propagation not being completely spherical in shape). It is argued that ETX is ideal for Mobile and Adhoc Networks (MANETs) due to mobility, but not true in a static Wireless Sensor Network (WSN) deployment where Four bit out performs ETX on its own as it relies on the 802.15.4 Level 2 acknowledgements (ACKs) to measure the ETX [39], [19].

**Four Bit(4B)**

Four bit LQE in essence is a hybrid estimator developed by Fonseca et al [19] where link failure is monitored by amalgamating 4 bits of data from different network layers that exist in most hardware interfaces. Fonseca's argument in developing four bit (referred in his paper as 4B) is due to that there is a need a for a narrow protocol independent link quality estimation

layer which uses 4 bits of data to tell if the link is reliable, or unreliable by using existing layers that can provide useful data to the LQE.
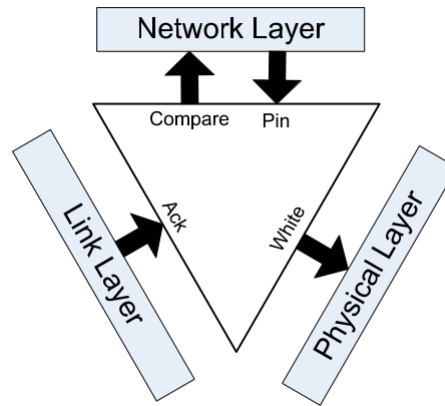


Fig. 2.1 Four bit LQE diagram from Fonseca et al [19]. Arrows pointing outwards represents information the estimator requests from the layers. Arrows pointing inwards represents the information that the layers provide

The Fourbit LQE takes 1 bit from the physical layer, 1 bit from the link layer and 2 from the network layer. The white bit is taken from the physical layer which denotes channel quality and can determine good or bad links. The acknowledge (ACK) bit taken from the link layer indicates whether an acknowledgement is received for a sent packet. The last two pieces of data are the pin and compare bit which are read from the network layer and are used to build the neighbour node tables for routing purposes. It then combines two link metrics which is the ETX for unicast packets (window size divided by number of acknowledged unicast packets). The second metric is the beacon packet which is calculated by applying an EWMA average of the window size, divided by the number of received beacons. These two metrics are then combined using a EWMA average.

**Score based**

In this subsection, score based Link Quality Estimators can be Channel State Information (CSI) or a hybrid form to include a score base aspect to analyse link quality.

**Hybrid Link Estimators - DUCHY**

A hybrid score based - CSI and Packet Data Reception (PDR) - LQE is DUCHY (Double Cost Field Hybrid link estimator) developed by Pucinella et al, [39] designed for network layer integration cost based protocols and was used over the Arbutus WSN routing protocol [38]. DUCHY selects the routes with the shortest hops and the highest quality links and it is based on two LQE's; the first is the CSI which is a normalised value between the RSSI and LQI which are collected from received beacons (see diagram 2.1.2) and then combines these two normalised values into a weighted sum. The second LQE is the RNP (ETX) which is used to refine CSI values which can be incorrect due to that these are based on beacon traffic.

DUCHY leverages on broadcast control traffic and unicast traffic and utilizes CSI and delivery estimates (ETX) to address typical problems found in WSN's such as weak signals and to strengthen low quality links by coding and using ARQ or Automatic Repeat Request (see diagram 2.1.2). The problem presented in [39] is that coding offsets the energy saving that it should bring whereas ARQ's are more commonly used and the problem in WSN nodes is that they are usually static and if the channel of two nodes are in a deep fade, then it may take an indefinite time for the fading pattern to change. Thus, lossy links will need many retransmissions if no other alternative is available.

DUCHY does not require neighbourhood tables but keeps the state of the parent node. RSSI is used to obtain information on good links and LQI is used to get information about bad links. It also borrows from Fonseca's idea [19] to use the L2 ACK's for unicast outgoing packets. The idea of DUCHY is specific to 802.15.4 since LQI although it could be implemented in non 802.15.4 standard.

The most common form of Channel State Information LQE is RSSI as mentioned previously and used to be considered a poor predictor due to limitations in the hardware [39] and [50]. However, because developers focus on the 802.15.4 stack, they use the CC2420 chipset which has a more reliable RSSI reading, [39].
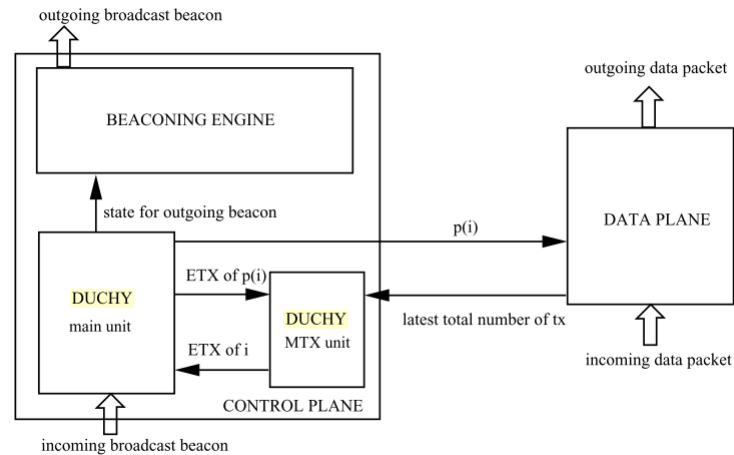
Fig. 2.2 Structure of DUCHY [39].

In evaluating DUCHY, Baccour [10] states that Arbutus was compared to MultiHopLQI (a hierarchical routing protocol based on LQI) as an LQE. In Puccinellis work [39], they found that Arbutus outperforms MultiHopLQI and deduce that DUCHY is better. Baccour argues that this is an unfair deduction due to that the two LQE's were compared in different contexts and suggested that it would be more reasonable to integrate LQI in Arbutus and compare DUCHY based Arbutus to LQI based Arbutus [10]. However, DUCHY does perform better than LQI because it integrates LQI and other estimator metrics and Baccour ends the analysis, noting that it would be interesting to compare DUCHY and other software LQE's to demonstrate its performance.

### 2.1.3 Link Inefficiency (LI)

Link inefficiency is a Link Estimator designed by Lal et al [27] to save energy by taking into consideration weak signals from neighbouring nodes by conducting a brief initialization audit as soon as the radio transceivers are powered up. More data can then be collected after this initialization phase. Although the test bed was conducted indoors during 7 days, Lal used sensor node hardware from Bosch Research with an 8 bit microcontroller. The transmitters are equipped with a quarter wavelength monopole wire antennas and use the

915 Mhz ISM band. If nodes have the ARQ protocol employed, it would mean that the node will send out a number of retransmissions until it has succeeded in sending the data packet to the neighbouring nodes. Thus, the more retransmissions there are on a weak signal, the less likely the packet will be sent and LI is modelled on how probable the data packet can be delivered by using the least amount of energy. This is done by getting the RSSI for every byte of data received and averaging the RSSI value for the complete data packet. The SNR was also collected and used to determine if links are good or bad quality; in their test bed, if the link is less than 15 dB, then it is considered a bad link. Lal also used Packet Success Rate or PSR, to get the ratio between the good packets and bad packets over a 300 second time frame where 3000 packets over 300 seconds would be a PSR of 100%. To determine link cost the author [27] proposes that the channel SNR is sampled, if the SNR is below a pre-determined threshold, the instantaneous link inefficiency as the reciprocal PSR is measured. If the SNR is above the threshold, then LI is calculated by inverting PSR and weighed with the factor that depends how away the threshold is from the ideal SNR. Then include the instantaneous LI value in a running average for all samples taken. Lal has shown in his work that only a few metrics are required to predict when links will fail and thus be able to take more data into account as soon as the neighbouring nodes are up and running. In Baccour's discussion [10], it is noted that PSP is a form of approximated Packet Reception Rate (PRR) and was shown by Aguayo [8], Yunqian [30], Senel [43] and Lal [27], that mapping from average SNR to an approximation of PRR can lead to an erratic estimation, thus using PSP instead of PRR might be unsuitable for link quality estimation.

**Non Traditional LQE's**

Other forms of hybrid LQE's used involve the use of fuzzy logic [11] in determining link quality, apply four bit in hardware implementations [19] or use mapping methods [43] to determine link quality. Unfortunately, fuzzy processing does require a certain amount of processing carried out by the node itself which its power source may be limited.

## 2.2    Environmental Effects on Radio Transceivers

In this section, we look at different types of wireless radio transceivers and examine what the authors have researched in terms of how these are affected by external factors such as heat, humidity and air pressure.

Bannister et al [12] studied the effects of temperature on Received Signal Strength, data collection and localization. In his work, it was aimed to characterize the effect of temperature on commercially available sensor nodes and to understand how it affects WSN deployments. In Bannisters' research, he used the IEEE 802.15.4 TI CC2420 Radio in a Tmote sky wireless mote. The CC2420 datasheet [5] discusses how temperature can affect the internal oscillator, however in the CC2400 datasheet [4], does include graphs of the output power and receiver sensitivity over an operating range.

Bannister sets up two motes to observe the effect that temperature has on RSSI. To eliminate noise from external sources, he connects both motes using a coaxial cable and a sequence of attenuators - see figure 2.2. The temperature inside the chamber started from an initial temperature of 45 °C and then rising to 65 °C before allowing it to cool down and then remained for a 45 minute period. The temperature was measured using the on-board Sensirion SHT11 sensor. The power readings were collected by averaging the RSSI over a 10 packet burst transmitted every 40 seconds which were sent over the maximum transmission

power of 0 dBm. Each mote was swapped as transmitter and receiver and inside and outside of the temperature chamber to see observable effects.
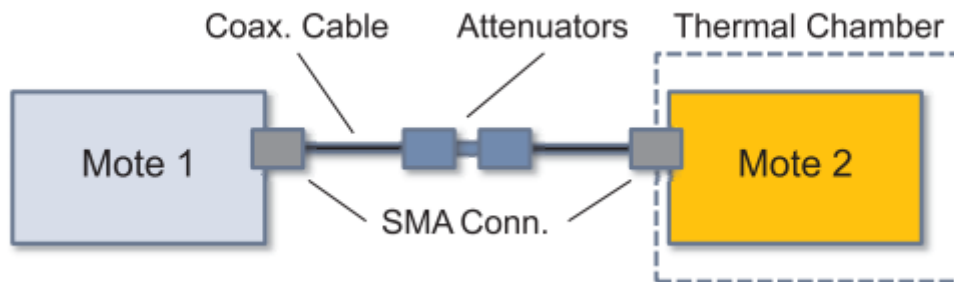


Fig. 2.3 Experimental setup in Bannisters' paper [12].

It was found that there is a loss in RSSI of 8 dB at 65 °C. A linear pattern was found to express the relationship between RSSI and temperature and it is presented in Bannisters' paper. He states in his paper that there is already work done previously that temperature decreases the efficiency of Radio Frequency (RF) circuitry [4], [47] [49].
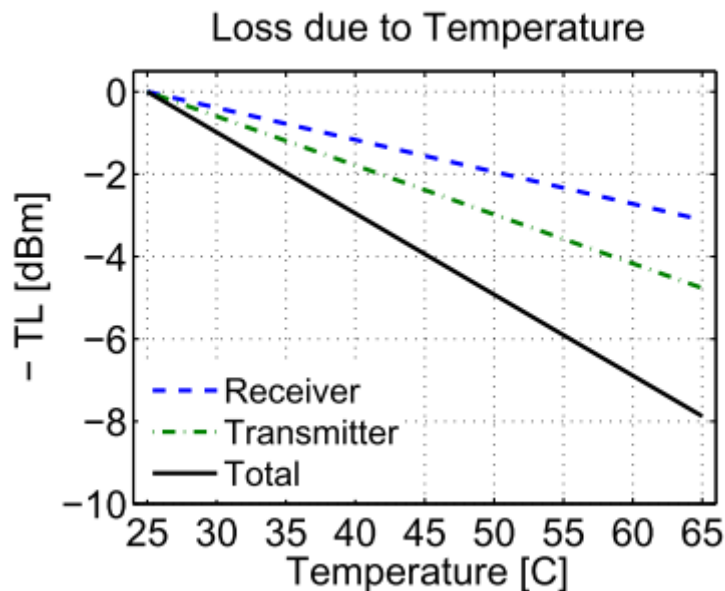


Fig. 2.4 Loss due to Temperature [12].

The increase of temperature at 65 °C has a negative impact on range as seen in figure 2.2 as it shows a 4 dBm to 5 dBm decrease in output from the transmitter and 3 dBm decrease in measured input power by the receiver for approximately 8 dB decrease combined. Communication range is also affected as can be seen in figure 2.2 when 65C is when there is a significant loss in range than operating in a 45C environment.
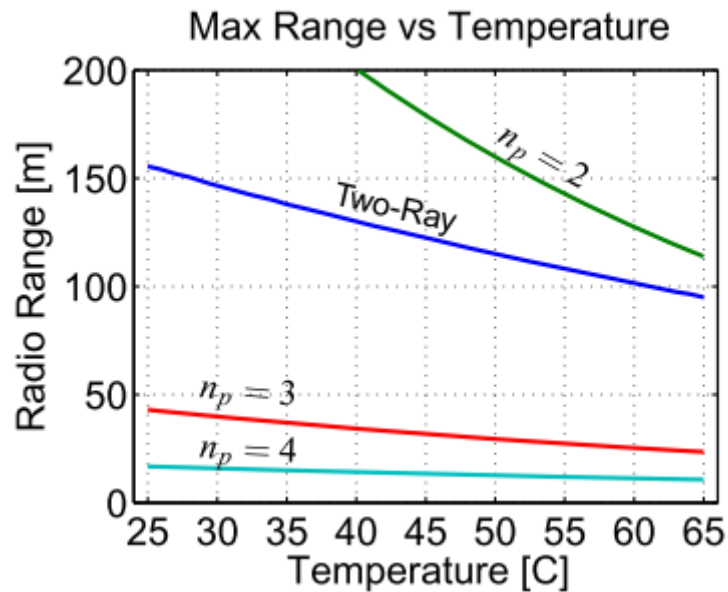


Fig. 2.5 Maximum Range Vs Temperature [12].

Thus by using a linear model function, it is possible to state a Log-Distance Path Loss Model to estimate the effect of temperature on the maximum communication range between two sensor nodes. Bannister concludes that this is not a malfunction of the circuitry that measures the RSSI but it effectively corresponds to a decreased ability for the radio to demodulate signals with low power and his findings is consistent with the findings of Wu, et al, [47] where temperature is shown to decrease the efficiency of the low noise amplifier stage in a Complementary Metal Oxide Semi-Conductor (CMOS) receiver.

In 2010, Boano et al [14], explores how ambient temperature affects an oil refinery WSN deployment in Portugal. The motes used were Tmotesky using the CC2420 radio chip [5]

using the 802.15.4 stack and the 2.4 Ghz ISM band. In an experiment to quantify how heat affects the motes, the sender and receiver mote were cooled to between -15 °C and -3 °C and then heated up to 50 °C in 90 minutes whilst sending data packets with a 12 byte payload every 4 seconds. The motes are separated 3 metres apart and transmission power is kept at -3 dBm throughout the experiment. The result from this experiment is that both sender and receiver had a loss of 4 dBm to 5 dBm in three separate runs - see figure 2.2. Tests were also conducted by placing the same motes inside ATEX compliant boxes to observe if heat affected the motes inside. The result of having motes inside ATEX compliant boxes is that temperature will be warmer inside the box than outside the box. It was observed that RSSI decreased as temperature increased.
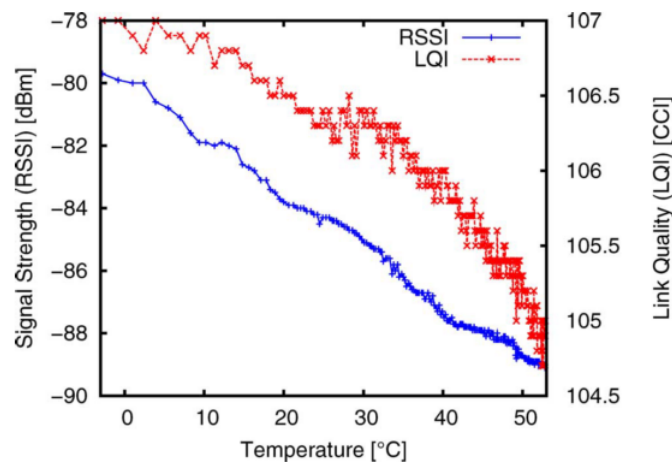


Fig. 2.6 RSSI and LQI falling as temperature rises [14].

In 2013, Boano et al [13] tried to quantify how temperature can dramatically reduce radio throughput. In his work, Boano attempts to design a low cost experimental infrastructure (WisMotes employing CC2520 and CC2420 using the ZigBee 802.15.4 stack at 2.4 Ghz ISM band) to vary the temperature of the low power transceiver in a repeatable and predictable manner. It was found that temperature can affect all platforms in the same way; in radio transceivers, it leads to a reduction of SNR which leads to a lower link quality and a shorter radio link which leads to lower physical throughput, delays or partitioning of the network.

Thelen et al investigated the effect of radio propagation for two months on a potato field utilizing Chipcon CC1000 radio transceivers using the Mica2Dot 433 Mhz version [45]. Relating to our studies, Thelen concludes that foliage does affect radio propagation and limits range to 10 metres, but radio waves propagate better in conditions that are high in humidity, especially at night and when raining. Thelen did dismiss the fact that the curvature of the Earth has no effect due to that the range between the radio nodes is very limited (up to 50 metres). This is in contrast to work done by Anastasi et al who used the 868 Mhz version and found that the presence of fog and rain decreased transmission range significantly [9].

Kang et al [25], wrote a paper which is based on WSN deployments in Hog Island, USA, under a project named LUSTER (Light Under Shrub Thicket for Environmental Research) and describes a long range setup (see figure 2.2), were WSN nodes powered by solar energy, sends data packets back to the main server over several kilometres using Gain antennas.
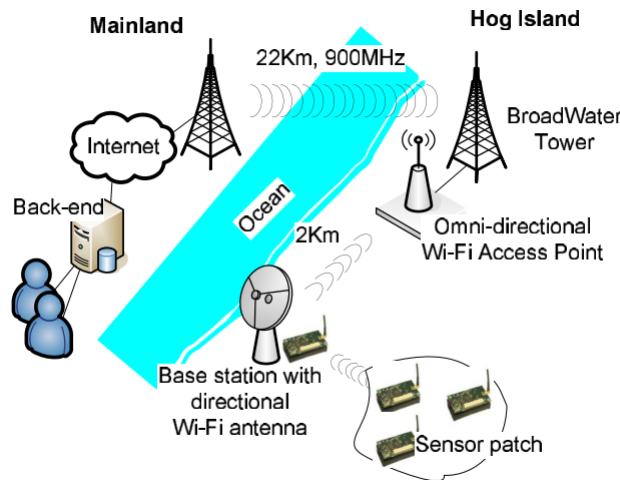


Fig. 2.7 LUSTER deployment in Hog Island [25].

One of the problems Kang described in the paper is that wind had a noticeable effect in packet drops and thus, Kang et al developed a delay/disruption-tolerant networking (DTN) technique as retransmitting data which were lost via the network would be lost due to wind. The reason highlighted in the paper that wind affects this deployment is due to the size of the antenna; small disturbances in the antenna can cause the signal to shift especially when Gain

antennas are used. Hence a weather aware DTN technique was developed to avoid the WSN to send data when there were wind speeds exceeding a particular threshold. In the discussion, it is highlighted that publicly available weather data was used to predict when outages may occur and hence delay transmission until wind speeds are more tolerable. Results were recorded and plotted on graphs seen in figure 2.2 where in a) is the wind level of the week and was observed that wind speed is strong between February 5th and February 10th. Plot b) reveals failure rates are much greater than in plots c) and d) where wind speeds at 15mph mitigates less packet drops than in plot d) which mitigates packet drops at lower threshold of wind speeds reaching 10 mph.



(a) Wind level of the week.

(b) Failure ratio without weather information.

(c) Failure ratio with weather information ($\alpha = 15mph$).

(d) Failure ratio with weather information ($\alpha = 10mph$).
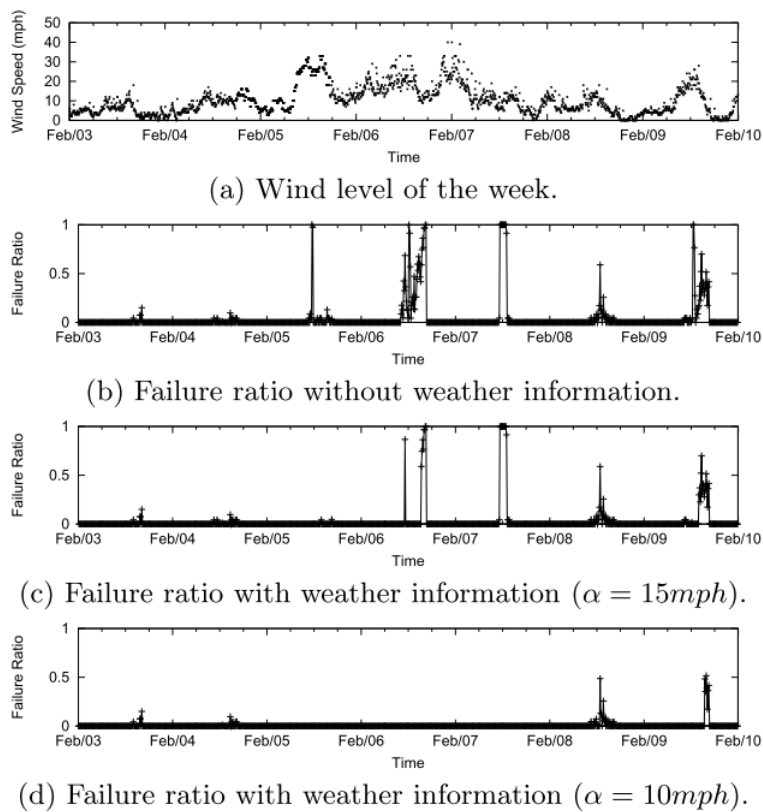
Fig. 2.8 Exploiting weather data to predict packet drops [25].

In Kang's paper, rain, fog and snow did not have any noticeable effects in their setup and these factors were not looked at since it is documented by Panagopoulos et al [36], that

radio operation under 10 Ghz frequency bands does not have an effect on rain, snow or fog. However, it is documented that a build-up of snow has a negligible effect as this degrades the sensitivity of the antenna.

In Hall's et al paper [22], work was done with Very High Frequency (VHF) and Ultra High Frequency (UHF) to confirm if anticyclonic weather conditions affects positively the range of radio signals. In his experiment, Hall used two trans horizon radio paths, the first radio path was 114 Km apart from Peterborough to Slough using a frequency of 90 Mhz and the second radio path was from Crystal Palace in London to Peterborough which are 121 Km apart using a frequency of 573 Mhz. Over a period of days from August to September in 1966, it was observed that during the night, there was an increment of 5 dB in signal power and the author demonstrates in his paper using ray tracing techniques that during periods of anticyclonic weather, abnormally high values of radio strength occurs at night and returns to normal during the sunset. This phenomenon is due to radio signals being reflected from the troposphere and down to the surface. To further explain the term anticyclonic, it is a region of high pressure that pushes cold air downwards to the surface from the upper atmosphere to the surface causing good weather. The effect of air pressure and anticyclonic weather is explained in more detail in section 3.2.3.

## 2.3   Link Selection Schemes

In this section, we look at previous related works in link selection algorithms.

Dube et al [17] proposed the Signal Stability Based Adaptive (SSA) routing protocol in MANETs due to the problem that in a dynamic network, fast changes in routing tables can cause nodes to have tables that are out of date and inaccurate and the constant changing topology would cause problems in looping routes. Dube et al performed simulations to show that the use of RSSI as a metric decreases route maintenance required by longer lived routes.

Work done by McDonald et al include a path availability model for wireless Ad-Hoc Networks [31] which proposes a routing metric which defines the probabilistic measure of availability of network paths that are prone to link failure. The paper highlights how more stable paths can be made and reduces overheads caused by node mobility.

Jiang et al [24] focuses on link prediction to estimate best availability in MANETS by introducing a prediction based link availability estimation and verified via a computer simulation. He highlights that nodes are aware of neighbours by defining how long each neighbour node has existed in the network and quantify the signal strength of each link. However, Jiang argues that this method does not address how a link status would behave in the future. He also proposes that his probabilistic link availability model can predict the status of future wireless links and thus select the strongest nodes to select reliable neighbours and form a strong cluster. It is also mentioned in his work that once the link of a path breaks, re-routing is required immediately.

Link selection schemes such as Yamaguchi, et al work [48] where evaluation of two schemes are made in usage of multi radio networks; link selection - selection of the most appropriate radio access - and link aggregation - bundles multi radio accesses which enhances transmission speed and reliability. In this paper, Yamaguchi focuses on link selection and improvements on the Transmission Control Protocol (TCP) throughput with an Analytical Hierarchy Process (AHP) algorithm and compares this with two schemes available which are fixed priority scheme (Priority) and maximum rate scheme (MaxRate). The AHP scheme was selected due to its simplicity in comparison with other approaches previously which is classed as a Multiple Attribute Decision Making (MADM). Other approaches within MADM are fuzzy logic, neural networks and genetic algorithms. The evaluation of the improved AHP method and using Round Trip Time (RTT) as a metric yields between 22% and 400% improvement in throughput although future studies are required to improve

MADM approach such as developing a hybrid system combing autonomous and centralized adjustment methods.

Gerharz et al [20] describes an adaptive metric to identify stable links in mobile wireless networks. This is achieved by obtaining online data of observed link evaluations and does not require signal strength, radio conditions or spacing of mobile devices or the availability of energy expensive devices such as GPS devices to keep track of distances. In his work, it is highlighted that many applications require stable connections to guarantee Quality of Service and transfers to access points can disrupt data transfer. The stability of a link is given by its probability to remain active for a certain time span thus measuring a links age to predict its lifetime is a relatively unexplored approach. However, it was found that selecting the oldest links sometimes works well, but may get bad choices.

## 2.4   Proposed Weather Based LQE Using RSSI and Weather Data

In the paper by Baccour et al [10], it is stated that there is a growing awareness that there is a need for a combination of hardware and software LQE that can provide a better predictor when nodes might fail and avoid frequent alterations of neighbourhood tables. Gungor et al [21] performed work in smart grids within an electric utility company and found out that Expected Transmission Count (ETX) and Fourbit performed better in terms of packet delivery ratio, average number of packet retransmissions, average number of parent changes and average communication delay on all nodes within the smart grid network. Other Link Quality Estimators in a harsh smart grid environment tested are PRR, RNP and WMEWMA which performed the worst. Although 4B and ETX have provided good results in the real setting [21].

In understanding the effects of meteorology on radio transceivers, heat was observed as a factor in affecting RSSI strength negatively when the radio transceiver was exposed to high levels of heat caused by an increase in resistance within the circuitry of the transceiver [13] but does not analyse other meteorological factors together with humidity and air pressure which others advocate is needed to better understand this issue holistically [34]. Interestingly Kang et al [25] uses weather aware algorithms but focusing on wind, to prevent data from being sent to the main server in order to preserve energy as WSN's are energy constrained.

In this paper, it is shown that Kang et al [25] developed a delay algorithm to stop the motes from transmitting data when wind speeds were high. We believe this is a step in the right direction when developing a new LQE method that involve weather parameters to predict outages.

Also to the best of our knowledge, there have been no LQE's that use the methods such as exploiting several environmental data sets; humidity, temperature and air pressure used to predict radio link outages. It is possible in developing a new LQE by combining current hardware LQE's such as RSSI with novel ones such as combining weather data, to be able to perform long range predictions when outages might occur.

We therefore need a long range predictor (by combining weather data) alongside a short range hardware based predictor (dropped packets and RSSI) to be able to predict when outages might occur, but by understanding the environmental data and implementing a model to carry out simulations. This proposed LQE would be hardware and score based since the hardware aspect is collected from the radio's RSSI register and the score base is used to calculate potential drops by analysing weather data.

We shall also demonstrate our claim for the need to have multi radio links with an enhanced Link Quality Estimator to predict packet drops and prevent network switching which can result in extra costs which we describe later.

The type of link selection scheme that we require in our test bed is to switch between an expensive GSM modem and a cheaper 868 Mhz modem. The test bed is static and not mobile as the work is geared towards industrial settings such as water companies (pumping stations), oil refineries and other large installations. The link selection process laid out in this thesis focuses on link selection based in decisions made by analysing meteorological data. The environmental conditions analysed are temperature, humidity and air pressure. Real world data is used on a link selection algorithm that is based on data collected over a year and use what we learn to select the best link depending on the environment that radio communication is subjected to.

## 2.5   Options For Radio Nodes

In deciding which radio node to select, in 2014, we selected the xbee pro series 5, 868 Mhz ISM band due to its long range and the fact that it is an unlicensed band by OFCOM; licensed bands and its usage requires payment of a fee and it is illegal to use a licensed band for a different purpose from what it was assigned to. The CC2420 chipset is used on motes such as the Tmote Sky, Imote2, TelosB, Iris and Sunspot, are all based on the Zigbee 802.15.4 2.4 Ghz band [37]. Zigbee is meant to be used as WPANs or Wireless Personal Access Networks which has an effective range of about 50 metres depending on environment [7]. Due to that our setup is based on distant wet wells, we require radio transceivers that are able to operate at greater distances of several miles and this is why the xbee 868 Mhz radio was selected at the time. Overcrowding of sources was also a factor since the 2.4 Ghz band is also used in many houses containing devices such as microwaves, WiFi LAN networks, baby monitors and cordless phones. Thus, there would be signal attenuation throughout our experiment if this band was used.

## 2.6   Chapter Summary

In this chapter, we have covered past related work on Link Quality Estimators and how a real setting have used the popular types of LQE's to some success and the growing awareness that exists that hardware and software LQE's can provide better quality estimation. We looked into what other researchers have done in the past and it was found that heat affects the internal circuitry of a radio transceiver which can impact RSSI output and thus decrease its effective range. We also discussed the effects of other weather phenomenon such as rain, snow and fog which there are mixed views between authors as to how these can impact U.H.F frequencies, particularly the 868 Mhz band. Humidity was documented as having a positive effect on radio communications at night over flourishing crops and disregards the effects of tropospheric ducting due to that communications is short range of several metres. There was also work done in the past to find out more about how anticyclonic weather can affect radio communications and it has been shown that this can have a positive effect especially during the night. We also looked into link selection schemes where this is built up on top of the LQE layer to route packets in the network which vary from simple algorithms to more complex AI algorithms. We also presented our vision for a new link quality estimator that uses weather data to predict radio link disruptions and then we presented options of different radio nodes that could be used in our test bed with justification of our selection.

# Chapter 3

# Meteorological Effects on Wireless Links

## 3.1 Chapter Overview

In this chapter, we discuss the meteorological factors examined in our experiments and discussing how link quality and meteorology are related. We then discuss our test results obtained from the test bed experiments and state how we use the new body of results to derive our new link quality estimator.

## 3.2 Weather Factors

All weather data has been collected using a WS1081 weather station that is linked via a 433Mhz module that transmits data to a headset wirelessly. This data is then processed using a framework called Pywws (Pi Weather Station) which fetches the data from the headset and records it in a human readable format. The polling time of the transmitter is once every 5 minutes which is the minimum setting.

### 3.2.1    Temperature

Air temperature is recorded in degrees centigrade. This gives us an indication of how cold or warm the air is that surrounds us. The warmer the air temperature is, the more moisture it can hold within an air packet, the cooler the air gets, the less moisture that air can retain within an air packet. As the air packet rises within the troposphere, the air packet becomes smaller and starts to condense as energy is being released. This causes the air packet to condense into tiny droplets of water known as precipitation. Thus air temperature has a relationship with air humidity and precipitation. We also suspect that a higher air temperature will have an effect on the xbee nodes circuitry as it was already proven in Bannister's work [12].

### 3.2.2    Humidity

Humidity is recorded as RH% or relative humidity as a percentage. To calculate RH% we obtain two metrics which are dew point and air temperature. We then use those two metrics by dividing the dew point with the air temperature to give us a percentage of how saturated the air is with water. The dew point is the temperature at which water vapour from the air starts to condense. For instance, if the air temperature is 15 °C and dew point is 14 °C, then dividing dew point with air temperature gives us a value of 93.33 %, where the air is almost saturated.

### 3.2.3    Air Pressure

Air pressure is the atmospheric pressure applied on to the surface of the Earth. The surface pressure on water level or mean sea level is approximately 1013.25 hPa, 29.92 inches of mercury or 1 atmosphere (Atm). The unit of pressure we use is hecta-Pascals where 1 hP is equal to 1 mm on a barometer. Atmospheric pressure on the surface of the Earth can change the weather of a particular location either bringing calm and sunny days to chaotic and destructive weather. A region with high air pressure may bring stability to the area with

warmer than usual weather. This is caused by a phenomena in the stratosphere known as the jet stream. Depending on how the jet stream is positioned on the atmosphere, it can force air downwards by compressing the lower tropospheric atmosphere. This causes the colder air to sink clockwise to the area of high pressure which leaves sunny skies as descending air reduces the chances of cloud formation; these areas are known as "Highs". On the contrary to this, the jet stream can cause a "Low" region where warm moist air ascends thus causing unsettled weather and are also associated with frontal systems associated with bad weather. Highs are known to be anticyclonic (anticlockwise) and Lows are cyclonic (clockwise) which flows to regions of High pressure areas - see figure 3.1.

In data that we collected during 2014 and 2015, we have observed that pressure also plays a role in determining weather patterns as this ultimately governs meteorological factors. We observe that changes in pressure (especially low pressure and when falling) seems to have a negative effect on the 868 Mhz radio link and the algorithm's behaviour is to switch when changes occur. We have seen for instance when the UK suffered from storms and weather bombs (an explosive cyclogenesis where a pressure drop of 24 hPa within 24 hours is observable) causing severe gales and long periods of heavy rain often with sleet as shown in this news article [1].

### 3.2.4   Experimental Setup

In this section, we highlight the need for having a multi-radio interface link so that middleware can use the optimal link when weather conditions threaten communication links. We highlight the importance that we want to limit rapid switching between transceivers as much as possible as this can be costly in terms of energy used, CPU cycles expended and idle time wasted in forming new links. The map on figure 3.3 shows the locations of the transceivers; to the south, an xbee node and to the north, a box carrying an xbee with a GSM modem.
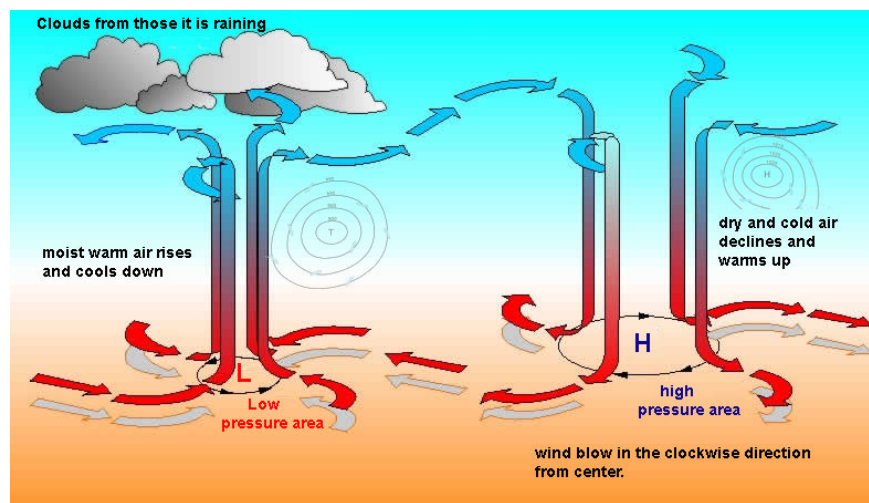
Fig. 3.1 Air Pressure diagram showing low and high regions

We conducted this experiment in order for us to gauge on the effects that weather environments have over radio propagation; more specifically, we want to know how the 868 Mhz band (non licensed band) and GSM bands (licensed) perform in different weather scenarios. During May 2014 to December 2015, we organised a test bed where we placed an xbee node 1.2 Km apart with no line of sight (obstacles such as trees and buildings interfere line of sight) that would send a data packet which is one character in length and would send one transmission; no retries were allowed. The nodes on each side would log a time stamp and the RSSI on each xbee node. One of the nodes had a GSM modem (Huawei E220) that is connected to a GSM carrier. A module was coded to fetch the GSM RSSI levels which normally receives signals from the carrier every 2 seconds which updates its RSSI level. The 868 Mhz radio (Xbee Pro Series 5) RSSI is fetched using local and remote Attention (AT) commands and the RSSI level is logged together with a time stamp that collects RSSI data once every 30 seconds

During the experiment, various challenges were faced which affected our results. Such errors such as erroneous RSSI fetched from the GSM, hardware bugs present in raspberry pi R1 with power issues, water penetration and equipment failure was experienced due to
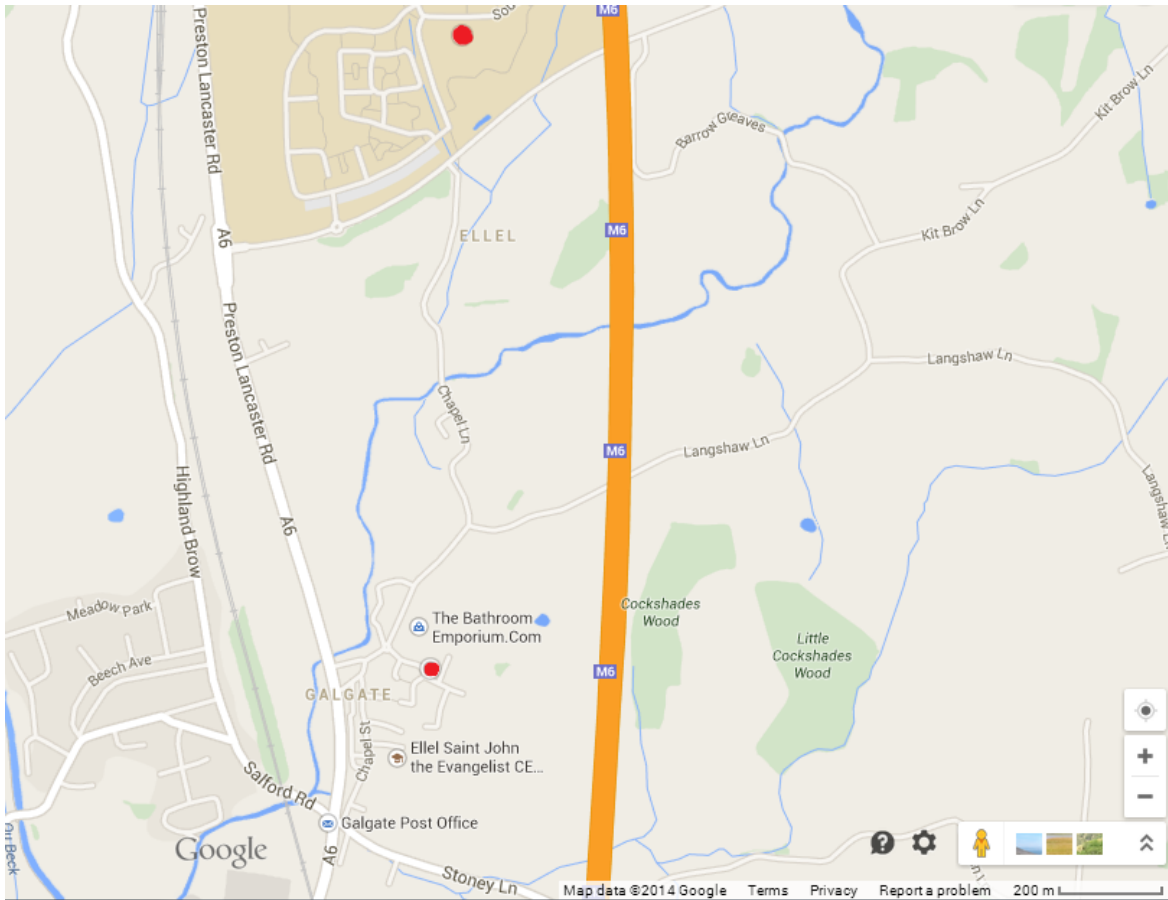
Fig. 3.2 Map showing locations of 868 Mhz sender node in the south and 868 Mhz receiver on the north with GSM receiver more than 1Km apart.

harsh weather conditions which slowed the experiments. We selected July 2014 to base our analysis with two xbee set-ups where we show packet losses as shown in time clusters and where the data was reliable to draw conclusions with weather correlations. the reason we select July is due to that it is the summer month and it is usually rainy, warm and humid. GSM RSSI signal is acceptable between -100 and -60.

During the month of July 2014, a smaller scale experiment between 3 xbee radio transceivers was conducted to understand if there was significant difference in RSSI levels by having a ground and elevated placement which we describe in the next section.

Fig. 3.3 Position of receiver end of the test bed.

## 3.3   Test Bed Experiment between Infolab21 and Galgate

One point of the radio transceiver was placed within the School of Computing area suspended on the third floor of the Infolab21. The reason for this is due to that the building external shield is made of copper and causes interference if placed indoors. Placing the sealed box with the xbee radio outside a window and secured with cables in our setup was more reliable in receiving signals. Other places were attempted such as in the Infolab21 grounds during 2014, but, these areas required a separate power source which was possible by using a 15Amp 5V USB battery which can supply the Xbee 868 Mhz radio with a few days of power until another battery is required. These had to be sealed in watertight boxes as during this period, rain is prevalent. One issue we found was the antenna positioning; to match the antenna vertically, it meant that a hole had to be made and this can cause leakage if not sealed properly. We saw that the RSSI signal is slightly lower to what is received on the one elevated, that is, the elevated transceiver had a better RSSI than the one below.

The method of testing RSSI on the ground level is to send a remote AT RSSI command to the xbee node located on the Infolab21 grounds which should then reply back by sending the RSSI level back to the transmitter located in Galgate. The reason of doing this is to preserve energy as we only required the radio to test if there are significant differences (e.g. 30 dBm to 50 dBm) in RSSI levels between the elevated transceiver and the one at ground level.
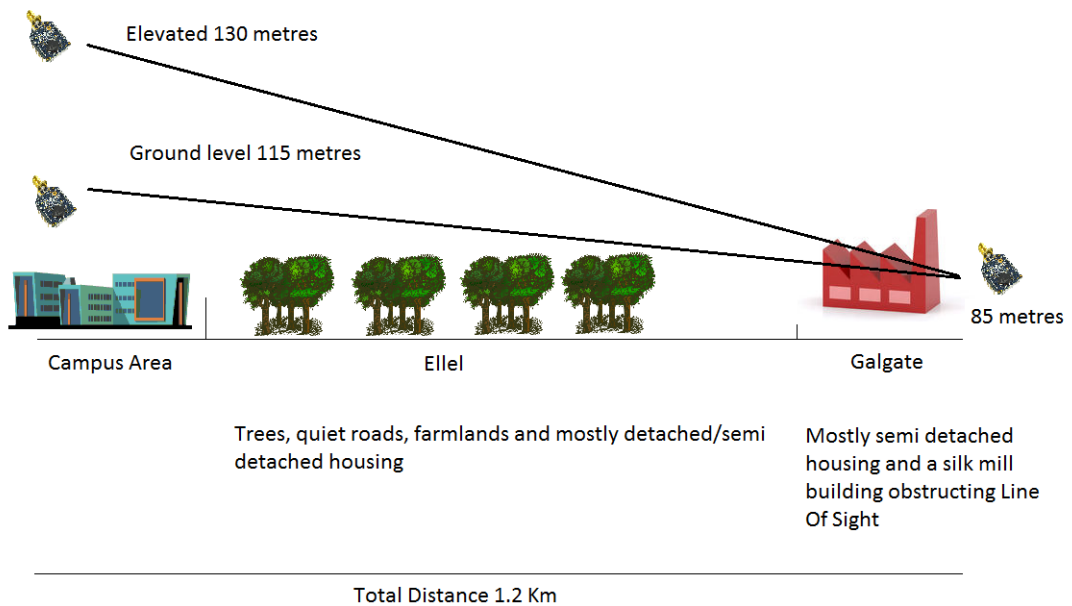
Fig. 3.4 Test bed layout between University campus area and Galgate

## 3.3.1 Ground And Elevated Placements

We collected data that is split into three separate graphs; the first shows 868 Mhz RSSI, GSM RSSI and cluster fail from 868 Mhz packet drops if failure rate is more than 30 % during 5 minutes. The reason for such measurement is that in an industrial scenario, no more than 30 % failures within a 5 minute would be acceptable, although this figure can be altered for other applications. We therefore collect weather data from a WS1081 weather station which makes a reading once every 5 minutes. When these drops occur, these are highlighted as cluster fail and cluster2 fail. The labels on the graphs on this section refers to xbee-EL, cluster fail-EL, xbee and cluster2 fail.

The weather data collected is as follows; the middle graph shows air temperature in degrees centigrade, dew point in degrees centigrade and rain in mm. The third graph shows barometric pressure in hecta pascals. We collected data over a 12 month period (using the elevated transceiver) and we selected at random the events where there have been observable effects including storms that have made headlines in the news media. What we aim to find

is if there is a correlation between the RSSI collected on our test bed and also observe if meteorological events has any effect. If there is such a correlation, we can then use this data in our model to better predict when failures are likely to occur and; 1) pre-empt unnecessary switching (evil switches) and 2) saving time, computation, real time actuations and energy costs from making those switches.

On this section, we focus mainly on our findings for the month of July in 2014 as a short experiment to see the difference in having a radio transceiver on the Infolab21 ground area and elevated on the 4th floor (D floor) of the Infolab21 which is approximately 130 metres from sea level. The ground level xbee radio transceiver height was 115 metres from sea level and the Galgate xbee radio transceiver was 85 metres from sea level. The total height from the elevated xbee radio transceiver from the Infolab21 building is 45 metres over a distance of 1.2 Km to Galgate and 30 metres from the ground level xbee from the Infolab21 building to Galgate.

Figure 3.4 diagrammatically shows how the test bed was laid out and what obstructions were present. We also show a photograph displaying the obstructions and the surrounding environment that the test bed experiment was conducted in figure 3.5. In the same photo, we highlight the large silk mill building which is over 300 years old and was an obstruction in our experiments. Measurements were taken from 22 satellites with a Global Positioning System (GPS which is the United States of America navigation system) and Global Navigation Satellite System (GLONASS which is the Russian navigation system) receiver with an accuracy of 5 metres or less.

Note that the range of readings extend from 0 dBm to -140 dBm and the reason for this is to appreciate packet losses marked as 0 on the graphs.

Whilst conducting experiments for one month on the outdoor grounds of the Infolab21, we have collected both the RSSI from the elevated radio transceiver and that of the transceiver

Fig. 3.5 View from the elevated xbee node to Galgate

on the ground. For the rest of 2014 and 2015, we collected data solely using the elevated radio transceiver.

**July 2014 Investigations**

In this section, we will present the results and focus on discussing our findings here. Some days are not included as data points were not available to examine. When calculating correlation, we calculate first without packet losses to see if there is a correlation with signal strength, then we calculate correlation with packet drops included. We define correlation weakness and strength in the following value range. A value of r between 0 and 0.19 is very weak, 0.2 and 0.39 is weak, 0.4 and 0.59 is moderate, 0.6 and 0.79 is strong and finally 0.8 to 1 is very strong. If a correlation r value is minus, it means that there is an inverse relationship; as one variable increases. the other decreases whereas in a positive correlation, both variables move in tandem.

During the 7th of July, we show a graph 3.6a displaying the elevated xbee radio nodes with their corresponding RSSI strength. The red points are for the elevated xbee. Recording of data on both elevated and ground level started on the 8th of July 2014; the elevated xbee is always powered and in some occasions, the ground level data was unavailable as we did not start collecting data from the ground level on the 7th of July (the ground level xbee node is powered by a 15 Amp USB battery which needs to be recharged often). We see that during the early morning between 7am and 8am, rain was collected and cluster failures occurred during this time. However, we do observe an improvement in RSSI signal when there was a cooling effect at around 6pm which there are still packet losses present, but far less than during the early afternoon.

Looking at the analysis of air pressure in 3.6b, there have been a number of drops at around 1011 hPa, however, we do see in graph 3.6a that there was a period of instability as air pressure was getting higher. We observe during the day that the elevated xbee node had more failures especially when the temperature was between 22 °C and 24 °C, at around 1pm and 5pm. There was a cooling effect by 5pm, more data packets was received successfully after that time. As we interpolate heat data for a best line fit, we can see that more packet losses can be seen as the temperature rises in 3.6c and there is also a relationship seen in graph 3.6d where more packet losses is observed when the air is dry; i.e. when relative humidity (RH%) was approximately 70 %. A very weak positive correlation was found between air pressure and RSSI with a value of 0.12. A very weak negative correlation was found between temperature and RSSI with a value of -0.01. A very weak negative correlation was found between relative humidity and RSSI with a value of -0.01.

When calculating correlation and taking into account dropped packets, a weak negative correlation was found between air pressure and RSSI with a value of -0.24. A moderate negative correlation between temperature and RSSI was found with a value of -0.44 and a

moderate positive correlation was found between relative humidity and RSSI with a value of 0.42.
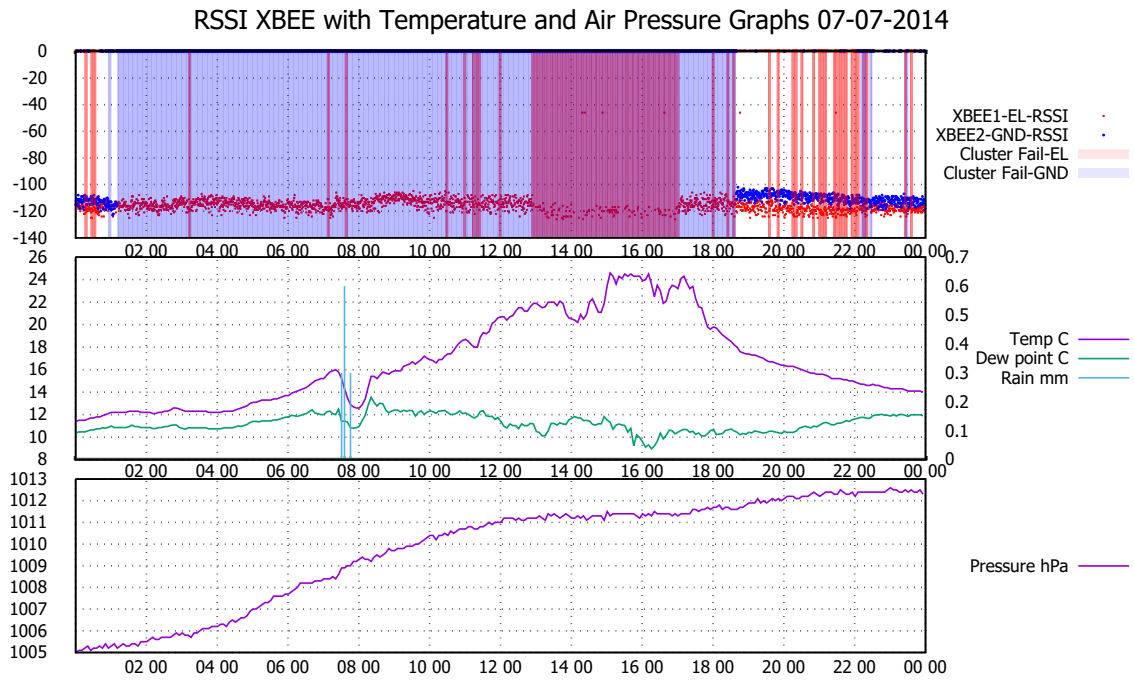
(a) Xbee1 as elevated 868 Mhz transceiver 07-07-2014
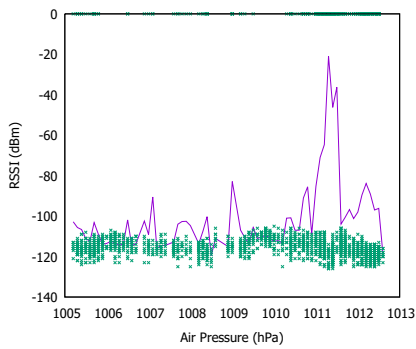


(b) RSSI and Air Pressure 07-07-2014
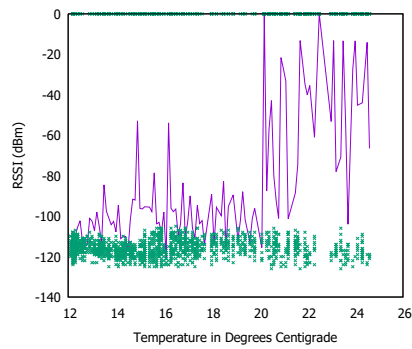


(c) RSSI and Air Temperature 07-07-2014
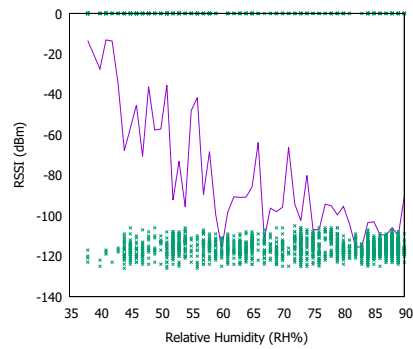


(d) RSSI and Relative Humidity 07-07-2014

Fig. 3.6 Analysis during the 07-07-2014 applying best line fit

On the 8th of July as can be seen on graph 3.7a, we observed that the RSSI on both xbee nodes were within -100 dBm and -120 dBm. It can be observed that during the day, temperature starts to rise and the air gets dryer as from 5 am and we see during noon on the same day that both transceivers had cluster failures; more than 30 percent of packets were dropped within 5 minutes. After 10 pm, the ground floor transceiver failed, but there were no failures on the elevated transceiver. Both elevated and ground xbee nodes had improved RSSI approximately between 4 am to 10 am and this is a period where humidity was very high and 1.8 mm of rain was collected. In the analysis of data points in 3.7b, we observe that air pressure has a best line of fit in different values, after 1013 hPa with a period of no packet drops before 1013 hPa. If we refer to graph 3.7a, we see that there was a period of air pressure instability from around 5pm to 11pm which represents the air pressure oscillations in 3.7b. Looking at temperature in graph 3.7c, we observe that more failures occurred when the air was warmer peaked at 18 °C and 24 °C. In analysing humidity in graph 3.7d, we see that there were more failures when the air was dryer when RH% is less than 70 %. A moderate positive correlation was found between air pressure and RSSI with a value of 0.49. A weak positive correlation was found between temperature and RSSI with a value of 0.21. A weak negative correlation was found between relative humidity and RSSI with a value of -0.23.

When calculating correlation and taking into account dropped packets, a weak negative correlation was found between air pressure and RSSI with a value of -0.06. A very weak negative correlation between temperature and RSSI was found with a value of -0.19 and a weak positive correlation was found between relative humidity and RSSI with a value of 0.19.
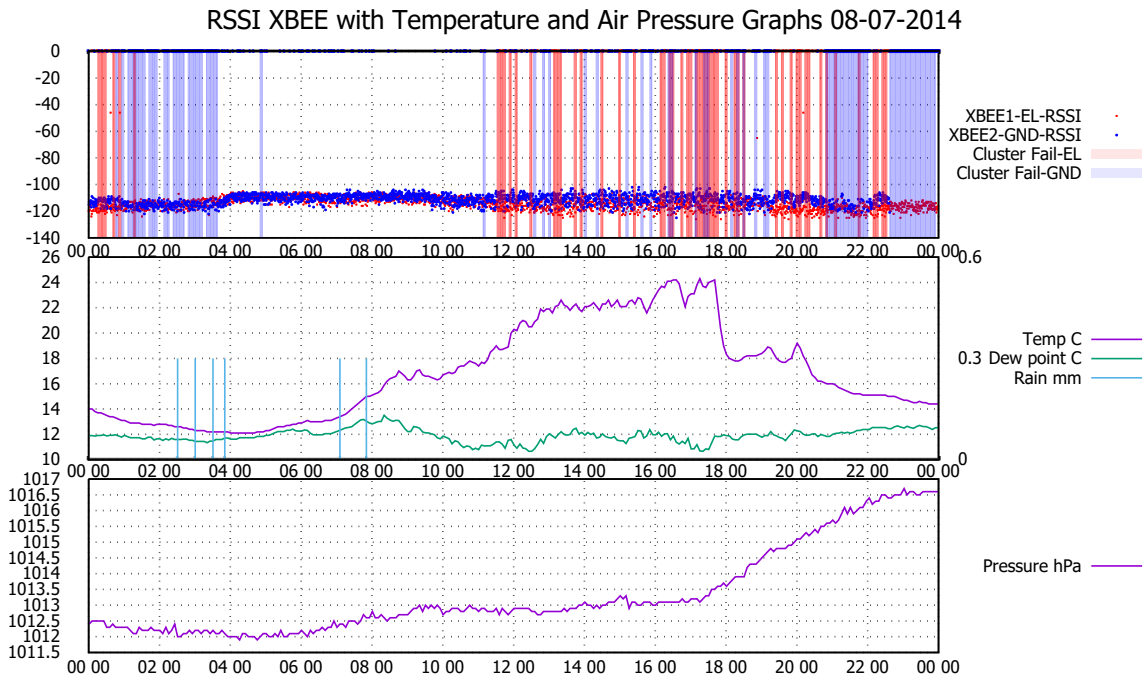
(a) Xbee1 as elevated and Xbee2 as Ground level 868 Mhz transceiver 08-07-2014
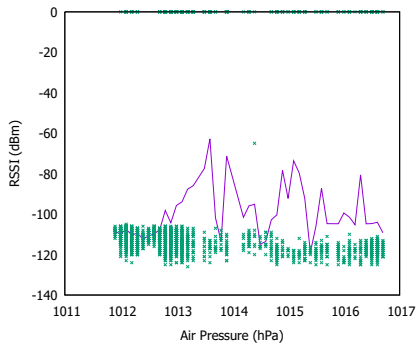


(b) RSSI and Air Pressure 08-07-2014
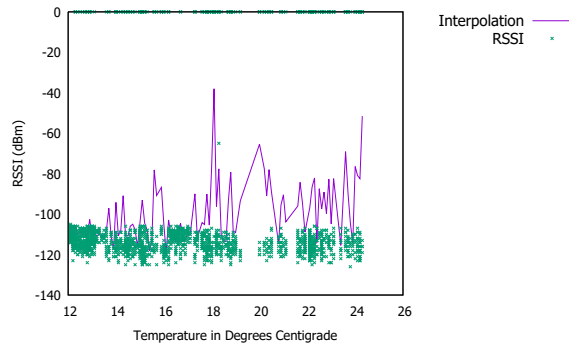


(c) RSSI and Air Temperature 08-07-2014
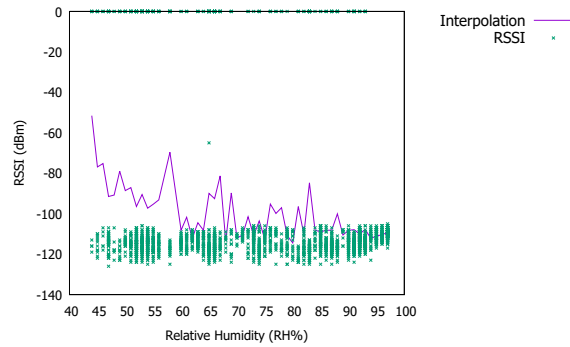


(d) RSSI and Relative Humidity 08-07-2014

Fig. 3.7 Analysis during the 08-07-2014 applying best line fit

In graph 3.8a which is on the 9th of July, we noticed that the ground level transceiver was operating after 3 am. However, the elevated transceiver was reporting cluster failures as from 3 am for the rest of the day. As from 8 am, there was some improvement of approximately 10dBm on the ground level transceiver to that compared with the elevated transceiver. Observing the analysis in 3.8a and 3.8b, we can see that air pressure was unstable but oscillated over a small range of air pressure; from 1016.4 hPa up to 1018 hPa. It can be observed that there is a gradual packet loss in 3.8b from 1016.6 hPa to 1017.9 hPa. In observing heat under 3.8c, it is difficult to conclude if heat had any impact as the line of best fit oscillates across all values. In observing humidity in graph 3.8d, we can see a pattern where packet drops suffer most in dryer conditions with the exception when RH% was nearly 99%. A very weak negative correlation was found between air pressure and RSSI with a value of -0.03. A very weak negative correlation was found between temperature and RSSI with a value of -0.14. A very weak positive correlation was found between relative humidity and RSSI with a value of 0.15.

When calculating correlation and taking into account dropped packets, a very weak negative correlation was found between air pressure and RSSI with a value of -0.12. A very weak negative correlation between temperature and RSSI was found with a value of -0.01 and a weak positive correlation was found between relative humidity and RSSI with a value of 0.02.
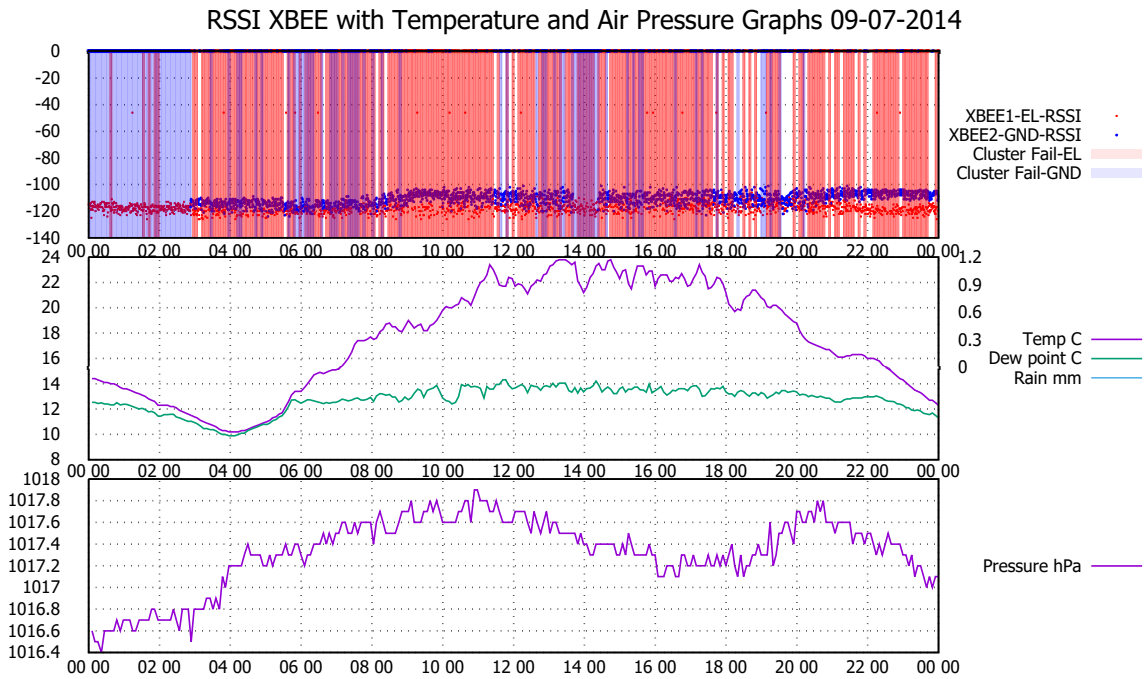
(a) Xbee1 as elevated and Xbee2 as Ground level 868 Mhz transceiver on 09-07-2014
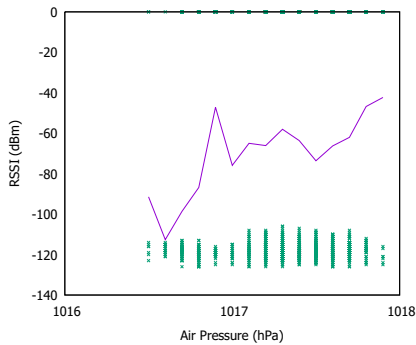


(b) RSSI and Air Pressure 09-07-2014
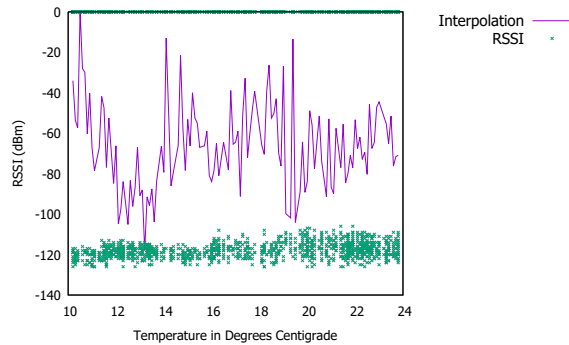


(c) RSSI and Air Temperature 09-07-2014
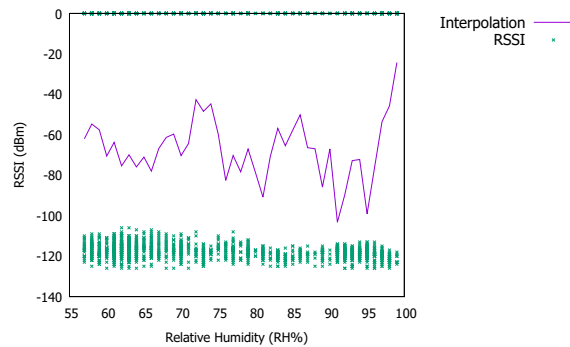


(d) RSSI and Relative Humidity 09-07-2014

Fig. 3.8 Analysis during the 09-07-2014 applying best line fit

On the 11th of July, 3.9a, we can observe xbee packet drops from 4 am to 8 am and then after 11 pm at night. This was unusual for the elevated radio node to fail since the ground level xbee node has been transmitting packets successfully over this same period. We do notice that the ground level xbee node has a reduced RSSI level during the afternoon, most notably between 2 pm and 8 pm which during this time, the sun was still on the horizon and temperature was over 20 °C during this period. In our analysis of air pressure in graph 3.9b, there was a mid range of values between 1015 hPa and 1016 hPa where packet losses were minimal whereas we see more packet losses in the lower and higher range which are 1014 hPa and 1016.5 hPa. In observing temperature in graph 3.9c, we can see that there were more packet losses when temperature was less than 20 °C. In analysing relative humidity in graph 3.9d, we observe that packet losses was greater when humidity was greater than 70%. A very weak positive correlation was found between air pressure and RSSI with a value of 0.14. A very weak negative correlation was found between temperature and RSSI with a value of -0.19. A very weak positive correlation was found between relative humidity and RSSI with a value of 0.18.

When calculating correlation and taking into account dropped packets, a very weak negative correlation was found between air pressure and RSSI with a value of -0.05. A moderate positive correlation between temperature and RSSI was found with a value of 0.51 and a moderate negative correlation was found between relative humidity and RSSI with a value of -0.51.
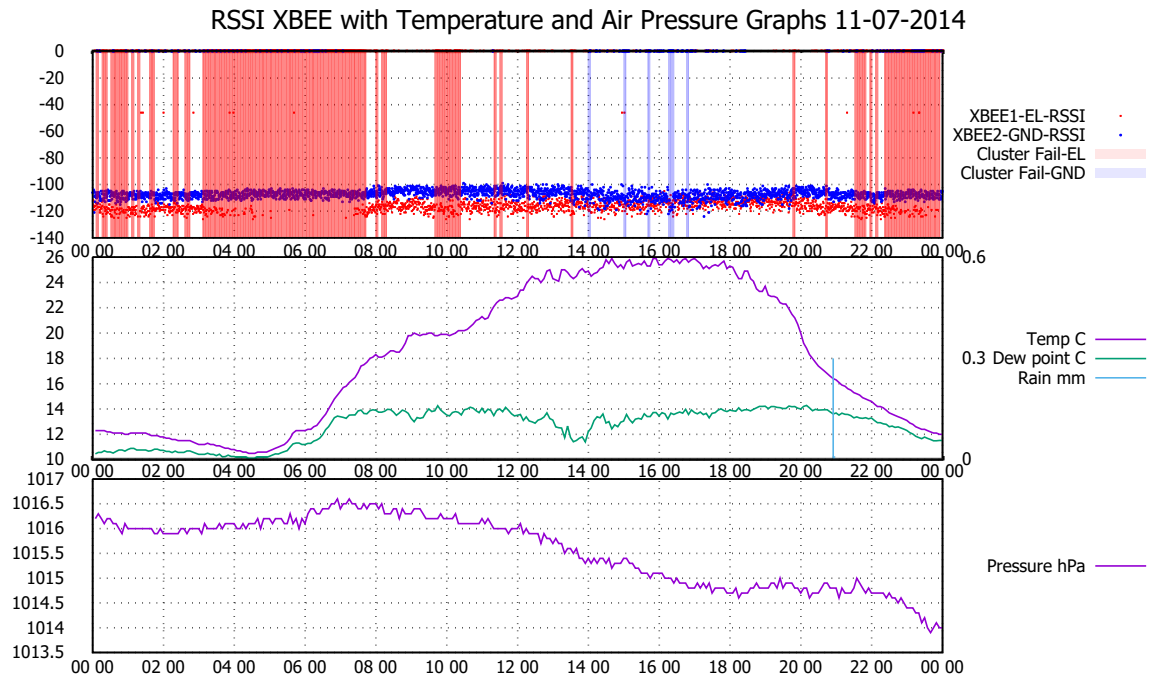
(a) Xbee1 as elevated and Xbee2 as Ground level 868 Mhz transceiver on 11-07-2014
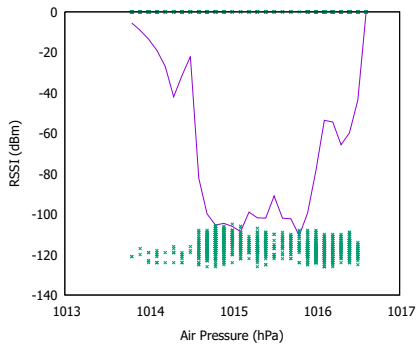


(b) RSSI and Air Pressure 11-07-2014
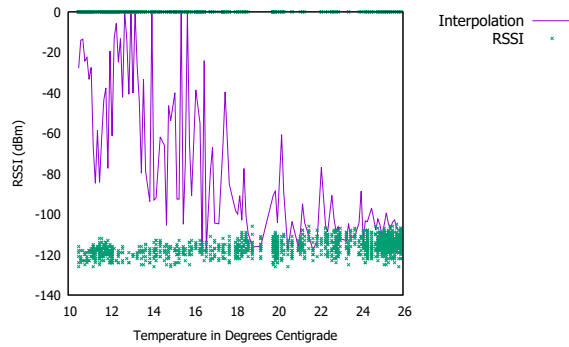


(c) RSSI and Air Temperature 11-07-2014
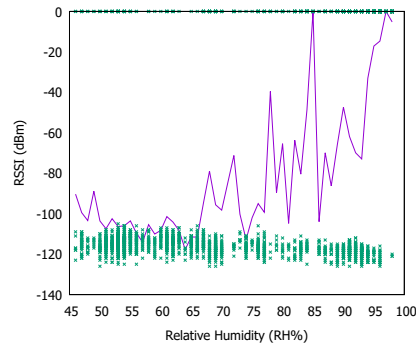


(d) RSSI and Relative Humidity 11-07-2014

Fig. 3.9 Analysis during the 11-07-2014 applying best line fit

On the 12th of July, 3.10a, we see on the graph that from midnight to 7 am, there were failures on the elevated transceiver and we can appreciate that heat has been rising from 5 am and cooling down as from 2 pm which has remained very dry during this period. We observe a slight improvement in RSSI signal on both transceivers at around 6pm when there was heavy rain (1.2mm in one hour) with scattered rain until close to 10 pm in the evening which at this point, humidity was very high, foliage and ground was wet. Temperature was high at approximately 17 °C at night and air pressure has been falling steadily - albeit fast - during the day signalling a low pressure area was incoming as pressure dropped from 1011 hPa down to 1001.5 hPa.

In discussing the analysis of air pressure, we see in graph 3.10b where data packets are lost as air pressure rises despite that RSSI improved when air pressure was below 1007 hPa; in this day, air pressure dropped throughout the day. In observing graph 3.10c, we look into temperature during the day and we see mixed results; failures when temperature was under 17 °C but a mixture of packet drops throughout the temperature range. In observing 3.10d, we see more drops in data packets when humidity was above 80% with mixed results when under this threshold. A moderate positive correlation was found between air pressure and RSSI with a value of 0.46. A weak positive correlation was found between temperature and RSSI with a value of 0.37. A moderate negative correlation was found between relative humidity and RSSI with a value of -0.42.

When calculating correlation and taking into account dropped packets, a strong negative correlation was found between air pressure and RSSI with a value of -0.71. A moderate positive correlation between temperature and RSSI was found with a value of 0.44 and a very weak negative correlation was found between relative humidity and RSSI with a value of -0.19.
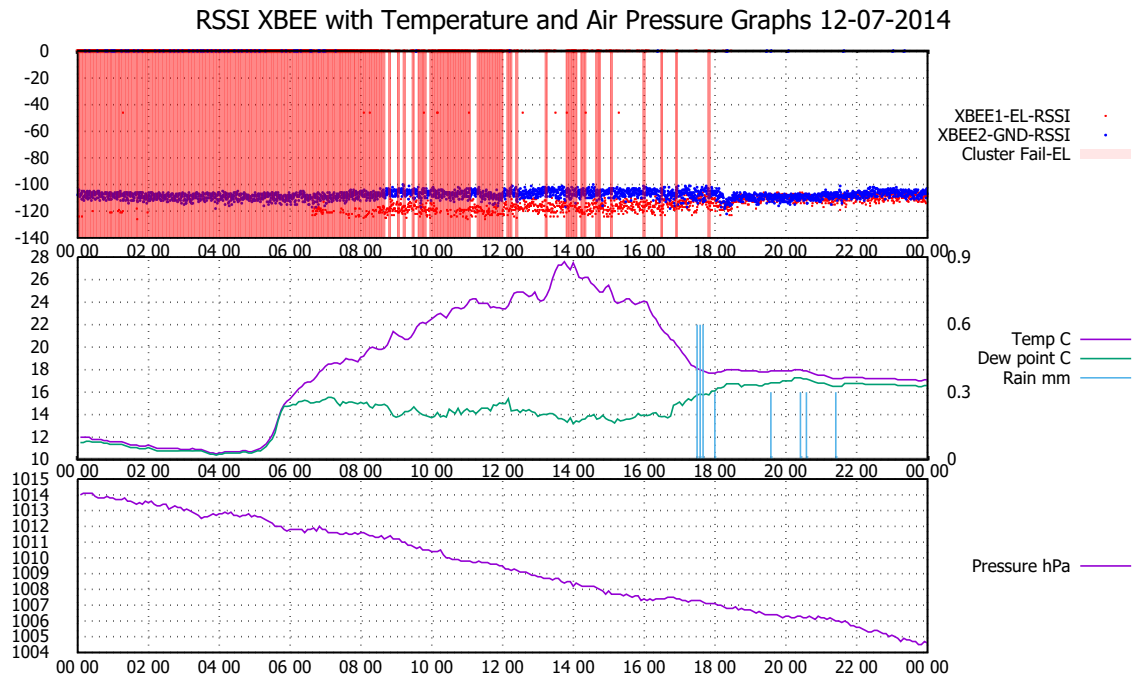
(a) Xbee1 as elevated and Xbee2 as Ground level 868 Mhz transceiver on 12-07-2014
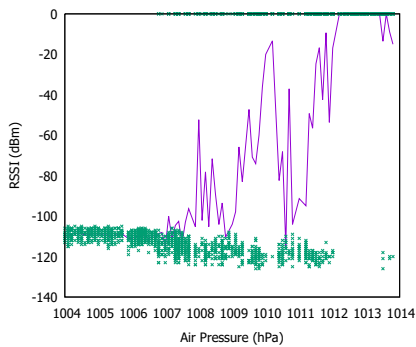


(b) RSSI and Air Pressure 12-07-2014
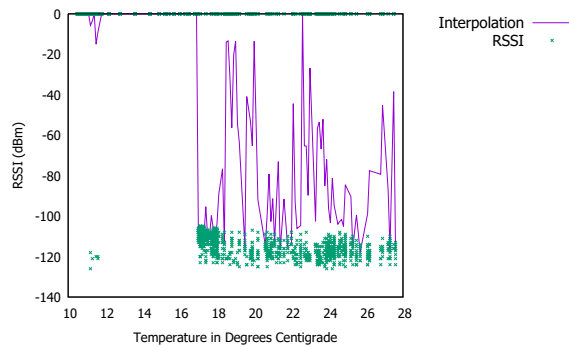


(c) RSSI and Air Temperature 12-07-2014
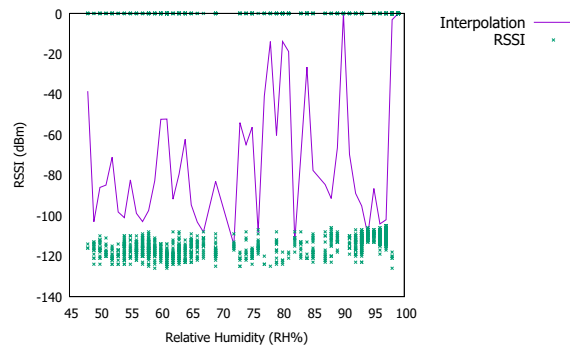


(d) RSSI and Relative Humidity 12-07-2014

Fig. 3.10 Analysis during the 12-07-2014 applying best line fit

On the 13th of July, 3.11a, we collected xbee data on the elevated node. During the morning, it rained and this had no effect on the xbee communications. We do see however later in the day as from 9 am, RSSI range was wider than before this time and there were packet drops after 12 pm. We do see that temperature was high at around 21 °C and a dew point was 10 °C at its lowest point which gives a relative humidity of 48 %; a very dry day. In observing graph 3.11b, we observe an improvement in RSSI signal when the air pressure was between 1003 hPa and 1004.5 hPa with few packet drops. However, as air pressure rose, there was an increase in packet losses as it approached 1009 hPa. In observing temperature in 3.11c, we see that RSSI was more favourable around 16 °C to 17 °C and RSSI weakened outside this temperature range. In observing graph 3.11d, we observe that a higher humidity level did improve RSSI and reduced packet drops at around 85 % of relative humidity. A moderate positive correlation was found between air pressure and RSSI with a value of 0.49. A weak positive correlation was found between temperature and RSSI with a value of 0.21. A moderate negative correlation was found between relative humidity and RSSI with a value of -0.47.

When calculating correlation and taking into account dropped packets, a moderate negative correlation was found between air pressure and RSSI with a value of -0.42. A very weak negative correlation between temperature and RSSI was found with a value of -0.09 and a weak positive correlation was found between relative humidity and RSSI with a value of 0.34.
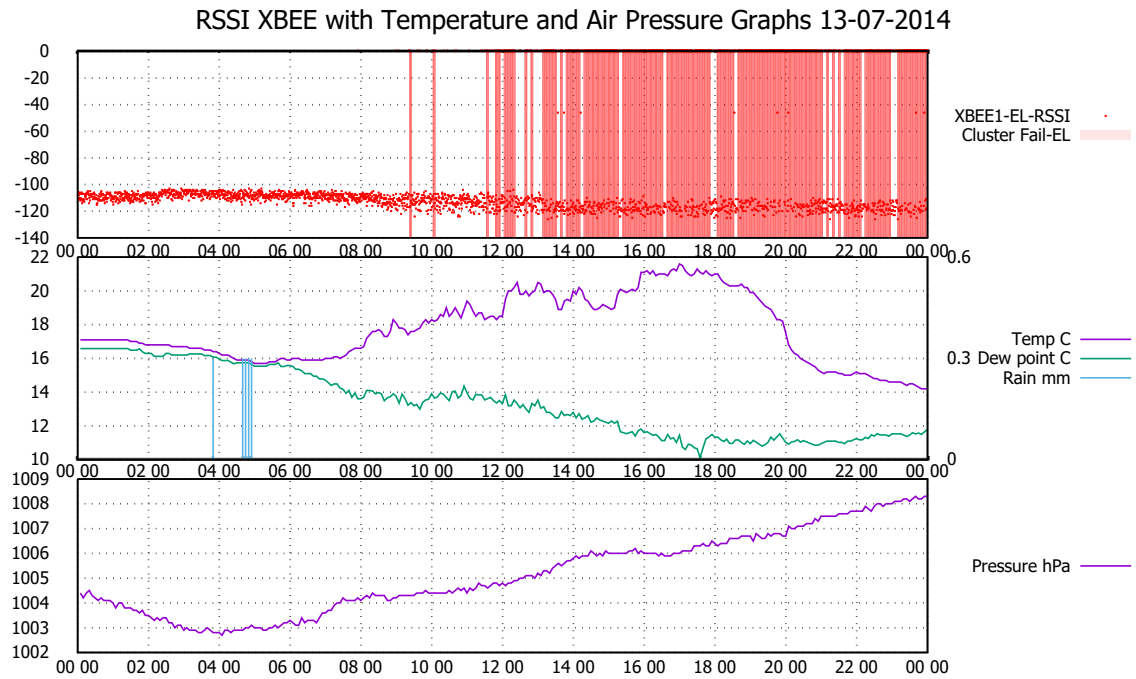
(a) Xbee1 as elevated and Xbee2 as Ground level 868 Mhz transceiver on 13-07-2014
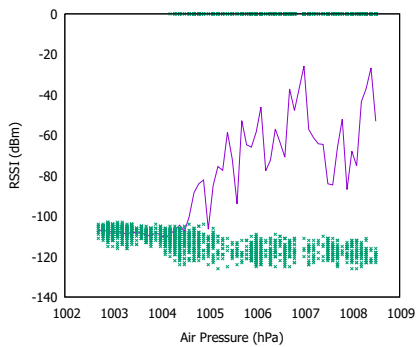


(b) RSSI and Air Pressure 13-07-2014
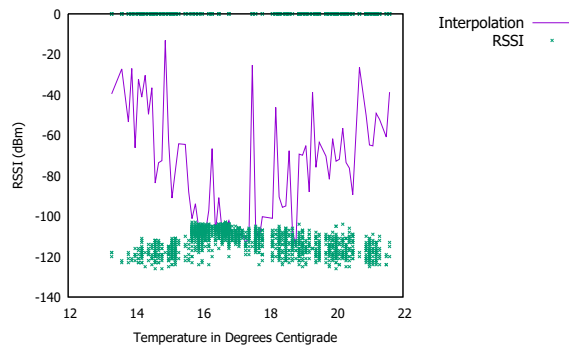


(c) RSSI and Air Temperature 13-07-2014
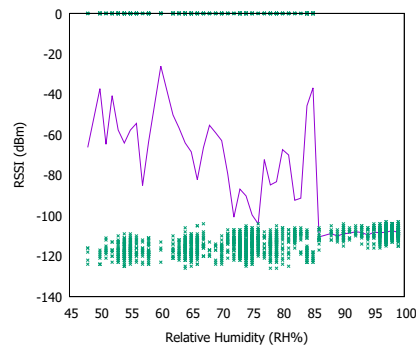


(d) RSSI and Relative Humidity 13-07-2014

Fig. 3.11 Analysis during the 13-07-2014 applying best line fit

On the 14th of July 2014, see graph 3.12a, we can observe that the elevated transceiver has numerous failures during the night with pockets of data being received from 7 am until 10 am with failures occurring until 3 pm. The ground level transceiver was unaffected but some failures started at around 2pm. We can observe that RSSI did improve for the elevated node as from 3pm which we can see a cooling effect with a drop in pressure and a rise in humidity. We observed rainfall of 1.5 mm collected which had no effect on the elevated transceiver. Packet drops occurred mostly when air temperature dropped rapidly in the early hours of the morning and rose during the day. In figure 3.12b, there were packet drops when air pressure was unstable between 1006.5 hPa and 1008 hPa. In observing air temperature in graph 3.12c, we saw that a temperature range of 15 °C to 17 °C did not produce as many packet failures as in other temperature values; more failures were observed when the air temperature was under 15 °C and greater than 18 °C. In observing relative humidity in graph 3.12d, the line of best fit signal strength dropped between 75 % and 80 % and then again deteriorated when RH% was near 99%. In 3.12d, there was a larger area of data sets of RSSI that was stronger between 90 % and 99 % of RH% which the RSSI signal was generally weaker when humidity was under 75 %. A weak positive correlation was found between air pressure and RSSI with a value of 0.27. A very weak negative correlation was found between temperature and RSSI with a value of -0.13. A very weak negative correlation was found between relative humidity and RSSI with a value of -0.16.

When calculating correlation and taking into account dropped packets, a weak negative correlation was found between air pressure and RSSI with a value of -0.25. A weak positive correlation between temperature and RSSI was found with a value of 0.26 and a very weak positive correlation was found between relative humidity and RSSI with a value of 0.1.
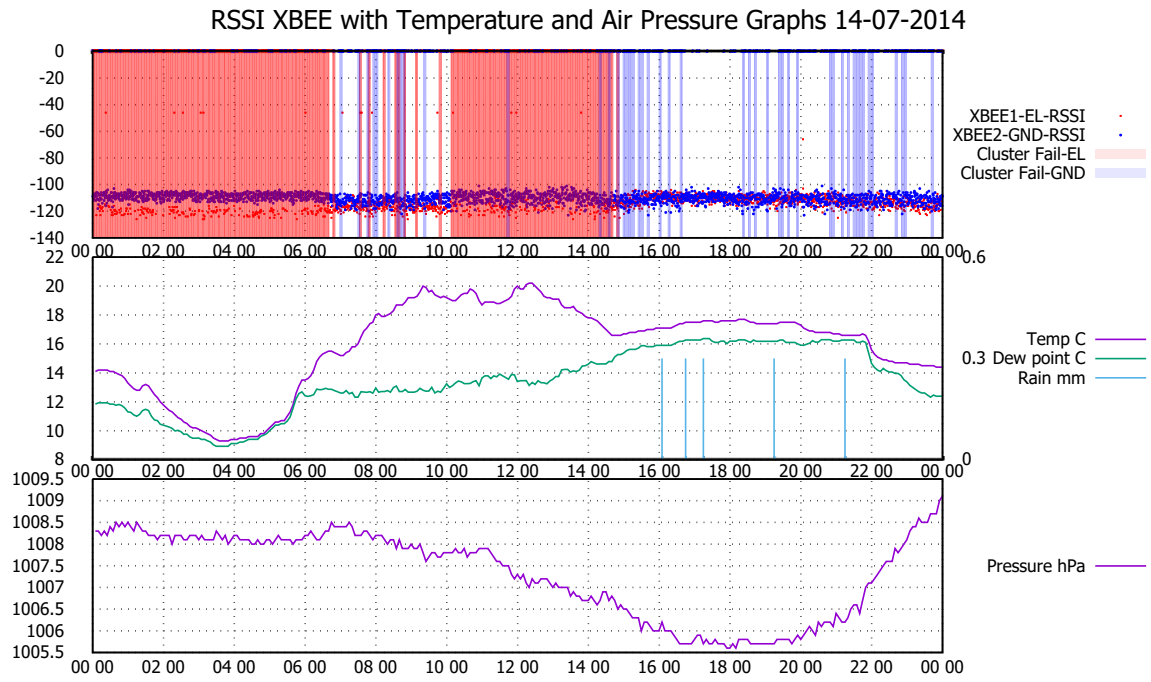
(a) Xbee1 as elevated and Xbee2 as Ground level 868 Mhz transceiver on 14-07-2014
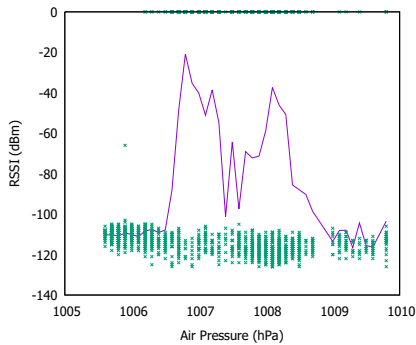


(b) RSSI and Air Pressure 14-07-2014
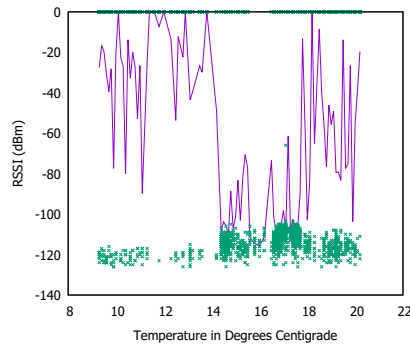


(c) RSSI and Air Temperature 14-07-2014
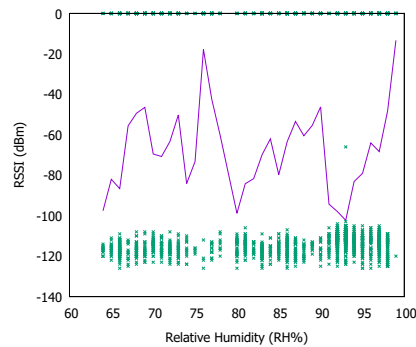


(d) RSSI and Relative Humidity 14-07-2014

Fig. 3.12 Analysis during the 14-07-2014 applying best line fit

On the 15th of July, 3.13a, the ground level xbee had cluster failures between 12 am and 4 pm during the day. We had a brief spell of rain during the early hours of the morning but there was no sign of packet drops during this time span. There was a rise in air pressure from 12 am to 2 pm and this usually represents unsettled weather - albeit improving - as air pressure remains constant for the rest of the day which at this point from 2 pm onwards, the ground level xbee node had fewer failures than the elevated xbee node. In observing air pressure in graph 3.13b, we saw that there was a large cluster of packets around 1016 hPa and 1017 hPa; this was a period when air pressure was becoming stable. In observing air temperature in graph 3.13c, we saw that there were more packet losses when temperature was less than 14 °C and packet losses oscillated with successful packets over the day. In observing graph 3.13d, packet drops oscillated between 37 % and 85 %.

A very weak positive correlation was found between air pressure and RSSI with a value of 0.16. A very weak negative correlation was found between temperature and RSSI with a value of -0.06. A very weak negative correlation was found between relative humidity and RSSI with a value of -0.02.

When calculating correlation and taking into account dropped packets, a very weak negative correlation was found between air pressure and RSSI with a value of -0.11. A very weak positive correlation between temperature and RSSI was found with a value of 0.05 and a very weak negative correlation was found between relative humidity and RSSI with a value of -0.02.
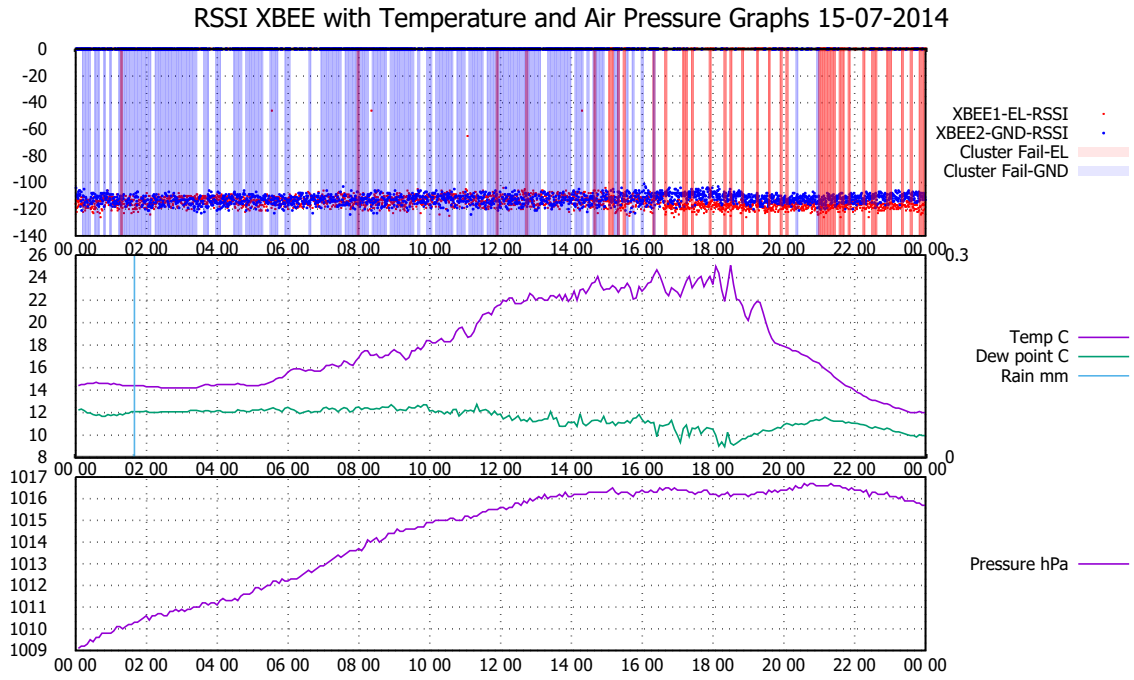
(a) Xbee1 as elevated and Xbee2 as Ground level 868 Mhz transceiver on 15-07-2014
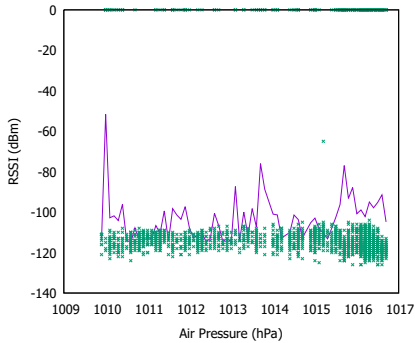


(b) RSSI and Air Pressure 15-07-2014
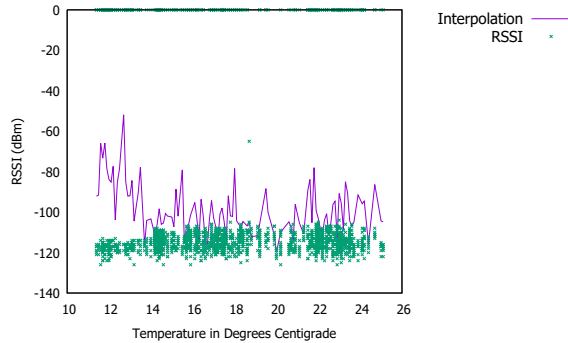


(c) RSSI and Air Temperature 15-07-2014
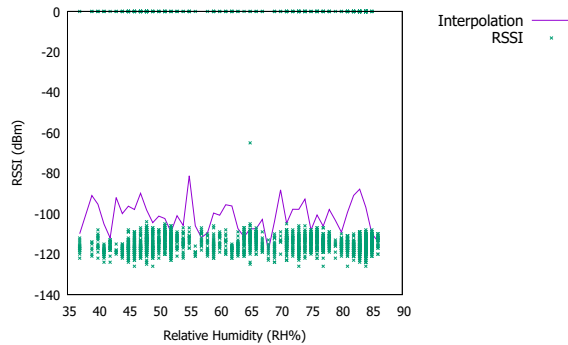


(d) RSSI and Relative Humidity 15-07-2014

Fig. 3.13 Analysis during the 15-07-2014 applying best line fit

On the 16th of July, 3.14a, relative humidity did not oscillate as much as in previous days and we saw failures occurring on both xbee nodes before 10 am. After 10 pm, we noticed that the ground level xbee RSSI improved but had more packet failures occurring than the elevated xbee node. During the afternoon, there was rain collected between 2 pm and 5 pm with no noticeable drops. Air pressure was erratic during the day oscillating from 1013.5 hPa to 1016 hPa throughout the day. In observing air pressure in graph 3.14b, we saw that packet reception was more stable at 1014 hPa to 1014.5 hPa which was a period of stability. As soon as air pressure starts to oscillate, we saw more packet failures at 1015 hPa which then became steady at around 1016.5 hPa. In observing air temperature in graph 3.14c, we observed that more packet reception failed at lower temperatures of less than 16 °C. Packet reception was steady between 16C and 21C which we saw a drop in packet reception when temperature exceeded 22 °C. In observing relative humidity in graph 3.14d, the line of best fit shows that RH% of less than 80 % had more failures when RH% was higher than 80 %.

A very weak positive correlation was found between air pressure and RSSI with a value of 0.09. A weak negative correlation was found between temperature and RSSI with a value of -0.21. A very weak positive correlation was found between relative humidity and RSSI with a value of 0.005.

When calculating correlation and taking into account dropped packets, a very weak positive correlation was found between air pressure and RSSI with a value of 0.01. A very weak positive correlation between temperature and RSSI was found with a value of 0.1 and a very weak positive correlation was found between relative humidity and RSSI with a value of 0.06.

RSSI XBEE with Temperature and Air Pressure Graphs 16-07-2014
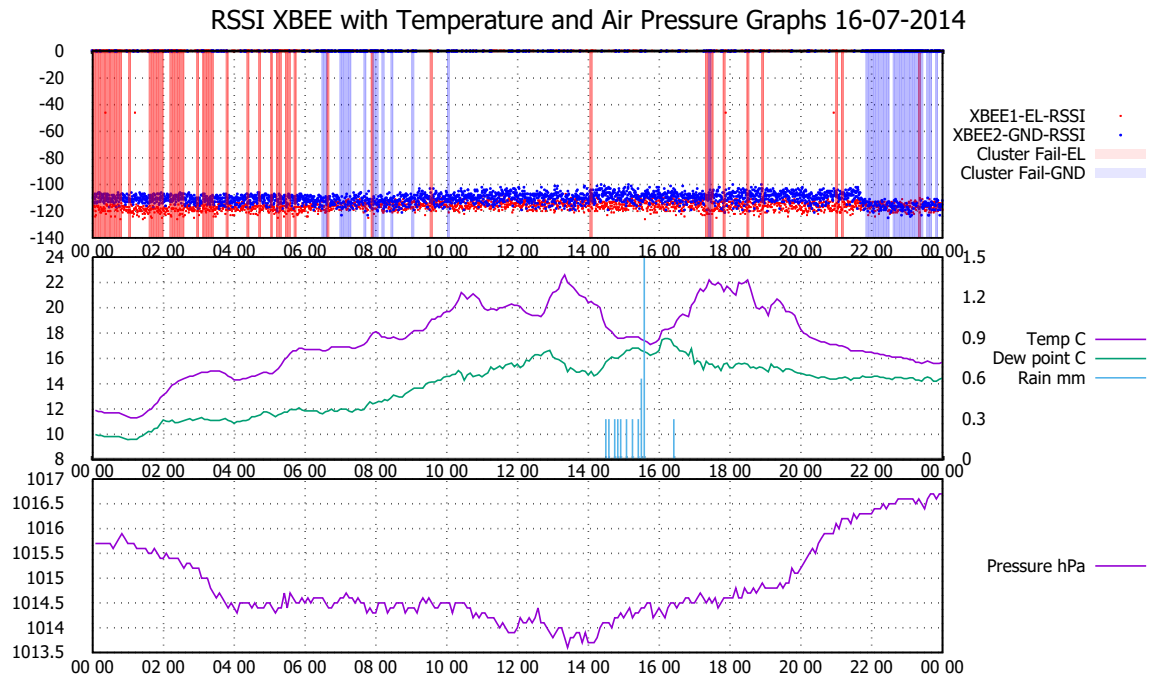
(a) Xbee1 as elevated and Xbee2 as Ground level 868 Mhz transceiver on 16-07-2014
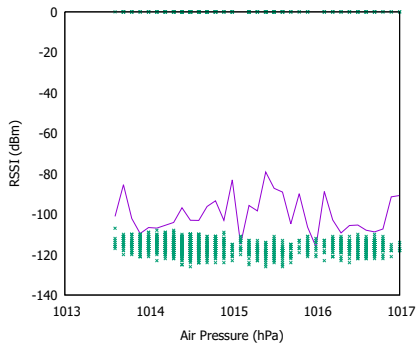
(b) RSSI and Air Pressure 16-07-2014
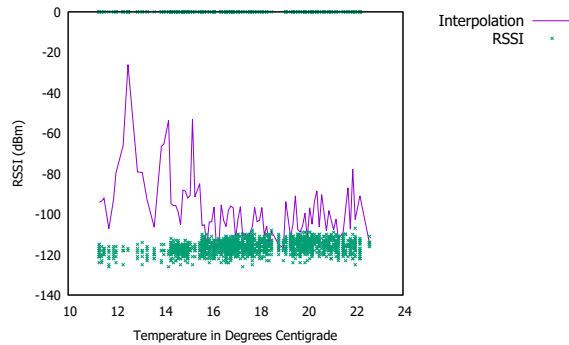
(c) RSSI and Air Temperature 16-07-2014
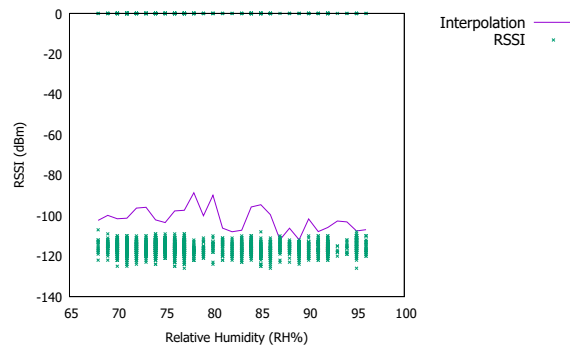
(d) RSSI and Relative Humidity 16-07-2014

Fig. 3.14 Analysis during the 16-07-2014 applying best line fit

On the 17th of July, 3.15a, the ground level xbee presented failures at around 8 am when humidity was dryer from the night. Relative humidity was low at around 40 % at around 6 pm with air temperature at 30 °C and dew point at 12 °C. During this time, we noticed that both xbee nodes had failures during the day, but later improved during the late evening. Air pressure oscillated during the day from 1014.5 hPa to a maximum of 1018.5 hPa with no rain collected during the day. In observing air pressure in graph 3.15b, there were packet losses at around 1016 hPa and 1016.5 hPa. This coincides when there was a drop in pressure during the afternoon. In observing air temperature in graph 3.15c, we observed that the majority of packet drops occurred when air temperature was over 28 °C which was around 6 pm and an improvement in RSSI signal at around 17 °C and 19 °C which was around 6 am and 7 am. In observing relative humidity in graph 3.15d, we observed that the RSSI signal improved when relative humidity was between 70 % and 80 %.

A very weak positive correlation was found between air pressure and RSSI with a value of 0.12. A very weak negative correlation was found between temperature and RSSI with a value of -0.12. A very weak positive correlation was found between relative humidity and RSSI with a value of 0.15.

When calculating correlation and taking into account dropped packets, a very weak positive correlation was found between air pressure and RSSI with a value of 0.06. A very weak negative correlation between temperature and RSSI was found with a value of -0.01 and a very weak positive correlation was found between relative humidity and RSSI with a value of 0.01.

RSSI XBEE with Temperature and Air Pressure Graphs 17-07-2014
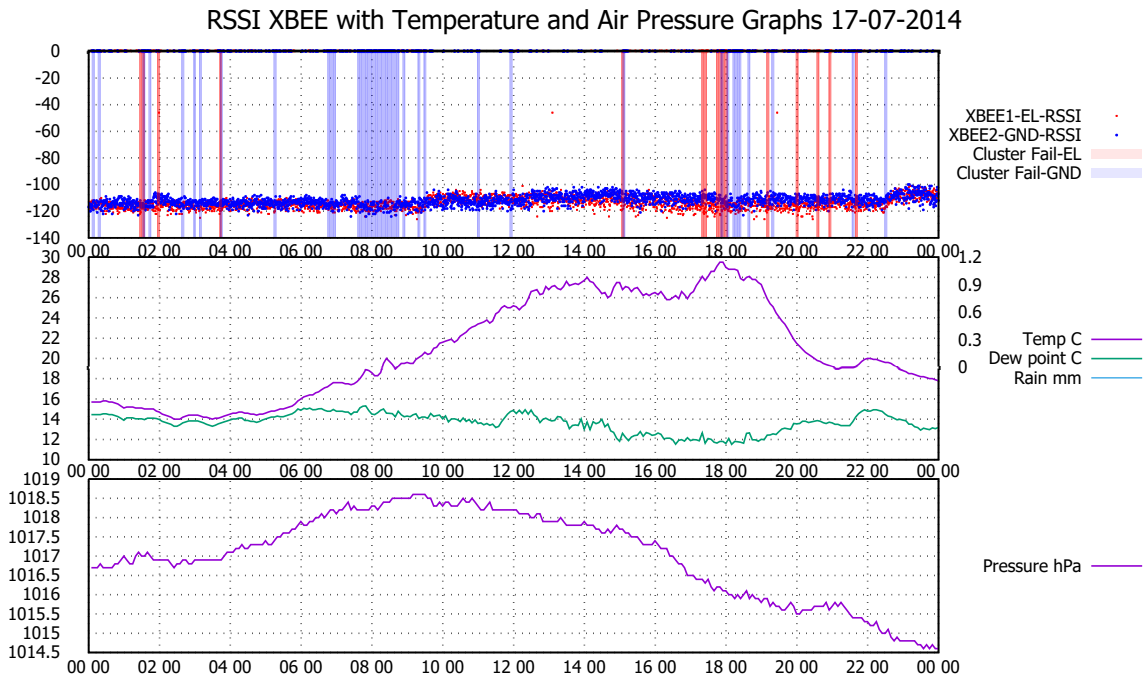


(a) Xbee1 as elevated and Xbee2 as Ground level 868 Mhz transceiver on 17-07-2014
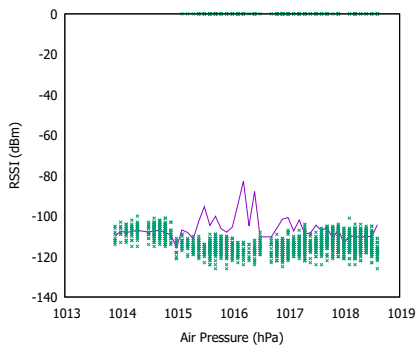


(b) RSSI and Air Pressure 17-07-2014
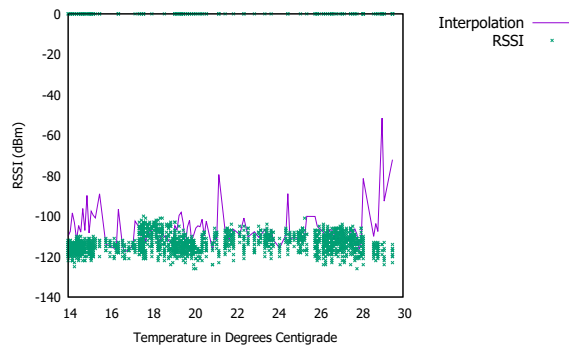


(c) RSSI and Air Temperature 17-07-2014
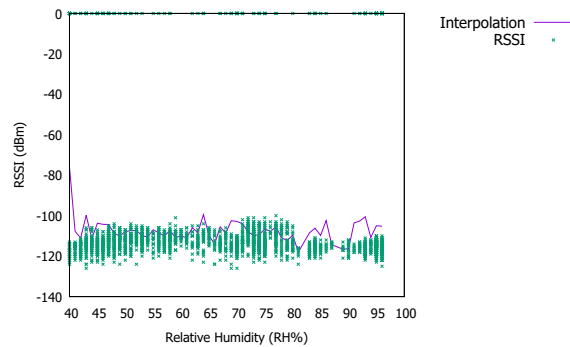


(d) RSSI and Relative Humidity 17-07-2014

Fig. 3.15 Analysis during the 17-07-2014 applying best line fit

On the 18th of July, 3.16a, only elevated xbee node data was collected. We observed a drop in air pressure from 1014.5 hPa to 1007.5 hPa signalling possible bad weather coming over the next day. Relative humidity was at around 60 % to 70 % between 12 pm and 6 pm rising to 90 % after 9 pm. In observing air pressure in graph 3.16b, we observed a series of packet drops from 1008 hPa to 1009.5 hPa which happened close to mid day. In graph 3.16c where we observed air temperature, we noticed that more failures occurred when temperatures were beyond 20 °C at around 10 am. More failures were seen at around 23 °C and 24 °C during 12 pm and 6 pm. In observing graph 3.16d, we observe that there was a drop in packets when RH% was 55 % and then again at around 73 % to 75 % of RH%.

A very weak negative correlation was found between air pressure and RSSI with a value of -0.02. A very weak positive correlation was found between temperature and RSSI with a value of 0.14. A very weak negative correlation was found between relative humidity and RSSI with a value of -0.19.

When calculating correlation and taking into account dropped packets, a very weak negative correlation was found between air pressure and RSSI with a value of -0.0009. A very weak negative correlation between temperature and RSSI was found with a value of -0.02 and a very weak positive correlation was found between relative humidity and RSSI with a value of 0.05.

RSSI XBEE with Temperature and Air Pressure Graphs 18-07-2014
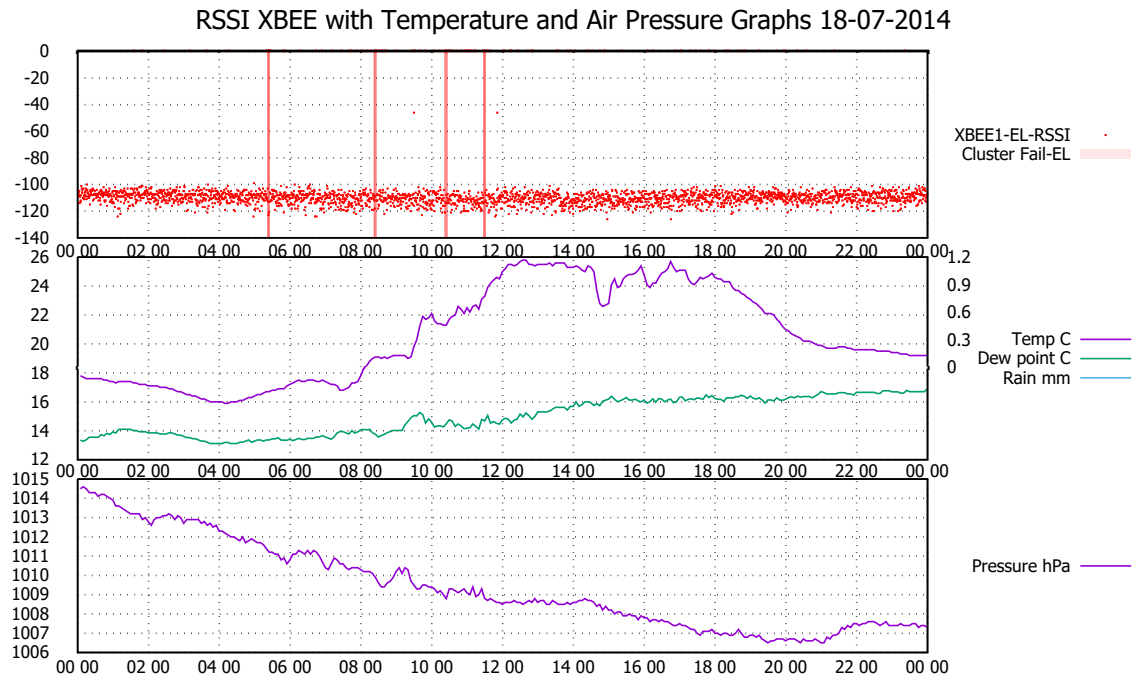
(a) Xbee1 as elevated 868 Mhz transceiver on 18-07-2014
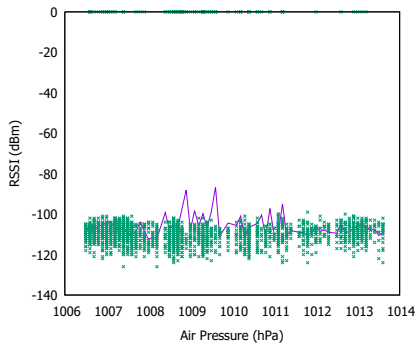
(b) RSSI and Air Pressure 18-07-2014        (c) RSSI and Air Temperature 18-07-2014
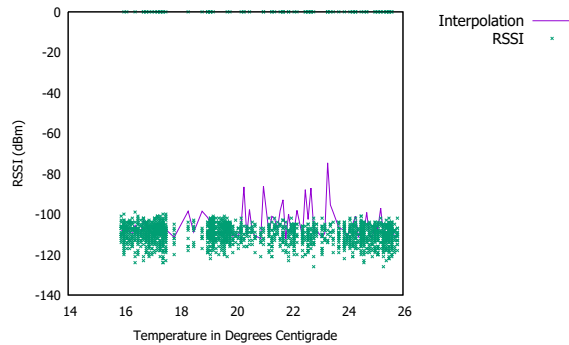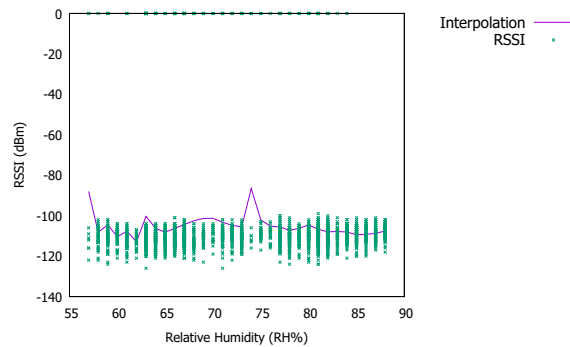
(d) RSSI and Relative Humidity 18-07-2014

Fig. 3.16 Analysis during the 18-07-2014 applying best line fit

On the 19th of July, 3.17a, the ground floor xbee had a new battery installed after 2 am. The elevated xbee had few failures during the day, but the ground level xbee node had more failures during the early morning between 6 am and 10 am, during the afternoon at around 2 pm and evening after 8 pm. Weather was unsettled as predicted by the air pressure drop from the previous day and there was scattered showers during the morning, mid day and evening. Air pressure was erratic during the day, although air pressure was going down at around 1005 hPa. We observed that humidity levels were high during the night approaching 99 % after 10 pm whereas during the day at around 5 pm, it was around 79 % of RH%. On observing graph 3.17b, air pressure between 1003.5 hPa and 1004.5 hPa showed a weakened RSSI signal and this was a period of instability between noon and 6 pm. In observing temperature in graph 3.17c, we observed a weakening in signal strength between 18 °C and 21 °C with some packet losses within this range. In observing graph 3.17d, there was a weakening of signal strength at 89 % of RH% followed by an improvement in signal strength at around 91 % RH%.

A weak negative correlation was found between air pressure and RSSI with a value of -0.22. A very weak negative correlation was found between temperature and RSSI with a value of -0.14. A very weak positive correlation was found between relative humidity and RSSI with a value of 0.17.

When calculating correlation and taking into account dropped packets, a very weak negative correlation was found between air pressure and RSSI with a value of -0.11. A very weak negative correlation between temperature and RSSI was found with a value of -0.09 and a very weak positive correlation was found between relative humidity and RSSI with a value of 0.1.
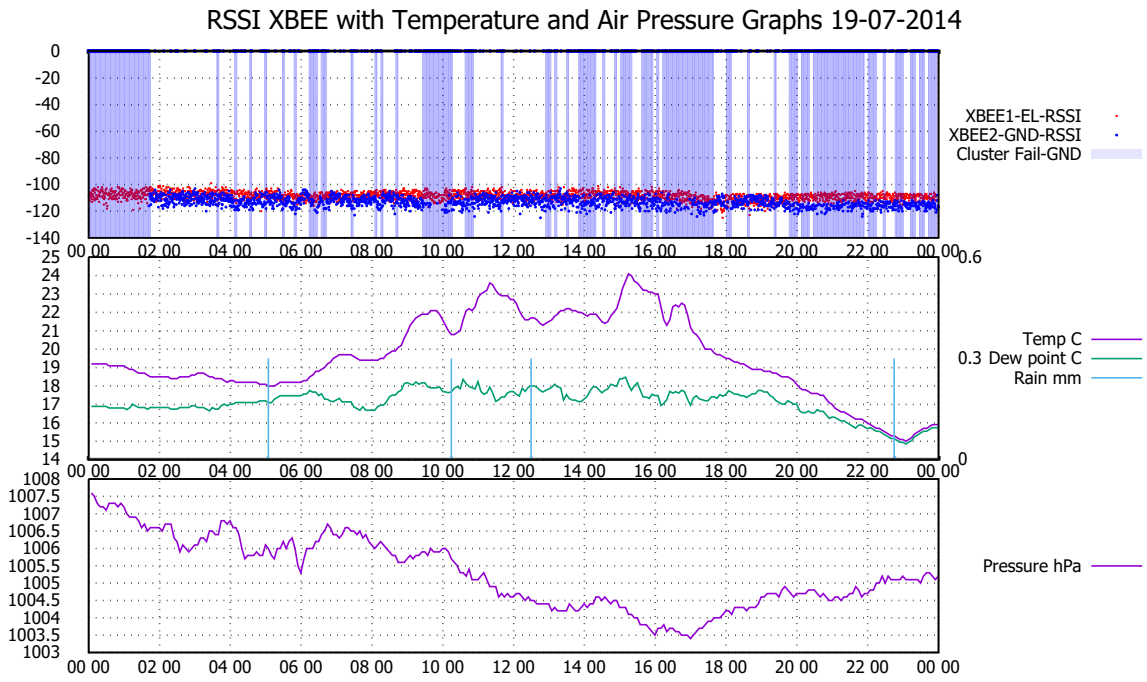
(a) Xbee1 as elevated and Xbee2 as Ground level 868 Mhz transceiver on 19-07-2014
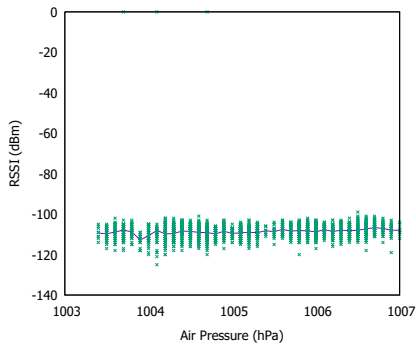


(b) RSSI and Air Pressure 19-07-2014
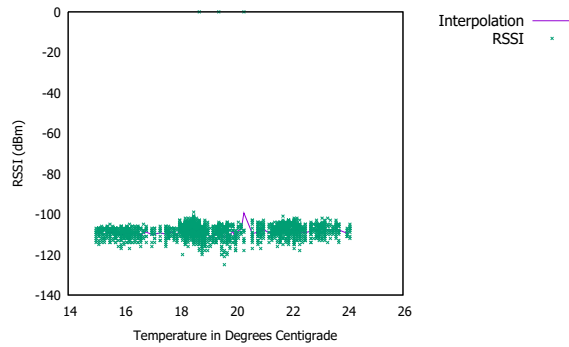


(c) RSSI and Air Temperature 19-07-2014
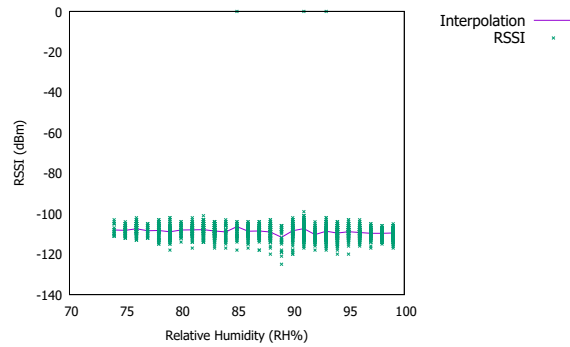


(d) RSSI and Relative Humidity 19-07-2014

Fig. 3.17 Analysis during the 19-07-2014 applying best line fit

On the the 20th of July, 3.18a, we observed air pressure was rising steadily throughout the day which signals that a possible heat wave is arriving. At around 8 am, we notice a slight drop in RSSI signal on the ground level although packet failures are fewer after this time. Air remains to be dry during the day with humidity ranging between 65 % and 75 % during the afternoon although humidity remains very high during the night at over 90 %. Intermittent failures were observed during the day for the ground level xbee and few failures occurring for the elevated xbee node. In observing graph 3.18b, we saw that data packet drops occurred between 1007 hPa and 1011 hPa as air pressure was rising steadily. We then saw in graph 3.18b, data packets dropped when air temperature was over 16 °C and worsened as it became warmer as it peaked close to 24 °C. In observing graph 3.18d, we notice that there were more packet drops when the air was dryer at 83 % and below. There were fewer packet drops when relative humidity was greater than 85 % and improved when at 98 % of relative humidity.

A weak positive correlation was found between air pressure and RSSI with a value of 0.28. A weak positive correlation was found between temperature and RSSI with a value of 0.36. A moderate negative correlation was found between relative humidity and RSSI with a value of -0.45.

When calculating correlation and taking into account dropped packets, a very weak negative correlation was found between air pressure and RSSI with a value of -0.02. A very weak negative correlation between temperature and RSSI was found with a value of -0.08 and a very weak positive correlation was found between relative humidity and RSSI with a value of 0.09.
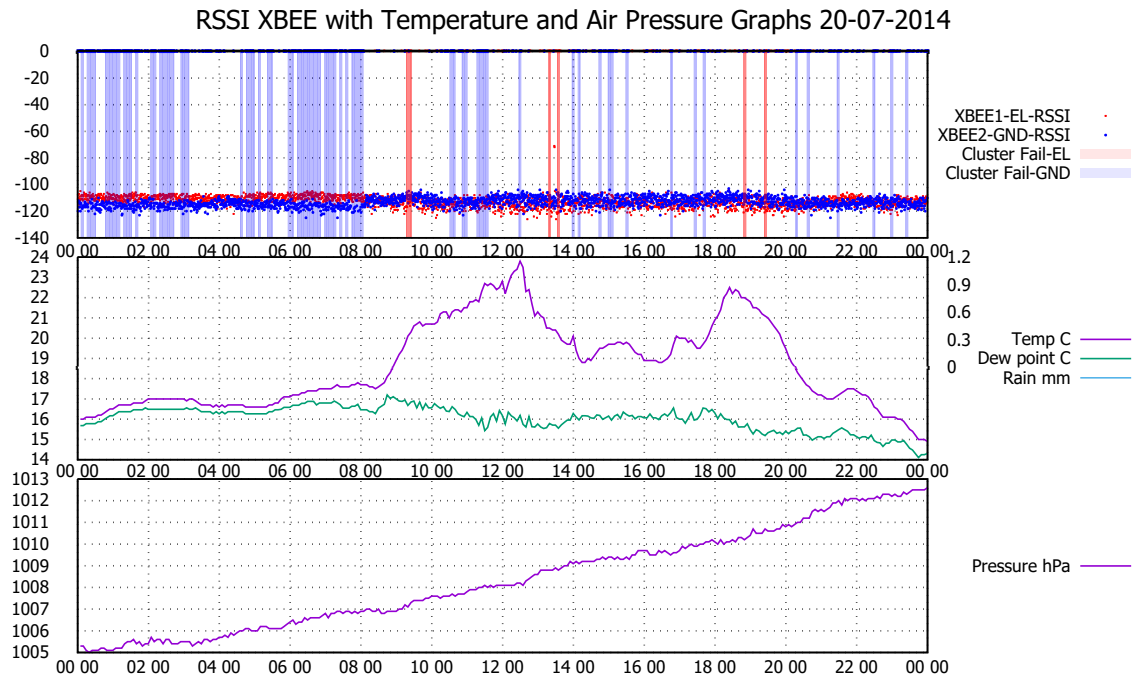
(a) Xbee1 as elevated and Xbee2 as Ground level 868 Mhz transceiver on 20-07-2014
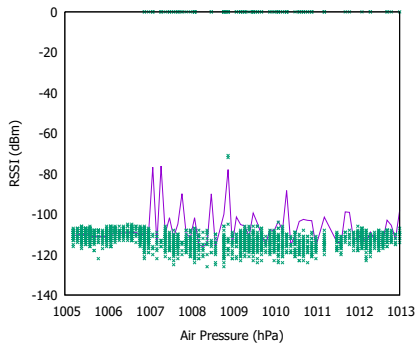


(b) RSSI and Air Pressure 20-07-2014
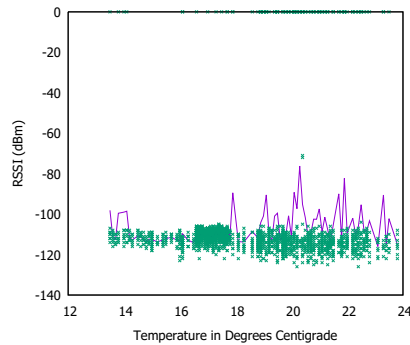


(c) RSSI and Air Temperature 20-07-2014
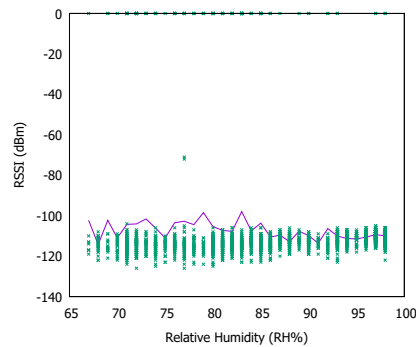


(d) RSSI and Relative Humidity 20-07-2014

Fig. 3.18 Analysis during the 20-07-2014 applying best line fit

On the 21st of July, 3.19a, as previously predicted on the 20th, a heat wave was approaching and we saw very dry and warm conditions during the day time where it peaked at around 46 % of RH% at 6 pm. We also observed that before 7 am, RH% was very high at almost 99% and more failures started to occur on the ground level when the air was dry and the sun was at its highest peak. During the afternoon, we observed that there were more failures between 12 pm and 7 pm and no failures were seen after this time. In observing graph 3.19b, we saw that air pressure rose steadily throughout the day and packet drops occurred between 1017 hPa and 1018.5 hPa. We do see also that RSSI was weaker between 1015.5 hPa and 1018 hPa. In observing graph 3.19c, packet drops occurred when the air temperature rose to 20 °C and worsened when it reached 26 °C. In observing RH% in graph 3.19d, we observed that more packets drops occurred when the air was dry at 46 % and up to 68 %. No packet drops occurred when relative humidity was close to 99 %.

A weak positive correlation was found between air pressure and RSSI with a value of 0.34. A moderate positive correlation was found between temperature and RSSI with a value of 0.44. A moderate negative correlation was found between relative humidity and RSSI with a value of -0.48.

When calculating correlation and taking into account dropped packets, a very weak negative correlation was found between air pressure and RSSI with a value of -0.12. A weak negative correlation between temperature and RSSI was found with a value of -0.27 and a weak positive correlation was found between relative humidity and RSSI with a value of 0.28.
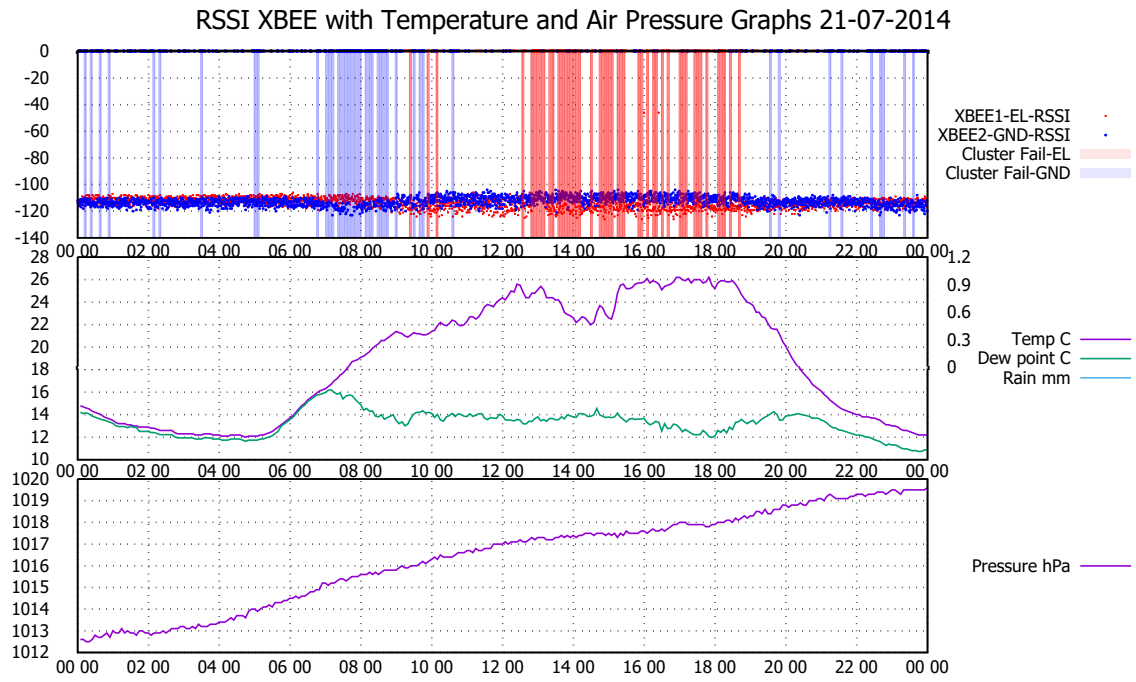
(a) Xbee1 as elevated and Xbee2 as Ground level 868 Mhz transceiver on 21-07-2014
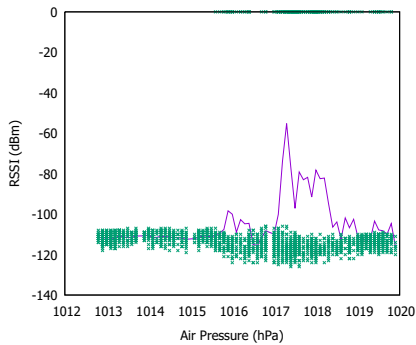


(b) RSSI and Air Pressure 21-07-2014
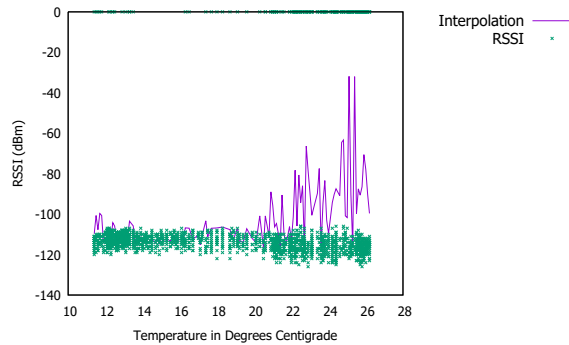


(c) RSSI and Air Temperature 21-07-2014
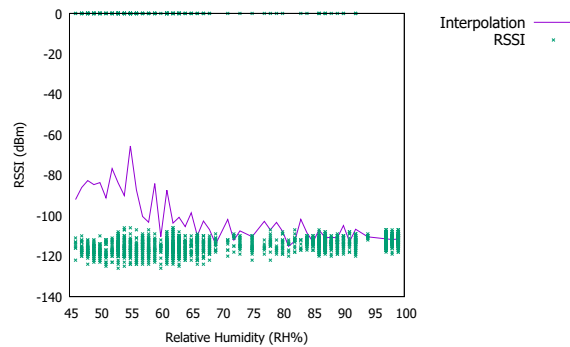


(d) RSSI and Relative Humidity 21-07-2014

Fig. 3.19 Analysis during the 21-07-2014 applying best line fit

On the 22nd of July, in graph 3.20a, we continue to see the same trend as on the 21st of July with the heat wave peaking at around 30C between 3 pm and 5:30 pm. We observed large cluster failures on the elevated xbee node when air temperature rose at around 10 am to 7 pm. The ground level xbee node had failures most notably during the night before 8 am when humidity was high after 11 pm. Air pressure oscillated between high pressures of 1019.5 hPa to 1021 hPa which gives an indication that the heat wave was present. In observing graph 3.20b, air pressure was unstable and packet drops occurred when air pressure was greater than 1020 hPa. In graph 3.20c, packet drops occurred when temperature exceeded 21 °C. In graph 3.20d, packet drops occurred when relative humidity was less than 70 % but improved when relative humidity rose to 99 %.

A very weak negative correlation was found between air pressure and RSSI with a value of -0.06. A weak positive correlation was found between temperature and RSSI with a value of 0.21. A weak negative correlation was found between relative humidity and RSSI with a value of -0.22.

When calculating correlation and taking into account dropped packets, a very weak negative correlation was found between air pressure and RSSI with a value of -0.07. A weak negative correlation between temperature and RSSI was found with a value of -0.32 and a weak positive correlation was found between relative humidity and RSSI with a value of 0.33.
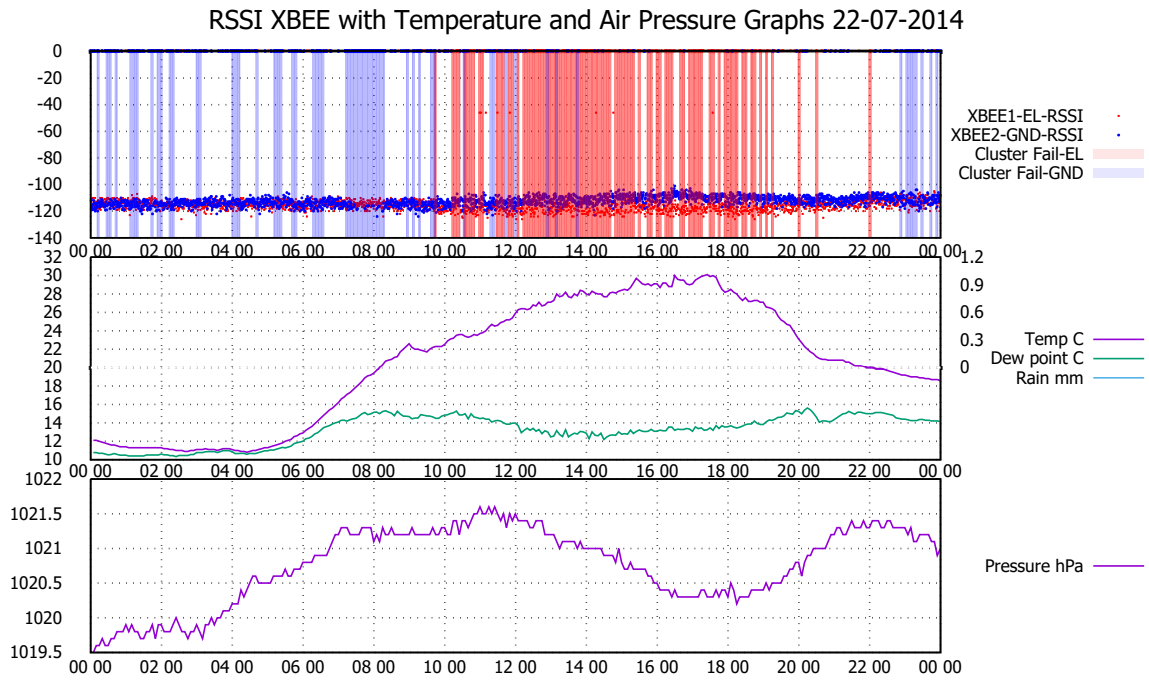
(a) Xbee1 as elevated and Xbee2 as Ground level 868 Mhz transceiver on 22-07-2014
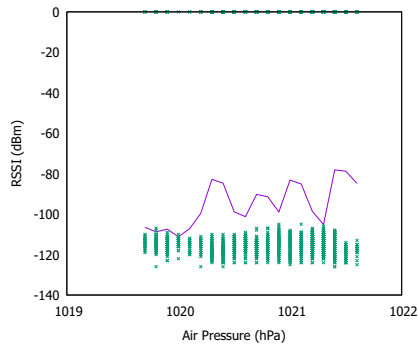


(b) RSSI and Air Pressure 22-07-2014
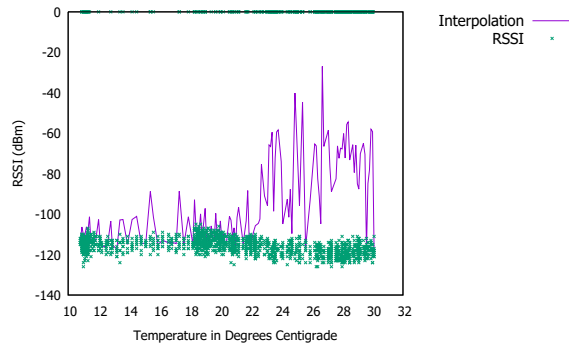


(c) RSSI and Air Temperature 22-07-2014
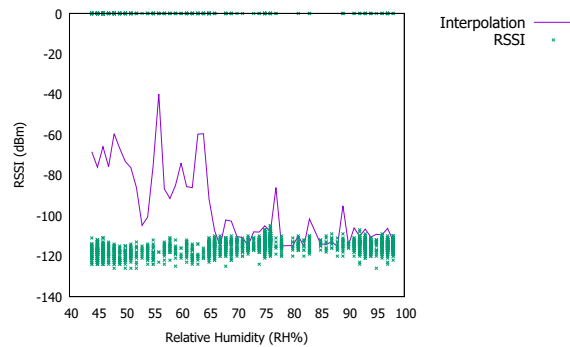


(d) RSSI and Relative Humidity 22-07-2014

Fig. 3.20 Analysis during the 22-07-2014 applying best line fit

On the 23rd of July, 3.21a, we observed that air pressure drops slightly from 1021 hPa to 1017 hPa. The heat wave was present as temperatures peaked over 30 °C between 1 pm and 5 pm. We saw a number of failures occur during the evening on the elevated xbee node, but not as many as observed on the 22nd of July which was predominant during the afternoon. There was a brief spell of rain of 0.3mm collected which had negligible change on RSSI on both radio nodes. In graph 3.21b, packet drops occurred when air pressure was below 1018.5 hPa. In observing air temperature in graph 3.21c, packet drops were between 16C and 20C and more drops occurred when air temperature reached between 28 °C and 30 °C range. In graph 3.21d, signal strength was weaker when RH% was below 45 %. We saw packet drops at around 60 % and 75 % of RH%.

A very weak negative correlation was found between air pressure and RSSI with a value of -0.09. A very weak positive correlation was found between temperature and RSSI with a value of 0.18. A very weak negative correlation was found between relative humidity and RSSI with a value of -0.17.

When calculating correlation and taking into account dropped packets, a very weak positive correlation was found between air pressure and RSSI with a value of 0.08. A very weak negative correlation between temperature and RSSI was found with a value of -0.02 and a very weak positive correlation was found between relative humidity and RSSI with a value of 0.03.
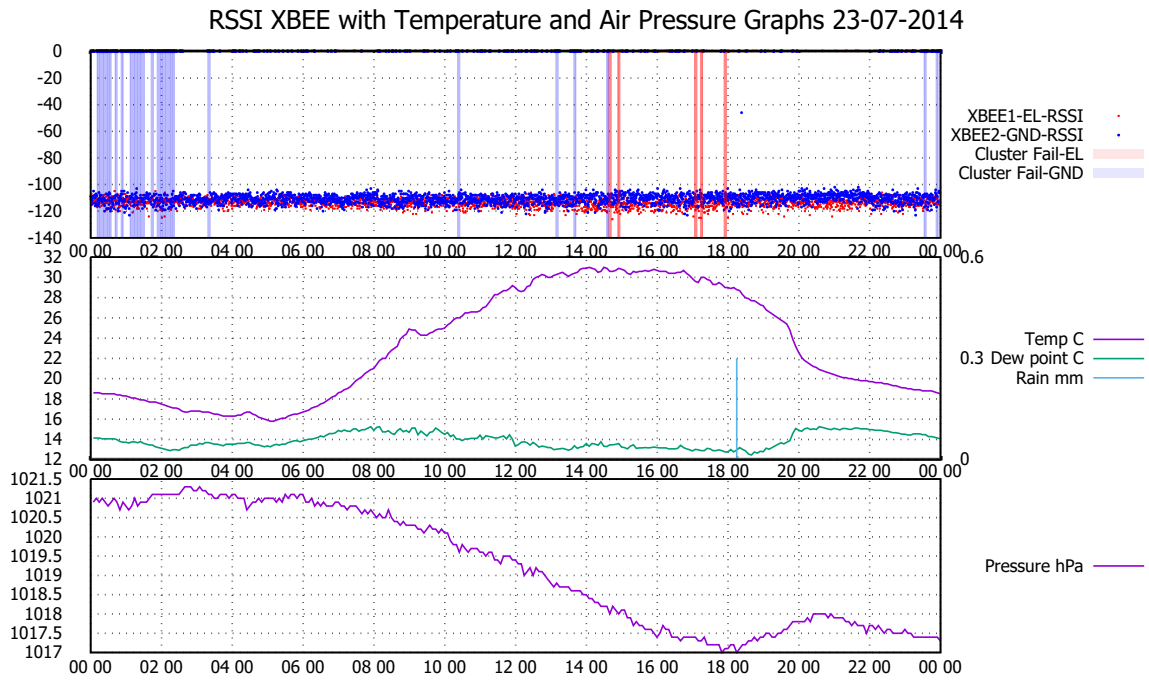
(a) Xbee1 as elevated and Xbee2 as Ground level 868 Mhz transceiver on 23-07-2014
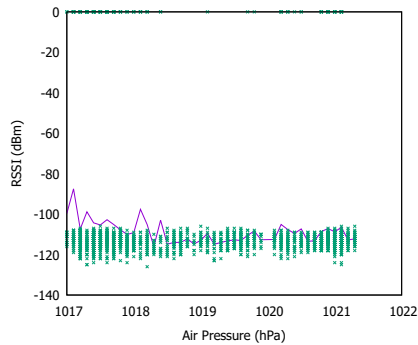


(b) RSSI and Air Pressure 23-07-2014
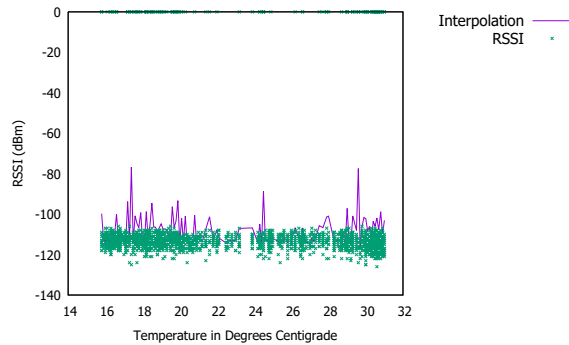


(c) RSSI and Air Temperature 23-07-2014
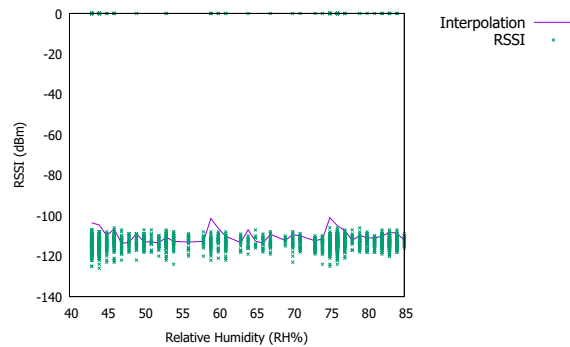


(d) RSSI and Relative Humidity 23-07-2014

Fig. 3.21 Analysis during the 23-07-2014 applying best line fit

On the 24th of July 2014 in graph 3.22a, we observed few packet losses during the day although we can appreciate an improvement on RSSI in both nodes between 3 am and 7 am. During these hours, the sun will rise at approximately 4 am and humidity was high at around 76 % of RH% (13C dew point and 17 °C air temperature at around 4 am). Air pressure was relatively steady oscillating from 1015.5 hPa to almost 1018 hPa. We saw a series of failures during the day from the elevated radio transceiver from 10:30 am to 4:30 pm which are the hours that the sun is present and temperature was very high peaking at 33 °C. As soon as the air temperature cooled down at 6 pm and humidity levels was rising, there was a slight improvement on RSSI in the elevated and ground xbee nodes. In graph 3.22b, signal strength weakened slightly when air pressure was around 1017.5 hPa. We see in graph 3.22c, most packet drops occurred at around 28 °C and 30 °C although drops happened when air temperature was over 20 °C and we saw that the interpolation line oscillates. In graph 3.22d, the interpolation line lies between the data sets between signal strength values of -100 dBm and -125 dBm .

A very weak positive correlation was found between air pressure and RSSI with a value of 0.1. A weak positive correlation was found between temperature and RSSI with a value of 0.27. A weak negative correlation was found between relative humidity and RSSI with a value of -0.29.

When calculating correlation and taking into account dropped packets, a very weak negative correlation was found between air pressure and RSSI with a value of -0.03. A very weak negative correlation between temperature and RSSI was found with a value of -0.01 and a very weak positive correlation was found between relative humidity and RSSI with a value of 0.01.
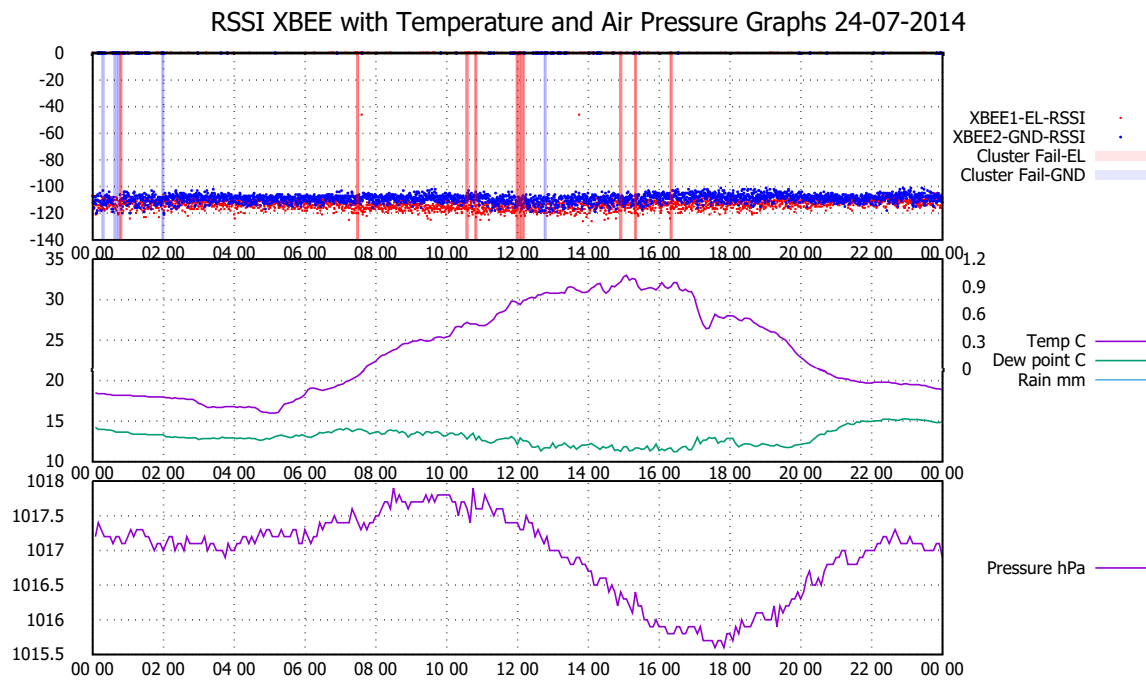
(a) Xbee1 as elevated and Xbee2 as Ground level 868 Mhz transceiver on 24-07-2014
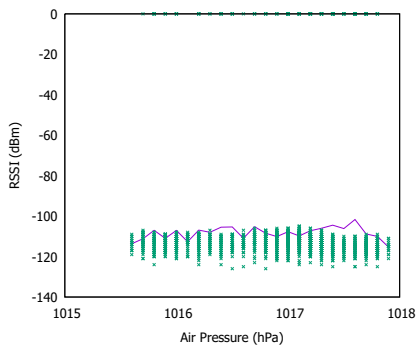


(b) RSSI and Air Pressure 24-07-2014
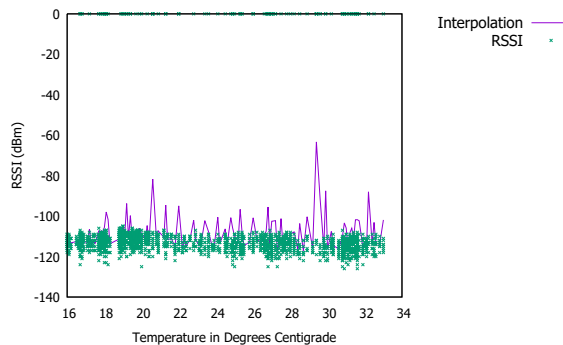


(c) RSSI and Air Temperature 24-07-2014
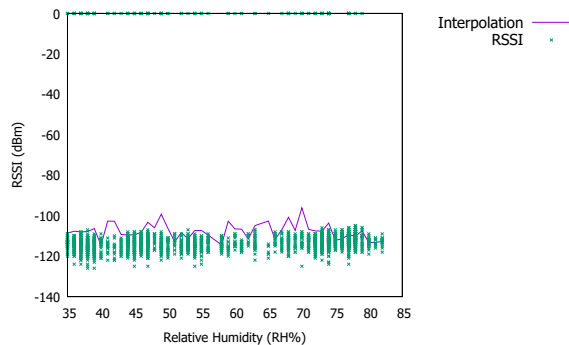


(d) RSSI and Relative Humidity 24-07-2014

Fig. 3.22 Analysis during the 24-07-2014 applying best line fit

On the 26th of July, 3.23a, air pressure was starting to lower from 1015.5 hPa to 1013 hPa and then rising back up to around 1014 hPa at around 6 pm. Failures on the elevated xbee node was observed at around 2 pm to 6 pm where temperature remains to be high between 23 °C to 27 °C. The RSSI on both nodes seem to improve for the ground level xbee node, but the xbee node that is elevated gets worse and the ground level xbee node improves during 2 pm and 10 pm. We also observed heavy rain after 9pm and we see humidity rising to almost 99 % where failures have occurred on the elevated xbee node. After 10 pm, we saw that the RSSI on the elevated xbee node improved and the RSSI on the ground level xbee gets worsens.

In graph 3.23b, we observe that there have been packet drops when air pressure was below 1014 hPa. In graph 3.23c, packet drops occurred when air temperature was between 16 °C and 19 °C and when air temperature was above 22C. In graph 3.23d, we saw more data packet drops from 40 % to 75 % although there were packet drops when RH% reached 92%.

A weak negative correlation was found between air pressure and RSSI with a value of -0.36. A weak positive correlation was found between temperature and RSSI with a value of 0.31. A weak negative correlation was found between relative humidity and RSSI with a value of -0.24.

When calculating correlation and taking into account dropped packets, a very weak positive correlation was found between air pressure and RSSI with a value of 0.16. A very weak negative correlation between temperature and RSSI was found with a value of -0.07 and a very weak positive correlation was found between relative humidity and RSSI with a value of 0.02.
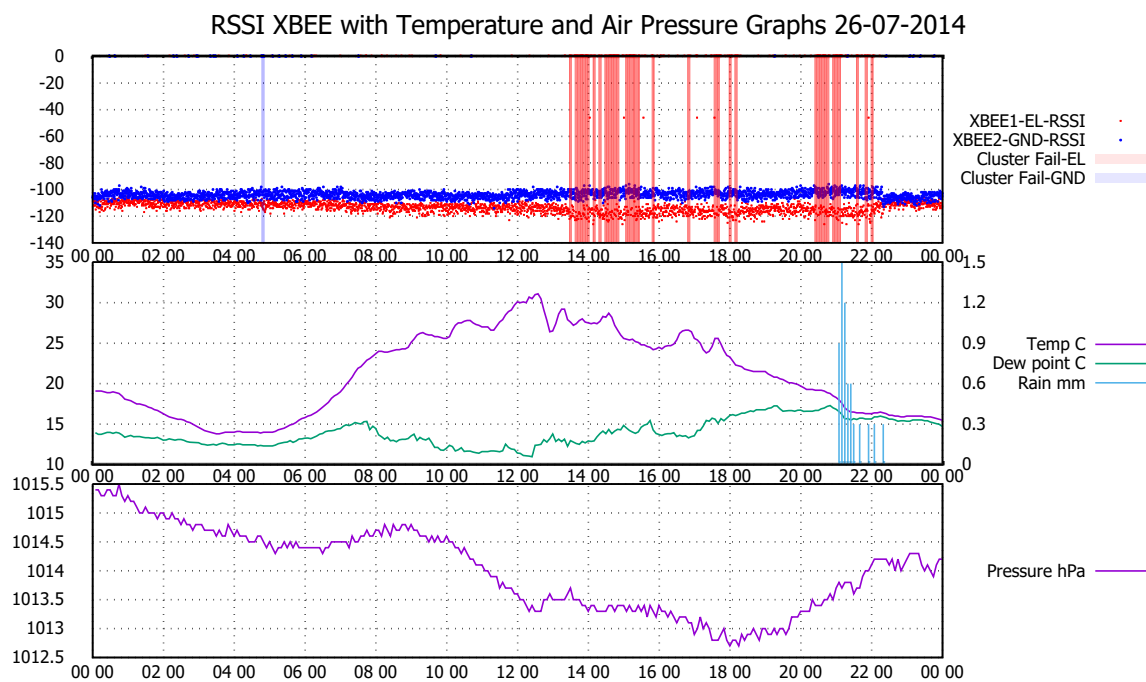
(a) Xbee1 as elevated and Xbee2 as Ground level 868 Mhz transceiver on 26-07-2014
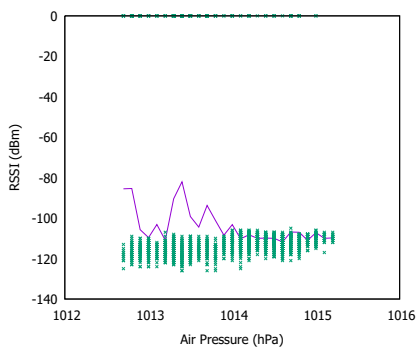


(b) RSSI and Air Pressure 26-07-2014
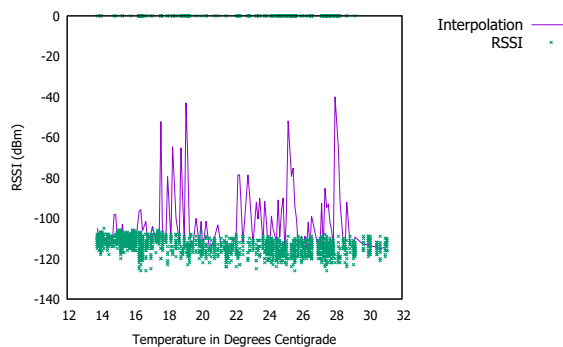


(c) RSSI and Air Temperature 26-07-2014
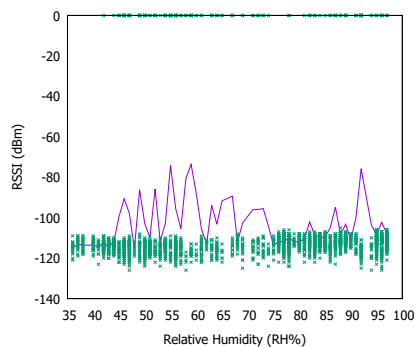


(d) RSSI and Relative Humidity 26-07-2014

Fig. 3.23 Analysis during the 26-07-2014 applying best line fit

On the 27th of July, 3.24a, we observed air pressure remaining steady until 12 pm which brought unsettled brief showers between 1 pm and 2 pm, and between 6 pm and 7 pm and then rains again near 12 pm. RSSI from the elevated xbee node worsens at around 8am which has more variable during the day and improves at night at around 8 pm when temperatures gradually cool down and relative humidity rises to around 80 %. We do see some packet drops occur when air temperature was between 14 °C and 15 °C and when greater than 18 °C.

A weak positive correlation was found between air pressure and RSSI with a value of 0.24. A weak positive correlation was found between temperature and RSSI with a value of 0.35. A weak negative correlation was found between relative humidity and RSSI with a value of -0.35.

When calculating correlation and taking into account dropped packets, a very weak negative correlation was found between air pressure and RSSI with a value of -0.003. A very weak negative correlation between temperature and RSSI was found with a value of -0.06 and a very weak positive correlation was found between relative humidity and RSSI with a value of 0.05.

RSSI XBEE with Temperature and Air Pressure Graphs 27-07-2014
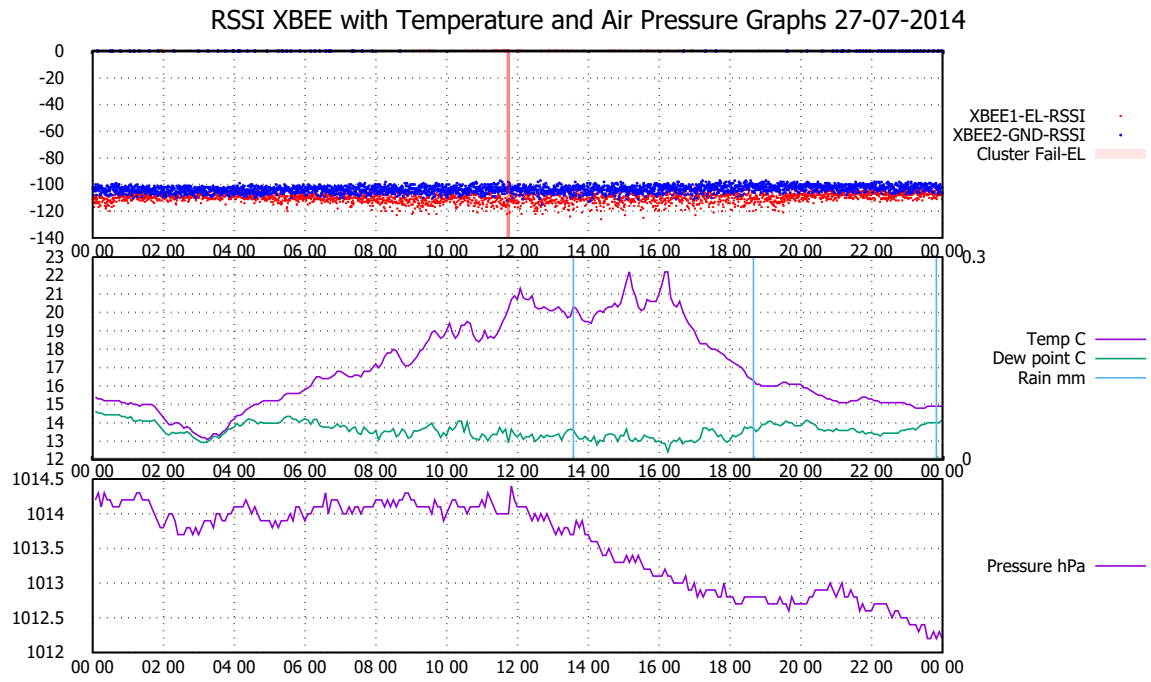


(a) Xbee1 as elevated and Xbee2 as Ground level 868 Mhz transceiver on 27-07-2014
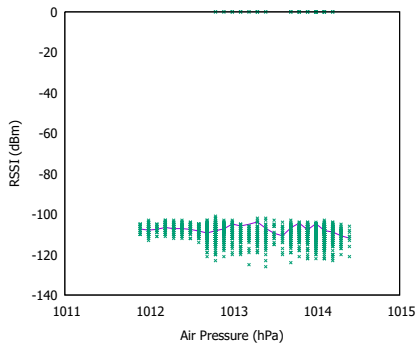


(b) RSSI and Air Pressure 27-07-2014
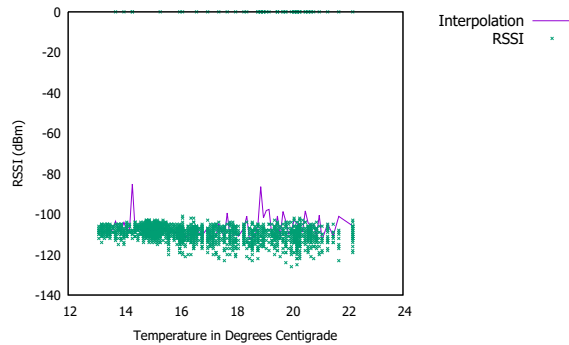


(c) RSSI and Air Temperature 27-07-2014
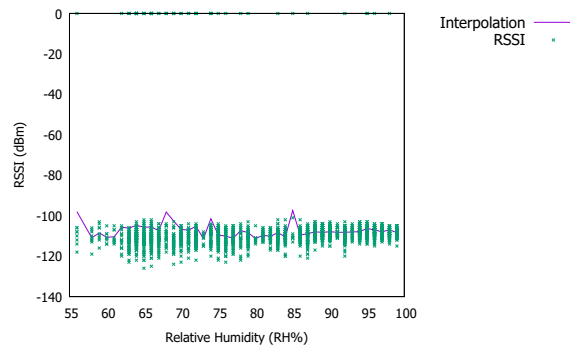


(d) RSSI and Relative Humidity 27-07-2014

Fig. 3.24 Analysis during the 27-07-2014 applying best line fit

On the 28th of July, 3.25a, we observed during the early morning early showers between 12 am and 2 am, we observed some packet losses for the ground level xbee with no large cluster failures, but the elevated xbee node had no failures during this time. Air pressure rose from 1012 hPa to around 1015 hPa and we observed that during the afternoon, the elevated xbee node RSSI strength suffered from 11 am until 9 pm which at this time, RSSI strength improved. Some packet losses occurred between 6pm and 7 pm for the elevated xbee node when temperatures were high at around 24 °C and 26 °C and RH% at around 46 %. In graph 3.25b, we saw that signal strength was weaker when air pressure was at 1014.5 hPa which then improved as pressure increased during the day. In observing air temperature, we saw that there were packet failures when temperatures reached 25 °C. We can also see that signal strength improves when it is colder. In graph 3.25d, we saw that there were packet drops when relative humidity was below 55% and we observed the same pattern from air temperature; as RH% increases, signal strength is improved.

A weak positive correlation was found between air pressure and RSSI with a value of 0.23. A moderate positive correlation was found between temperature and RSSI with a value of 0.46. A moderate negative correlation was found between relative humidity and RSSI with a value of -0.48.

When calculating correlation and taking into account dropped packets, a very weak negative correlation was found between air pressure and RSSI with a value of -0.006. A very weak positive correlation between temperature and RSSI was found with a value of 0.008 and a very weak negative correlation was found between relative humidity and RSSI with a value of -0.01.
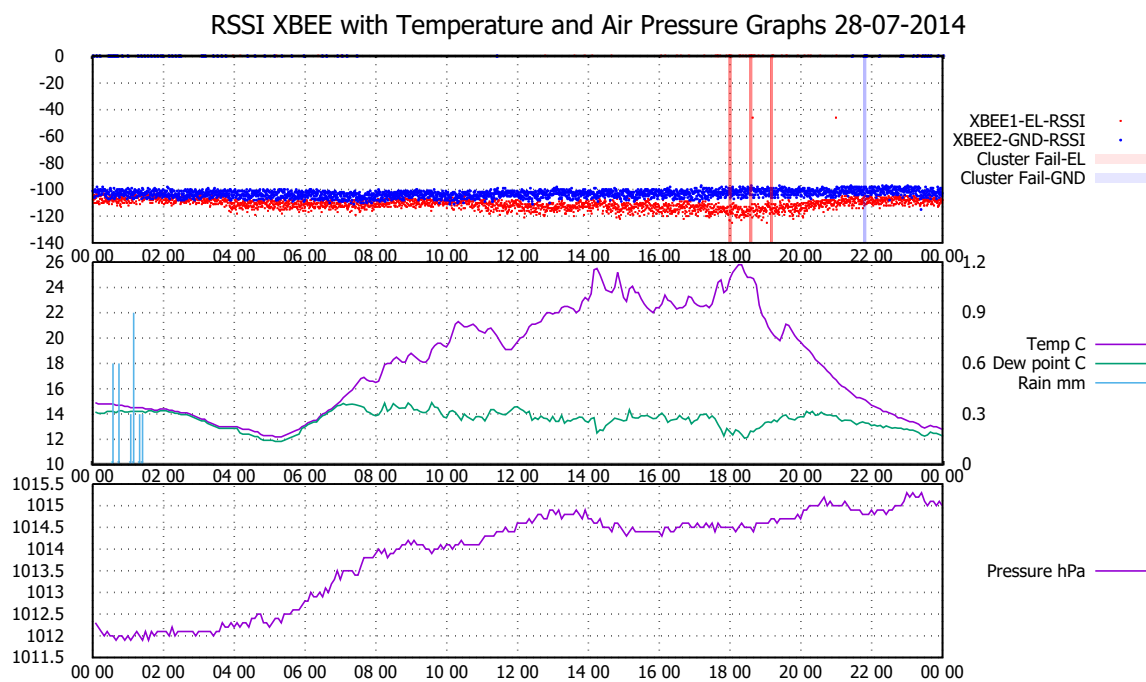
(a) Xbee1 as elevated and Xbee2 as Ground level 868 Mhz transceiver on 28-07-2014
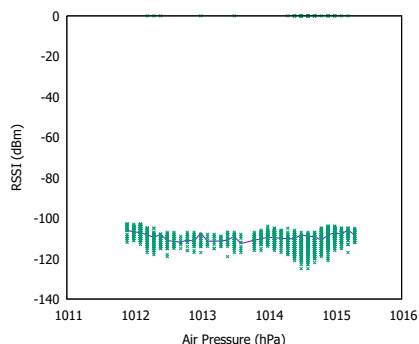


(b) RSSI and Air Pressure 28-07-2014
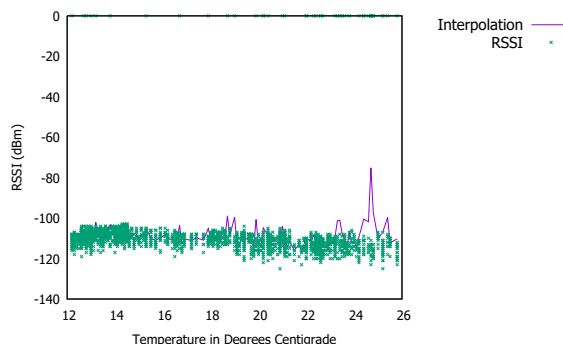


(c) RSSI and Air Temperature 28-07-2014
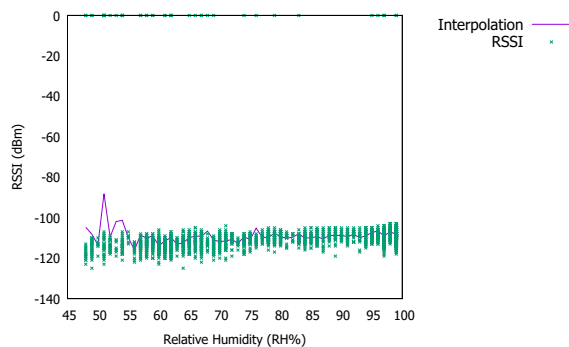


(d) RSSI and Relative Humidity 28-07-2014

Fig. 3.25 Analysis during the 28-07-2014 applying best line fit

On the 29th of July, 3.26a, air pressure started to drop throughout the day from 1015 hPa to 1013 hPa and relative humidity remained between 95 % and 99 % during the early hours of the morning between 12 am and 7 am. Air temperature oscillated during the day and we noticed a brief improvement in RSSI for the elevated xbee node between 2 pm and 4 pm where afterwards, we observed that signal strength weakened as it was before 2 pm. After 5pm, we observed multiple failures for the elevated xbee node which continued into the night. We noticed that humidity was dryer than it was in the morning at around 70 % to 80 % after 8 pm. In observing graph 3.26b, there were packet drops when air pressure was below 1013.5 hPa. We observed that as air pressure decreases, signal strength becomes weaker. In observing air temperature in 3.26c, we observed that packet failures occurred when temperatures reached 16 °C with signal strength worsening as temperature increased. In observing relative humidity in 3.26d, we observe that there were packet drops when humidity was less than 80 % with some instability happening at around 65 % to 70 % relative humidity.

A moderate negative correlation was found between air pressure and RSSI with a value of -0.43. A very weak positive correlation was found between temperature and RSSI with a value of 0.17. A weak negative correlation was found between relative humidity and RSSI with a value of -0.33.

When calculating correlation and taking into account dropped packets, a very weak positive correlation was found between air pressure and RSSI with a value of 0.19. A very weak negative correlation between temperature and RSSI was found with a value of -0.05 and a very weak positive correlation was found between relative humidity and RSSI with a value of 0.15.
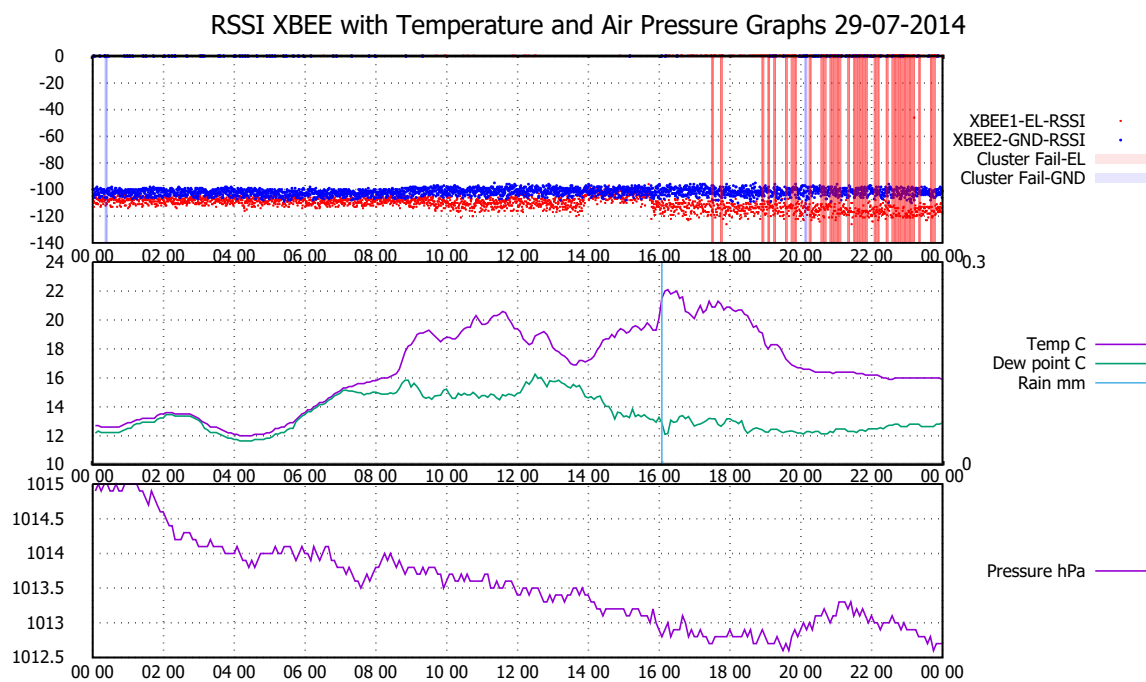
(a) Xbee1 as elevated and Xbee2 as Ground level 868 Mhz transceiver on 29-07-2014
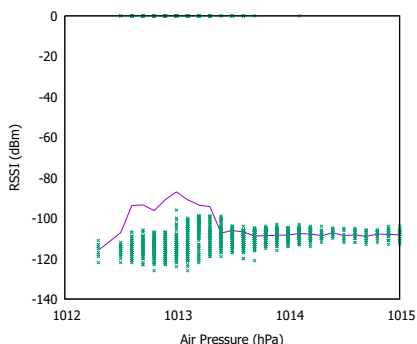
(b) RSSI and Air Pressure 29-07-2014          (c) RSSI and Air Temperature 29-07-2014
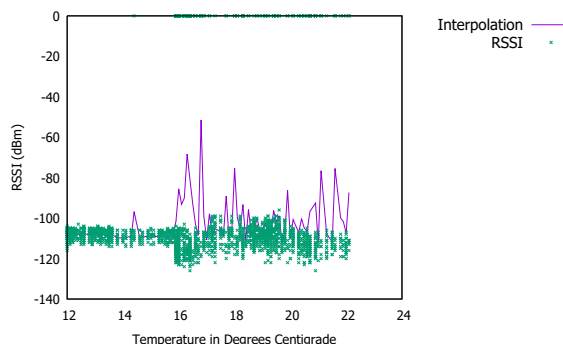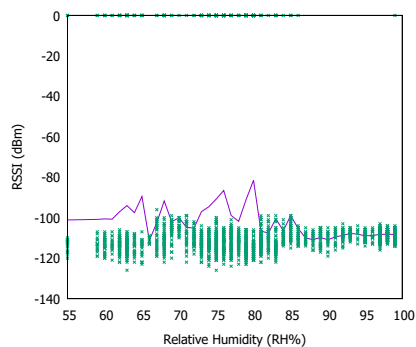
(d) RSSI and Relative Humidity 29-07-2014

Fig. 3.26 Analysis during the 29-07-2014 applying best line fit

On the 31st of July, 3.27a, we observed that the heatwave was waning as pressure dropped from 1010 hPa to 1005 hPa. We observed rain in the early hours of the morning where we saw a negligible effect on both xbee nodes. We noticed an improvement in RSSI on the elevated xbee node where -100 dBm or less signal strength was recorded between 1 pm and 6 pm. During this time, we observed that temperature was high at around 22 °C oscillating to 20 °C in the same period. As from 9 pm, there was heavy rain which had a negligible effect on both xbee nodes. The day ended with a relative humidity approaching 99 %. In observing air pressure in graph 3.27b, we observed that signal strength improved when air pressure was between 1006.5 hPa and 1008 hPa. As pressure rose, signal strength became weaker although during the day, air pressure was dropping. In graph 3.27c, signal strength improved as air temperature reached 20 °C. We can see however that signal strength was more scattered (RSSI range was greater between minimum and maximum values) as temperature increased past 20 °C. In observing graph 3.27d, RH% was less than 70 % and had a stronger signal strength than when RH% was greater than 70 %.

A very weak negative correlation was found between air pressure and RSSI with a value of -0.07. A borderline weak to moderate negative correlation was found between temperature and RSSI with a value of -0.39. A weak positive correlation was found between relative humidity and RSSI with a value of 0.35.

When calculating correlation and taking into account dropped packets, a very weak negative correlation was found between air pressure and RSSI with a value of -0.03. A very weak negative correlation between temperature and RSSI was found with a value of -0.19 and a very weak positive correlation was found between relative humidity and RSSI with a value of 0.17.

We did notice an increase in signal strength followed by a decrease between 12:50pm and just until 6pm. We calculated the correlation of air pressure, humidity and air temperature

excluding packet drops during the previously mentioned times and there is a strong correlation with values of -0.64, -0.68 and 0.63 respectively.
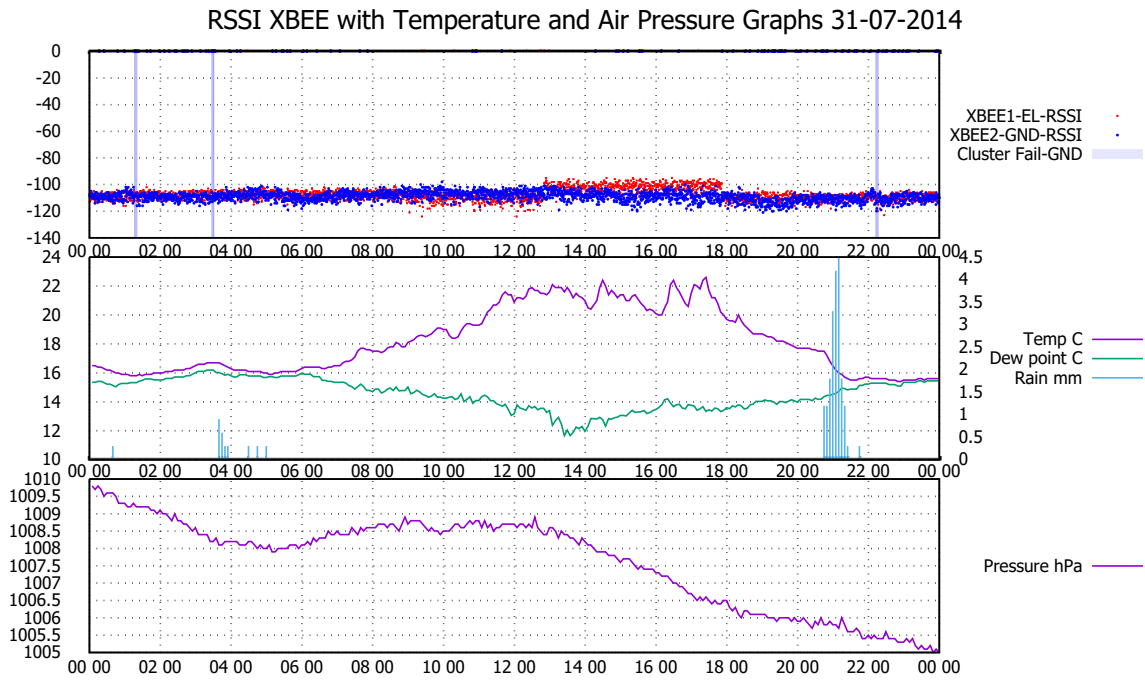
(a) Xbee1 as elevated and Xbee2 as Ground level 868 Mhz transceiver on 31-07-2014
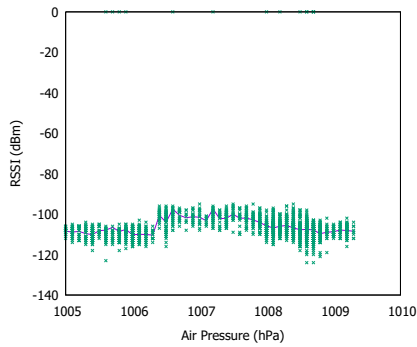


(b) RSSI and Air Pressure 31-07-2014
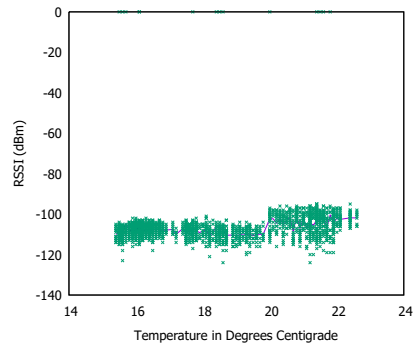


(c) RSSI and Air Temperature 31-07-2014
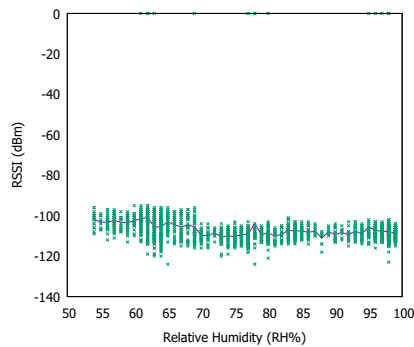


(d) RSSI and Relative Humidity 31-07-2014

Fig. 3.27 Analysis during the 31-07-2014 applying best line fit

### 3.3.2   Summary On July 2014 Data Collection

We made a brief summary for the days in July 2014 together presenting correlation data for the days available. We also highlight in this experiment that the RSSI between the elevated and ground level xbee were not too distant from each other and we could focus on our findings on the elevated xbee node which was constantly powered.

On some of the days analysed, there were strong, moderate and weak correlations with air temperature, air pressure and relative humidity. These correlation figures gives us clues as to the possibility if these weather factors could have a relationship with signal strength, although it may not be true for all days as other forms of interference were not monitored. In the next section, we give an overview on the observable effects of the 868 Mhz link. In calculating correlation, we did two calculations; the whole day for successful packets which we ignored dropped packets as this would skew correlation results and the second is a correlation value with the full data set with RSSI signal strength and dropped packets.

On the 7th of July we saw a moderate correlation between temperature and humidity with RSSI was found including and excluding dropped packets.

On the 8th of July, we saw a moderate correlation between air pressure with RSSI was found excluding dropped packets.

On the 11th of July, we saw a moderate correlation between temperature and humidity with RSSI including dropped packets.

On the 12th of July, we saw a moderate correlation between air pressure and humidity with RSSI excluding dropped packets. We also found a strong correlation between air pressure (a drop of 10 hPa during the day) and RSSI including dropped packets and a moderate correlation between temperature and RSSI including dropped packets.

On the 13th of July, we saw a moderate correlation between air pressure and humidity with RSSI excluding dropped packets. We also found a moderate correlation in air pressure with RSSI including dropped packets (a rise of 5 hPa).

On the 20th of July, we saw a moderate correlation between humidity and RSSI excluding dropped packets.

On the 21st of July, we saw a moderate correlation between temperature and humidity with RSSI excluding dropped packets.

On the 28th of July, we saw a moderate correlation between temperature and humidity with RSSI excluding dropped packets.

On the 29th of July, we saw a moderate correlation in air pressure and RSSI excluding dropped packets.

On the 31st of July, we saw a borderline weak to moderate correlation between temperature and RSSI excluding dropped packets. A strong correlation was found when calculating half of the day where an increase in signal was detected and then a dip was followed in air pressure, humidity and temperature.

Of the 22 days that were analysed in July 2014, we had 10 days which had a moderate correlation between air pressure, temperature and humidity. There was 1 day where air pressure had a strong correlation with RSSI. On certain days, air pressure did not vary as much as in other days. For instance, we had on the 12th and 13th of July, air pressure was rising or dropping much more than in other days.

On the days were we had a very weak to weak correlation, we observe on most days such as on the 14th (3.12), 17th (3.15), 18th (3.16), 19th (3.17), 23rd (3.21), 24th (3.22), 27th (3.24), and a borderline weak to moderate correlation - although a strong correlation was found when half of the day was analysed - on the 31st (3.27), we observe that the slope of the interpolation line was mostly horizontal and could distort any possible correlation as the variance of the dependent variable of y is almost 0. This is were the best line fit is applied to see if there is a relationship between signal strength and dropped packets with the three weather factors being measured.

Other days which had a poor correlation could be due to other sources that were not measured such as heavy traffic or interference from other electromagnetic sources. There was no specific threshold when air pressure, temperature or humidity will trigger failures although we could use another LQE mechanism to predict when failures can happen by using RSSI.

Since we have several days where we have moderate and strong correlation, this does not mean that air pressure, humidity and temperature are the cause of poor signal and packet drops; there are other factors which can cause signal degradation and packet drops to occur. However, this observation does give use a pattern that we see useful in applying to our model; we would be looking for a significant shift in air pressure of several hPa (which is a sign of incoming poor weather), dry air and high air temperature can affect signal strength and cause packet losses. However, there is a caveat in this observation; during the summer, heat waves are usually caused by high air pressures arriving from the south winds, but, in the winter, low temperatures and stable weather are caused by high air pressures that arrive from the north polar winds.

## 3.4   Observable Effects On 868 Mhz Link

In this section, we focus on data collected on the elevated transceiver in July 2014 and other days which are notable. We also compare our findings with what previous authors have found.

The data collected during May 2014 showed that there is effect on RSSI when it rained; see figure 3.29. We did also notice a slight decrease in RSSI when there was heavy rain on the 12th of July as seen in figure 3.10a. However, we do observe an improvement on RSSI levels during the evening when the air has cooled down and humidity is rising (The ratio between air temperature and dew point). On this observation, we would need a variable in our formula that takes into account that high humidity levels seems to improve radio propagation
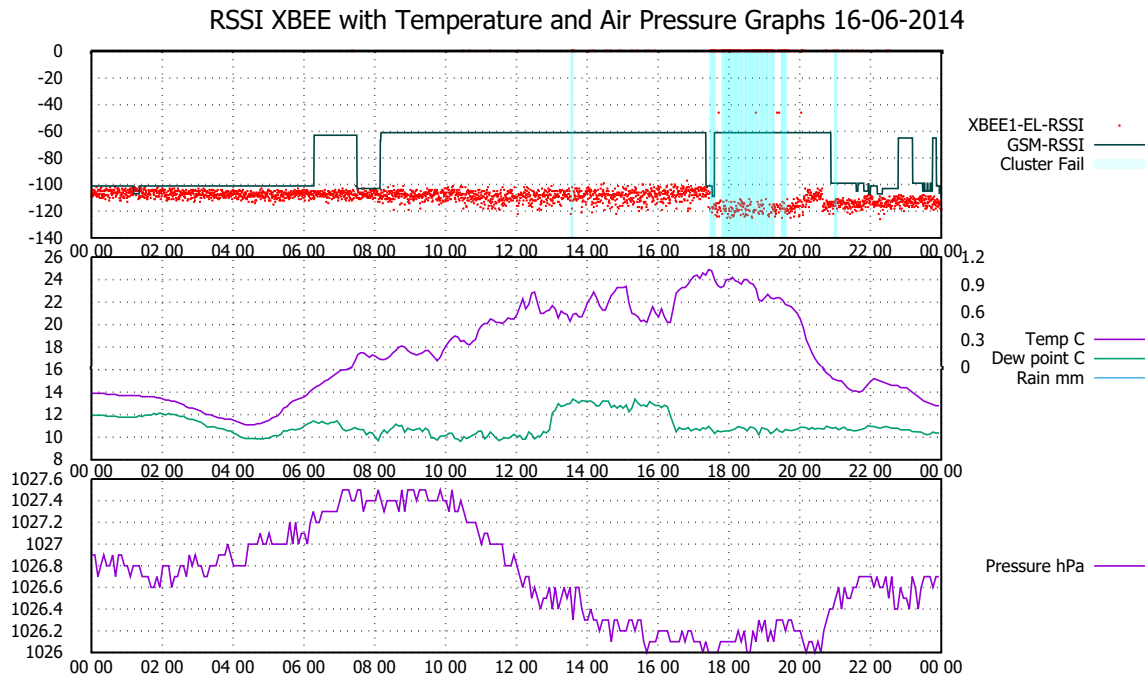
Fig. 3.28 June 16th 2014

at the 868 Mhz band. We observed similar occurrences in the following months and we noticed that GSM seems to be largely unaffected from environmental factors.

We noticed in the 16th of June, figure 3.28, there was a large group of cluster failures and shows a drop in RSSI levels whilst temperature was high, humidity was low (dry air) and air pressure dropped. This pattern of a wide RSSI range seems to improve and narrow further, and improve, during the evening which may correlate with what Thelen stated in his paper [45] on improved RSSI levels when humidity was high during the night. We also observe that 868 Mhz failure tends to be most prominent during the day when air temperature peak in figure 3.28.

We do suspect however that changes in air pressure may have a negative effect as we observed that packet failure seem to occur when there are sudden disturbances in air pressure which is an indication that there is a quick shift in air masses that flow from a region of high pressure to a region of low pressure that are either cold or warm [40]. However, during the winter in December 2014 (graph 3.30) and news article [1]), we observed many packet
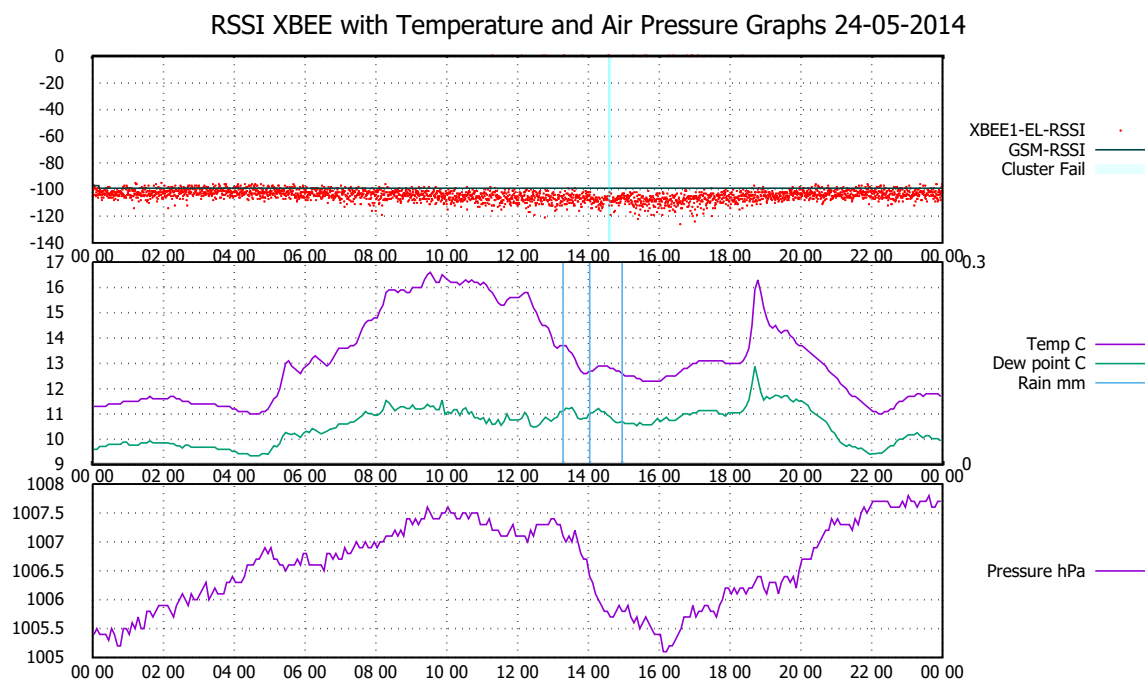
Fig. 3.29 May 24th 2014

failures and we noticed that air pressure dropped very rapidly and temperatures oscillated rapidly during the day. This behaviour followed for a few days as there was a storm in the north of Scotland which also affected parts of North England. We were not able to observe significant cluster failure when small changes in air pressure were occurring, however, rapid changes in air pressure does seem to play a role which merits further investigation to back this claim. On this basis, we need variables assigned for temperature, relative humidity and air pressure, and within our formula, express that a high level of temperature, dry air and rapid drops in air pressure, does affect negatively 868 Mhz propagation. These variables will be expressed as L which will be our long term predictor.
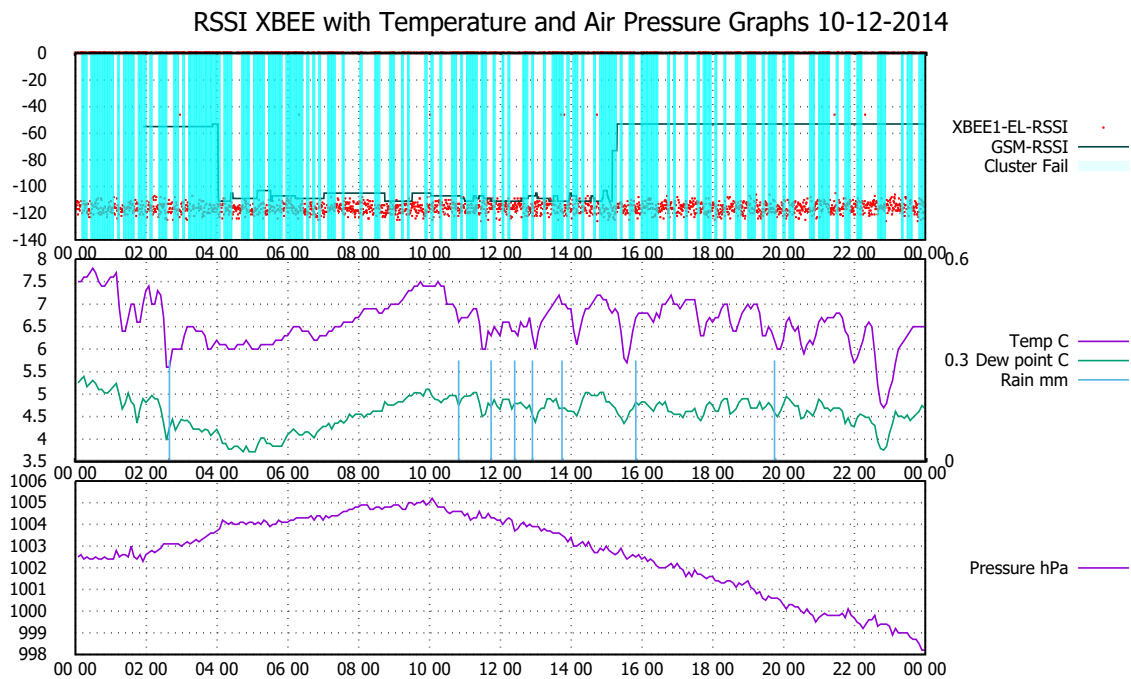
Fig. 3.30 RSSI severely affected by an explosive cyclogenesis

## Temperature

We observe that we do see that RSSI levels do improve when approaching night time during the summer month and we hypothesize that it could be either falling temperatures which correlates with Boano et al findings [13], [14] at the node level. However, we are also looking at the propagation level which heat alone cannot explain hence we look at humidity and air pressure next. During our data collection in July 2014, it was observed that there was a correlation between heat and RSSI in that the higher the heat, the weaker the signal will be.

## Humidity

With relative humidity, we generally observed that the lower relative humidity was, the worse the signal strength was received. The opposite was also true when relative humidity was at its highest at 99% which there might be presence of thick fog and wet foliage. Although we do know that at the 868 Mhz ISM band, fog should not impair xbee radio signals [36], there

are two works which mention different results. Meng, et al found that in low radio signals, wet vegetation especially humid tree trunks, can attenuate low signal frequency propagation [33]. In Thelen's work, [45], it was observed that humidity did improve signal strength over a potato crop over night and dismissed the tropospheric ducting effect due to that range was too short of several metres.

**Rain**

Rain does not seem to have a detrimental effect on the 868 Mhz band. As we can observe on figure 3.29 that there was precipitation and there was no significant packet losses. It is also mentioned in Meng's work [33] that rain is an unclear factor in low signal propagation, especially in forested areas.

**Air Pressure**

It is known from previous research that atmospheric conditions can affect radio propagation [15], [22]. We don't observe a direct relationship between RSSI and air pressure when rise and drops in air pressure occur, but we can use air pressure to predict when 868 Mhz will fail. For example, during the summer, a high pressure would mean that we would have a very warm front incoming which can negatively affect 868 Mhz RSSI levels. During winter, typically we can experience high air pressure; meaning that cold weather conditions will ensue and that would improve RSSI levels. We have seen for instance when the UK suffered from storms and weather bombs (an explosive cyclogenesis causes a pressure drop of 24hPa within 24 hours) causing severe gales and heavy rain often with sleet as shown in this news article [1]. We observed that packet drops were significantly high during this event. One explanation we can give is that of tropospheric scattering and ducting; the former occurs when radio propagation is scattered when there is a region of warm air and the latter is a phenomena that can affect UHF signal propagation by sudden changes in the atmosphere's

vertical moisture content and temperature profiles. In tropospheric ducting, we can observe radio signals are propagated further during periods of stable anticyclonic weather.

## 3.5 Observable Effects On GSM Band

In general, we did not observe poor signal strength during our experiment - even when it rained. However, we did observe that signal strength deteriorated when sudden and large drops in pressure occurred. This is normally an indication that a storm is approaching. In figure 3.30, we observe constant drops within a five minute period and GSM signal strength deteriorates below -100dBm between 0400 hours and 1430 hours. This article mentions the drop in pressure that happened on the 10th of December 2014, [1].

## 3.6 Chapter Summary

We have discussed in this chapter the weather factors that we have been analysing throughout our experiments and describe what each parameter is in meteorological terms - temperature, relative humidity and atmospheric pressure. We described two test beds to know if there is a significant difference in RSSI strength in having a receiver elevated placement or on the ground level in campus with the sender located in Galgate. We discussed the days available during the month of July 2014 and gave a summary on each day providing correlation data. We have observed that most days presented a weak to moderate correlation between the weather factors analysed and signal strength (for successful packets). This gave us clues to formulate our weather based link quality estimator. We then describe the observable effects on the elevated 868 Mhz radio link which fluctuates when certain environments prevail. However with GSM, we have seen that it is much more robust except when severe storms prevail in the area.

# Chapter 4

# Weather Based Link Selection Scheme

## 4.1 Chapter Overview

In this chapter, we shall review the weather based link selection scheme that was derived from our test bed. We look into what short term LQE's accomplish and what long term LQE's accomplish. We will discuss how it makes the decision based on predefined parameters and make a decision based on what it senses. We then go on to discuss its possibilities on how it can be deployed in practise and highlight its strengths and weaknesses.

### 4.1.1 Short Term Link Quality Estimators

Link Quality Estimators (LQE) are used to describe how the quality of a link is developing over time. Generally, LQE describe short term link developments. For example, the success rate of recent packet transmissions or RSSI of recently received packets is used to estimate link quality for the near future on sender and/or receiver side. LQE are a useful tool to decide if a link is still available for the next packet transmission but they generally do not capture long-term developments of a link.

In this work we use a particular LQE to estimate quality of the short range wireless link. Nodes transmit a probe packet every $t_S$ seconds. The transmitter records if the transmission was successful or not. The LQE (referred to as short term LQE $S$) describes the percentage of probe transmissions lost within a time window $T_S$. Threshold $S(pf)$ is used to decide at which point the cheaper link is considered unusable. If data is transmitted, these can be used as probe transmissions and dedicated link probing is not required.

In this work we used the aforementioned LQE metric; however, other methods could be used to decide if the short range wireless link is usable.

## 4.1.2   Long Term Link Quality Estimators

Link selection based on short term link quality estimation does not necessarily lead to the selection of a stable radio link (in our case, GSM and Xbee) over a longer period. Especially in situations where a link is in a transition phase short term LQE often leads to oscillation between links. We argue that this can be avoided by including long term link quality estimation in the decision. In particular we have shown that weather conditions have an impact on link quality and, therefore, weather information can be used as long term LQE.

As our experiments have shown there is not one single environmental parameter that describes how the link quality is developing over long time periods. Temperature, humidity and pressure was analysed as to how these metrics will affect wireless communications in our test bed. We construct a link quality estimator based on each of the parameters and then combine the result into a single link quality estimator which is subsequently used to decide if a link can be used or not. $L_t$ is the temperature LQE, $L_h$ is the humidity based LQE and $L_p$ is the pressure based LQE. All three LQE are represented as binary value of 0 or 1. We decided to use this binary notation instead of a sliding value between 0 and 1 as we found that this simpler representation is sufficient. A weather parameter is either taken into account when

making decisions or left out depending on weather conditions. We then use $\alpha$, $\beta$ and $\gamma$ to weigh these three binary LQE values and then combine them to create a single LQE.

Table 4.1 Parameters assigned to the S + L LQE

| Symbol | Purpose |
|---|---|
| c | Current moving time |
| t | Temperature value in degrees Centigrade (°C) |
| h | Humidity value in RH% |
| p | Pressure value in hectapascals (hPa) |
| $T_{trs}$ | Temperature Threshold in degrees Centigrade (°C) |
| $H_{trs}$ | Humidity Threshold in RH |
| $P_{trs}$ | Pressure Threshold in hPa |
| $Q_t$ | Quality Estimator result |
| $T_Q$ | Time to remain on the expensive transceiver |
| $T_t$ | Current Temperature |
| $H_t$ | Current humidity |
| $P_t$ | Current Air Pressure in hectapascals (hPa) |
| $T_L$ | Time when S+L algorithm started |
| $\alpha$ | Truth value determined for L with temperature either 0 or 1 |
| $\beta$ | Truth value determined for L with humidity either 0 or 1 |
| $\gamma$ | Truth value determined for L with air pressure either 0 or 1 |
| $S(pf)$ | Short term predictor packet failure |
| $L_t(t)$ | Long term predictor for temperature assigned a weighting value if true |
| $L_t(h)$ | Long term predictor for humidity assigned a weighting value if true |
| $L_t(p)$ | Long term predictor for pressure assigned a weighting value if true |
| $Score_{trs}$ | Score threshold is predetermined and determines the behaviour of S+L |

We define the short term packet failure in the following manner:

$$S(pf) = \begin{cases} 0.3 > pf \leq 1, & \text{if } pf \geq 0.3 \\ 0, & \text{else} \end{cases} \tag{4.1}$$

If the packet failure for $S(pf)$ is greater than 0.3, then it would activate the L component of the algorithm, thus the resulting equation for our LQE can be given as:

$$L(t) = \alpha \cdot L_t(t) + \beta \cdot L_h(t) + \gamma \cdot L_p(t) \tag{4.2}$$

The temperature related LQE $L_t$ is defined as follows:

$$L_t(t) = \begin{cases} 1, & \frac{T(t-t_t)}{T(t)} < T_{trs} \vee T(t) \geq T_{trs} \\ 0 & \text{else} \end{cases} \tag{4.3}$$

Here $T(t - t_t)$ is the temperature value recorded $t_t$ seconds in the past. If the ratio of past and current temperature value is above the set threshold $T_{trs}$ the value of $L_t$ is set to 1 as in this case temperature is likely to have an impact on the communication link. If the temperature is above a maximum temperature $T_{max}$ is also set to 1 as in this case an impact on the communication link will be noticed.

Similar the value considering humidity is calculated:

$$L_h(t) = \begin{cases} 1, & \frac{H(t-t_h)}{H(t)} < H_{trs} \vee H(t) < H_{trs} \\ 0 & \text{else} \end{cases} \tag{4.4}$$

$H(t - t_h)$ is the humidity value recorded $t_h$ seconds in the past. $H_{trs}$ is a humidity ratio threshold and $H_{max}$ is the maximum humidity threshold above which an effect on the communication link is to be expected.

The pressure contribution $L_p$ is calculated slightly different. Here we take into account the calculated temperature value $L_t$ as pressure changes are only an indicator for link disturbances if temperature is as well within the considered range:

$$L_p(t) = \begin{cases} 1 \cdot L_t(t), & \frac{P(t-t_p)}{P(t)} > P_{trs} \vee P(t) \leq P_{trs} \\ 0 & \text{else} \end{cases} \tag{4.5}$$

$P(t - t_p)$ is the pressure value recorded $t_p$ seconds in the past. We only consider pressure if there is a significant change in pressure over time (determined by threshold $P_{trs}$) or exceeds a predefined threshold.

In reading the results tables, as an example, table 4.2, we will explain what the definitions of each line on the table. Total Traversed readings is the amount of readings that was used as we need to discard data that either has no weather data available, no RSSI data or was skipped by the L blocking algorithm (different parameters can change this value). Used traversed readings is the amount of readings used that was either switched on 868 Mhz or GSM and the packet was not dropped. We coined the term "short term switch" as an Evil switch, hence we used Evil Switch S which is the amount of switching that would have taken place on the following scenario; in t1, we received a good packet, t2 was a packet drop and t3 we received a good packet. Evil switching S+L is the algorithm used to determine how many switches there are on the following condition where Ts is the score obtained on a particular time frame and $Score_{trs}$ is the predefined score threshold used:

$$(T_s \geq Score_{trs}) \tag{4.6}$$

The above statement determines if the L score has exceeded the threshold that was predetermined. If so, it will stop using the 868 Mhz radio in exchange for a more expensive radio transceiver.

$$(T_s - 1 < Score_{trs}) \wedge (Ts \geq Score_{trs}) \wedge (T_s + 1 < Score_{trs}) \tag{4.7}$$

The above equation detects if there is an evil switch in L. This means that the previous time frame, the calculated threshold must be below the set threshold $Score_{trs}$ and that the 868 Mhz radio was on and the current time frame ($T_s$) threshold should be greater than or equal to the set threshold and the future time frame ($T_s + 1$) should be less than the set threshold. If all conditions pass, then it is considered an evil switch under S+L. The higher the figure between 0 and 1, the longer it will block the decision to either switch or not. We also have times used in S and S+L times expressed in seconds. The bottom part of the table (e.g 4.2)

highlights which thresholds and weights were used for the month which are self explanatory. We then display the amount of time in seconds spent on S and S+L respectively.

### 4.1.3 Link Selection Using Short and Long Term LQEs

Using only short term link quality estimators to select a link is not desirable. As we will show this leads to a situation where a link is chosen and shortly after the decision is reverted. As a consequence, links frequently change and no stable routing topology can be established. To avoid this situation we combine short term link estimators and long term estimators as described in the previous section. We give both estimators an equal weight and create an overall link estimator $Q(t)$:

$$Q(t) = \frac{S(t) + L(t)}{2} \tag{4.8}$$

If $Q(t)$ is above a set threshold the link is selected. The link is then used for a time period $T_Q$ before the expression is re-evaluated to decide if the link should not be used any more. The time $T_Q$ is calculated using a decaying Euler function which avoids frequent link switching from occurring and is responsible of blocking any decisions to be taken and remain on a reliable radio communication until the time expires:

$$T_Q = e^{\frac{\left(\frac{-(T_L - c)}{1000}\right)}{Q_t.10}} \tag{4.9}$$

The function $T_L$ - c needs to be converted to a positive number by multiplying this result by -1 as subtracting a past time with a future time yields a negative number.

## 4.2   Processing of Data and Parameter Discovery

In this section, we shall describe how parameters and results were obtained by using Java code as our simulator. We will show some tables with sub optimal values and other tables with optimal values.

### 4.2.1   Simulation Data Processing

As weather data, dropped packet data and RSSI data were gathered and used in our algorithm, we could determine the best parameters by having a simulator run through a range of parameters. Such parameters are described in table 4.1.2 and we choose a suitable range to run based on the weather data collected. Such an example can be from the lowest temperature a month has seen to its highest temperature recorded. The same applies to low and highest pressure, low and high values of humidity. Running this simulator has several nested for loops which is processing intense and thus results for a 6 month period could take up to two and a half months on a standard office PC to obtain.

### 4.2.2   Java Code

Below we give the portion of code and the nested for loops that processes the data to find the optimal values. The code to find optimal values has been explained mathematically in the previous section.

```java
public void run() {


        double minT = 49, maxT = -110, minRH = 99, maxRH = -1, minPres = 2000
        double  maxPres = -1;
        double alpha = 0.25;beta=0.25;gamma=0.5;
        double b = maxT;
```

```
        double c = maxRH;

        double d = maxPres;

        double e = 1.05, f = 1.05, g = 1.03, x = 0.01, y = 0.01, z=0.01;


   for(double i = minT; i <= maxT;i++) {

for(double j = minRH; j <= maxRH;j++) {

for(double k = maxPres; k >= minPres;k--) {

// find out ratios for temp, hum and pressure respectively

for(double l = 0.95; l <= e;l = l + x) {

for(double m = 0.95; m <= f; m = m + y) {

for(double n = 1.03; n >= 0.97; n = n - z) {

this.doSim(0.3, i, j, k, l, m, n,alpha,beta,gamma);

...
```

### 4.2.3   Finding Optimal Values

In this section, we give examples of hits found by the simulator and use the optimal value for the corresponding month. Once we run the simulator, it will save text files with the parameters listed. It will not record parameters if the efficiency of the parameter combination does not exceed the one before. The efficiency is calculated by the following:

$$eff = (xbeeOnTarget/usableReadings) * 100 \qquad (4.10)$$

Where xbeeOnTarget is the value where the 868 Mhz communication was used and there were limited communication drops and then we have usableReadings which is the amount of readings that the pass made which is where the RSSI was either a 0 (dropped packet) or greater than 0. Anything else is considered an error. Depending on the algorithm's pass,

traversed readings can change due to the blocking algorithm that has been used during that pass and thus some readings would be ignored.

Table 4.2 May 2015 suboptimal Parameters 1

| May 2015 | Value |
| --- | --- |
| Total Traversed Readings: | 88904 |
| Usable Traversed Readings: | 70699 |
| Evil Switches on S | 1297 |
| Evil Switches on S+L | 46 |
| Time spent with S 868 Mhz: | 2606420 |
| Time spent with S+L 868 Mhz: | 1443467 |
| Score Threshold: | 0.3 |
| Temp Threshold: | 1.1 |
| Humidity Threshold: | 33.0 |
| Pressure Threshold: | 1022.7 |
| Temp Ratio: | 0.95 |
| Humidity Ratio: | 0.95 |
| Pressure Ratio: | 1.03 |
| Temp Weighting | 0.25 |
| Humidity Weighting | 0.25 |
| Pressure Weighting | 0.5 |

Table 4.3 May 2015 suboptimal Parameters 2

| May 2015 | Value |
| --- | --- |
| Total Traversed Readings: | 88905 |
| Usable Traversed Readings: | 70680 |
| Evil Switches on S: | 1297 |
| Evil Switches on S+L: | 41 |
| Time spent with S 868 Mhz: | 2606420 |
| Time spent with S+L 868 Mhz: | 1513674 |
| Score Threshold: | 0.3 |
| Temp Threshold: | 1.1 |
| Humidity Threshold: | 33.0 |
| Pressure Threshold: | 1022.7 |
| Temp Ratio: | 0.95 |
| Humidity Ratio: | 1.02 |
| Pressure Ratio: | 1.03 |
| Temp Weighting | 0.25 |
| Humidity Weighting | 0.25 |
| Pressure Weighting | 0.5 |

Table 4.4 May 2015 optimal values

| May 2015 | Value |
|---|---|
| Total Traversed Readings: | 87213 |
| Usable Traversed Readings: | 66808 |
| Evil Switches on S: | 1174 |
| Evil Switches on S+L: | 24 |
| Time spent with S 868 Mhz: | 2606420 |
| Time spent with S+L 868 Mhz: | 2394063 |
| Score Threshold: | 0.3 |
| Temp Threshold: | 19.1 |
| Humidity Threshold: | 33.0 |
| Pressure Threshold: | 982.7 |
| Temp Ratio: | 0.95 |
| Humidity Ratio: | 1.04 |
| Pressure Ratio: | 1.07 |
| Temp Weighting | 0.25 |
| Humidity Weighting | 0.25 |
| Pressure Weighting | 0.5 |

In table 4.3, we observe that a low temperature setting was chosen to be traversed, low humidity setting and a high pressure setting was selected. The idea behind traversing possible values is to find the setting that has the largest time spent on S+L whilst keeping Evil switching S+L as low as possible. As traversing through all the possible values, we then found a suitable combination of parameters which are displayed. The best values for May 2015 are found in table 4.4 with the simulation run in graph 4.1.

In table 4.3, we observe a change as an increase in the humidity ratio where the ratio is greater than 1. This means that there has to be an increase in humidity to have less evil switching taking place. We will now look at another hit where the algorithm found with a higher efficiency.

In table 4.5 which are readings collected in May 2015, we observe that all three weather parameters have changed. An increase in temperature is noted where we now see a jump from 1.1 °C to 14.1 °C, humidity remains the same (dry) and pressure has fallen from 1022.7 hPa down to 996.7 hPa. At this point, we know that a rise in temperature starting from a
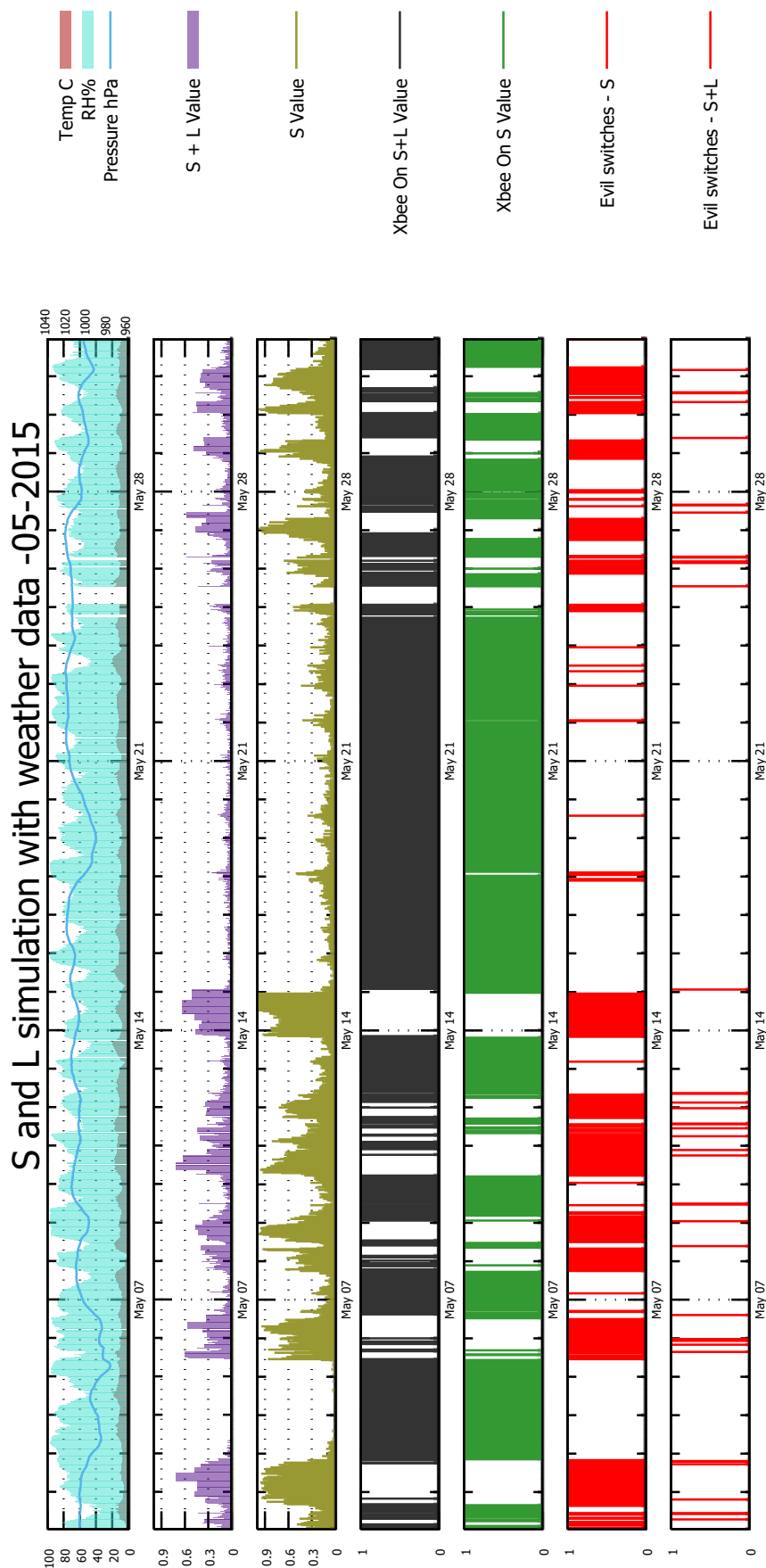
Fig. 4.1 Simulation run during May 2015 data using values that causes S+L evil switching based from table 4.4

Table 4.5 May 2015 suboptimal Parameters 3

| May 2015 | Value |
|---|---|
| Total Traversed Readings: | 88689 |
| Usable Traversed Readings: | 68064 |
| Evil Switches on S | 1297 |
| Evil Switches on S+L | 23 |
| Time spent with S 868 Mhz: | 2606420 |
| Time spent with S+L 868 Mhz: | 2336271 |
| Score Threshold: | 0.3 |
| Temp Threshold: | 14.1 |
| Humidity Threshold: | 33.0 |
| Pressure Threshold: | 996.70 |
| Temp Ratio: | 0.95 |
| Humidity Ratio: | 1.02 |
| Pressure Ratio: | 1.03 |
| Temp Weighting | 0.25 |
| Humidity Weighting | 0.25 |
| Pressure Weighting | 0.5 |

Table 4.6 May 2015 - 2nd best optimal values

| May 2015 | Value |
|---|---|
| Total Traversed Readings: | 88699 |
| Usable Traversed Readings: | 68114 |
| Evil Switches on S: | 1297 |
| Evil Switches on S+L: | 23 |
| Time spent with S 868 Mhz: | 2606420 |
| Time spent with S+L 868 Mhz: | 2352471 |
| Score Threshold: | 0.3 |
| Temp Threshold: | 19.1 |
| Humidity Threshold: | 48.0 |
| Pressure Threshold: | 993.7 |
| Temp Ratio: | 0.95 |
| Humidity Ratio: | 1.02 |
| Pressure Ratio: | 1.03 |
| Temp Weighting | 0.25 |
| Humidity Weighting | 0.25 |
| Pressure Weighting | 0.5 |

mild range, a dry humidity level and a low pressure level that is rising, gives a better result in predicting when radio interfaces should be switched.

In table 4.4, we see that the algorithm found the best values followed from table 4.6 values and we see that there was an improvement in evil switching as humidity value was set to be dryer.

## 4.3 Evaluation

During the month of July 2014, we observe several meteorological patterns; 1) During the day, it is typically warm with temperatures over 15 °C and colder during the night and 2) Relative humidity is low during the day (dry) and high during the night (air is almost saturated with water vapour). Pressure oscillates and periods when the pressure is high indicates good weather and sudden drops indicates a storm may be arriving. We then use this data to calculate the factor L.

From the period between 01 of July and 05 of July, we observe that S (the metric used for short term switching) is below 30%. We chose this figure as a suitable value between more aggressive policies which activates GSM more often and opt for a reliable connection or a lenient policy which sacrifices reliability and limits switching. This policy translates that if failures within a 5 to 30 minute period occur, then we calculate L and use both values to determine for how long we should switch to the more expensive and reliable transceiver (GSM). We observe a few instances during the first day of July that factor L was activated because the failure rate for S was greater than 30%. This is drawn on the "xbee On S+L" graph 4.2 where the coloured lines indicates when the xbee was activated whilst using S+L factors. We also observe that in graph 4.2 "xbee On S value" shows when the S value exceeded our value of 30%. On graph 4.2, we observe no short term switching for S+L but switching does occur for the S factor alone.

During the period of 05 July to 12 July 2014 in graph 4.2, we observe a more extreme period when switching takes place. The 8th, 9th and 10th of July are days when the S value was high with periods reaching 100% of packet failures occurring within a short time frame of 5 minutes (in 2015, we extend the time frame to be less than 30 minutes). This caused the S value to be greater than 30% and switch from the cheap transceiver (868 Mhz) to GSM radio. This behaviour is reflected on the "xbee On S+L" and "xbee On S" as seen on graph 4.2. We can also appreciate how the S+L graph normalises the S values and thus the decision was taken to use the more expensive radio transceiver as this was a time of instability. We sacrifice more time spent on the cheaper radio and switch to the expensive radio transceiver, but we save on possible network switches taking place unnecessarily within a short period of time (less than 30 minutes).

On the 29th of July, we can see in a zoomed graph 4.3 that between 5pm and 11:59pm, the value of S was rising steadily. At 10pm, the S value exceeded the threshold and L was triggered according to the parameters that would cause L to be triggered. The S+L LQE was blocked twice between 10pm and 11:59pm which saved from several switches occurring.

A high value of $Q_t$ would thus cause the curve to be steeper and cause a long interval which prevents the node from switching back to the more expensive and reliable transceiver. Once the time has elapsed, it would cause the node to re-check the status and re-evaluate if the conditions for the cheaper radio are favourable, or remain on the expensive transceiver (GSM). A lower value $Q_t$ would mean that conditions are favourable for 868 Mhz and the checking interval is reduced ($T_Q$).

Table 4.7 July 2014 based on figure 4.2

| July 2014 | Value |
| --- | --- |
| Total Traversed Readings: | 89018 |
| Usable Traversed Readings: | 77474 |
| Evil Switches on S | 510 |
| Evil Switches on S+L | 129 |
| Time spent with S 868 Mhz: | 2303637 |
| Time spent with S+L 868 Mhz: | 1533459 |
| Score Threshold: | 0.3 |
| Temp Threshold: | 24 |
| Humidity Threshold: | 26 |
| Pressure Threshold: | 1027.5 |
| Temp Ratio: | 0.95 |
| Humidity Ratio: | 0.95 |
| Pressure Ratio: | 1.03 |
| Temp Weighting | 0.2 |
| Humidity Weighting | 0.2 |
| Pressure Weighting | 0.6 |

Table 4.8 July 2014

| July 2014 | Value |
| --- | --- |
| Total Traversed Readings: | 89018 |
| Usable Traversed Readings: | 77473 |
| Evil Switches on S: | 510 |
| Evil Switches on S+L: | 91 |
| Time spent with S 868 Mhz: | 2303637 |
| Time spent with S+L 868 Mhz: | 1729538 |
| Score Threshold: | 0.3 |
| Temp Threshold: | 20 |
| Humidity Threshold: | 66 |
| Pressure Threshold: | 988 |
| Temp Ratio: | 0.65 |
| Humidity Ratio: | 1.0 |
| Pressure Ratio: | 1.03 |
| Temp Weighting | 0.25 |
| Humidity Weighting | 0.25 |
| Pressure Weighting | 0.5 |

Table 4.9 June 2015 using May 2015 parameters

| June 2015 | Value |
|---|---|
| Total Traversed Readings: | 86045 |
| Usable Traversed Readings: | 64813 |
| Evil Switches on S | 1407 |
| Evil Switches on S+L | 39 |
| Time spent with S 868 Mhz: | 2505430 |
| Time spent with S+L 868 Mhz: | 2096297 |
| Score Threshold: | 0.3 |
| Temp Threshold: | 19.1 |
| Humidity Threshold: | 48.0 |
| Pressure Threshold: | 993.7 |
| Temp Ratio: | 0.95 |
| Humidity Ratio: | 1.02 |
| Pressure Ratio: | 1.03 |
| Temp Weighting | 0.25 |
| Humidity Weighting | 0.25 |
| Pressure Weighting | 0.5 |

Table 4.10 June 2015 suboptimal Parameters

| June 2015 | Value |
|---|---|
| Total Traversed Readings: | 85900 |
| Usable Traversed Readings: | 64456 |
| Evil Switches on S: | 1407 |
| Evil Switches on S+L: | 63 |
| Time spent with S 868 Mhz: | 2505430 |
| Time spent with S+L 868 Mhz: | 1187295 |
| Score Threshold: | 0.3 |
| Temp Threshold: | 3.29 |
| Humidity Threshold: | 30.0 |
| Pressure Threshold: | 1033.19 |
| Temp Ratio: | 0.95 |
| Humidity Ratio: | 0.96 |
| Pressure Ratio: | 1.03 |
| Temp Weighting | 0.25 |
| Humidity Weighting | 0.25 |
| Pressure Weighting | 0.5 |

Table 4.11 June 2015 Optimal parameters

| June 2015 | Value |
|---|---|
| Total Traversed Readings: | 86049 |
| Usable Traversed Readings: | 65341 |
| Evil Switches on S | 1407 |
| Evil Switches on S+L | 34 |
| Time spent with S 868 Mhz: | 2505430 |
| Time spent with S+L 868 Mhz: | 2171897 |
| Score Threshold: | 0.3 |
| Temp Threshold: | 32.29 |
| Humidity Threshold: | 37.0 |
| Pressure Threshold: | 1005.19 |
| Temp Ratio: | 0.96 |
| Humidity Ratio: | 1.05 |
| Pressure Ratio: | 1.03 |
| Temp Weighting | 0.25 |
| Humidity Weighting | 0.25 |
| Pressure Weighting | 0.5 |

# 4.4   Results And Optimization Problem

In this section, we describe how we predefine values for our simulation and present an optimization problem as to find the best values that would bring our efficiency close to 100%. In the following tables, we give details of the parameters which we get varying results.
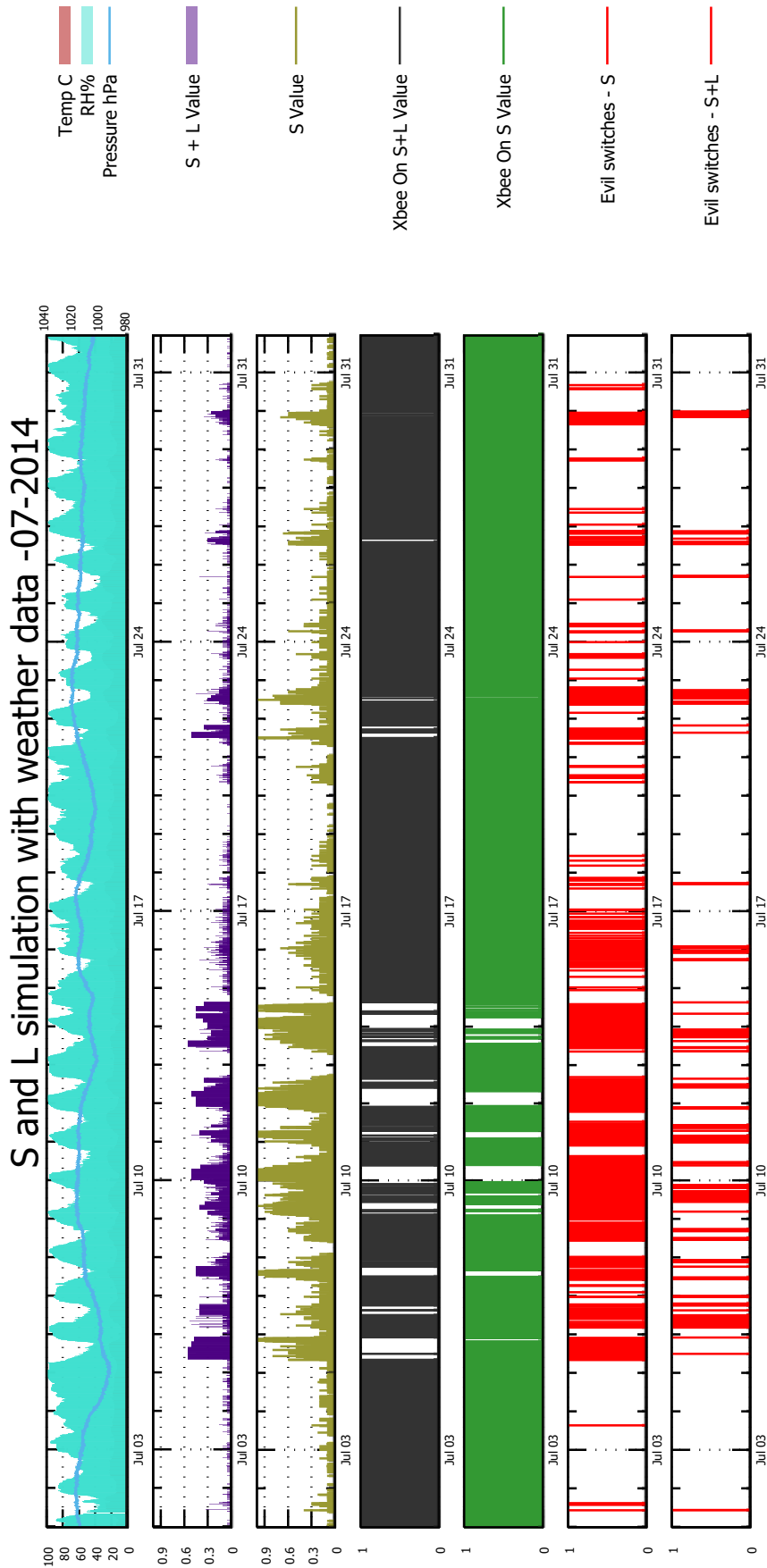
Fig. 4.2 Simulation run during July 2014 data using values that causes S+L evil switching -
table showing details on table 4.7
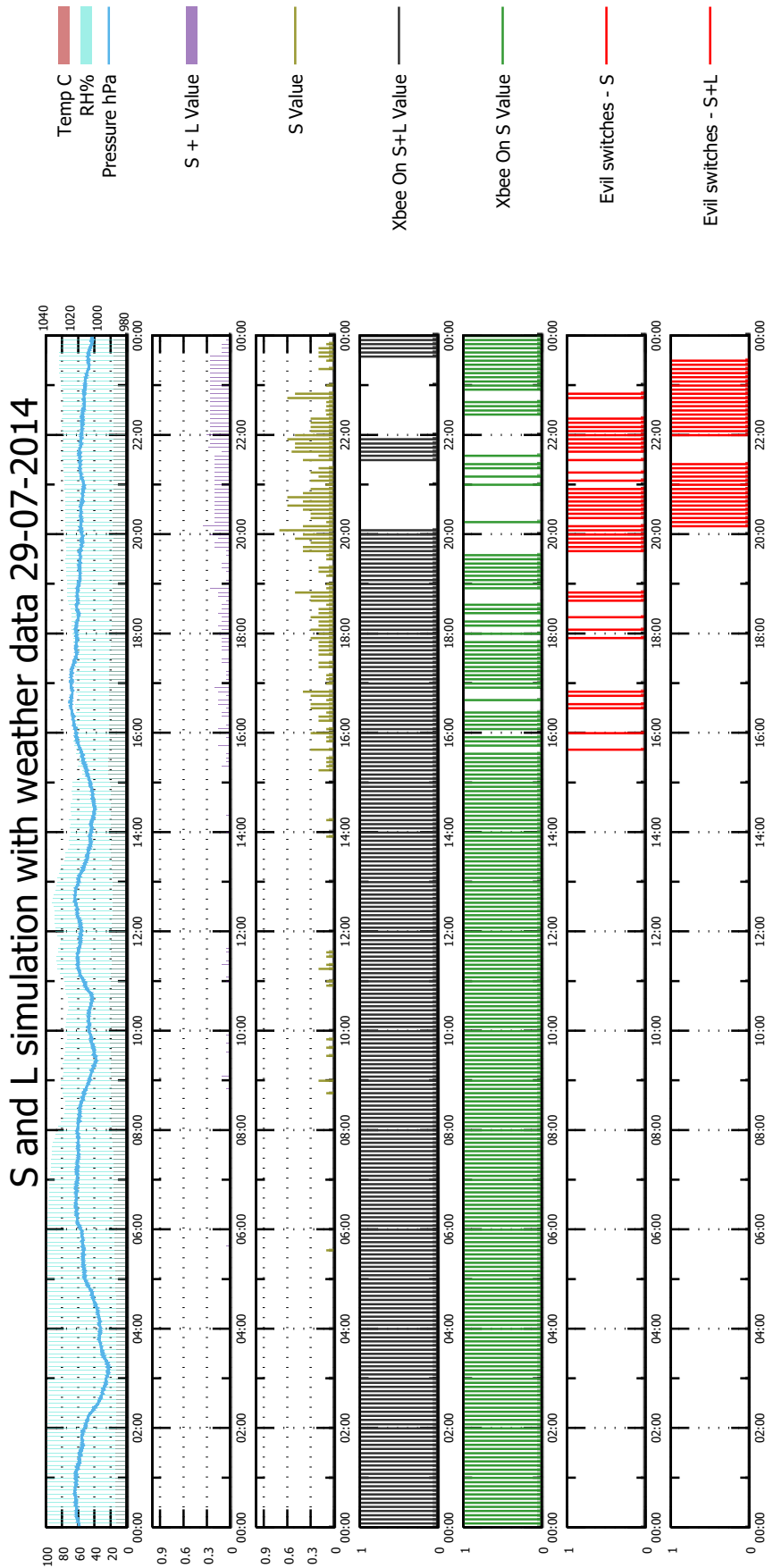
Fig. 4.3 A day period on the 29th July 2014

Table 4.12 August 2015 Optimal Parameters

| August 2015 | Value |
|---|---|
| Total Traversed Readings: | 80517 |
| Usable Traversed Readings: | 71400 |
| Evil Switches on S | 830 |
| Evil Switches on S+L | 56 |
| Time spent with S 868 Mhz: | 2626839 |
| Time spent with S+L 868 Mhz: | 2453704 |
| Score Threshold: | 0.3 |
| Temp Threshold: | 24 |
| Humidity Threshold: | 32.0 |
| Pressure Threshold: | 992 |
| Temp Ratio: | 0.95 |
| Humidity Ratio: | 1.04 |
| Pressure Ratio: | 1.07 |
| Temp Weighting | 0.25 |
| Humidity Weighting | 0.25 |
| Pressure Weighting | 0.5 |

## 4.4.1 August 2015

In August 2015, we could see a remarkable shortage of evil switching taking place as seen in table 4.12 were there was 830 S switches; down to 56 switches using S+L. We contrast this amount of reduced switching taking place with table 4.13 were only 73 S+L switches took place; 20 more evil switches taking place if parameters are not correctly tuned. We also see in graph 4.4 were S had a significant amount of switching taking place and fewer switches took place with S+L.

## 4.4.2 UK Storms in 2015

In the UK, the national MET office decided to name storms so that the public can be better prepared of an incident. Such incidents that a storm can cause can be flooding, disruptions to water, electricity and gas utilities which can cause billions of pounds worth of damage. During 2015 storm season, 4 storms made landfall on the UK; in Lancaster storms Abigail, Barney and Clodagh left significant rainfall which saturated the ground. When Storm Desmond
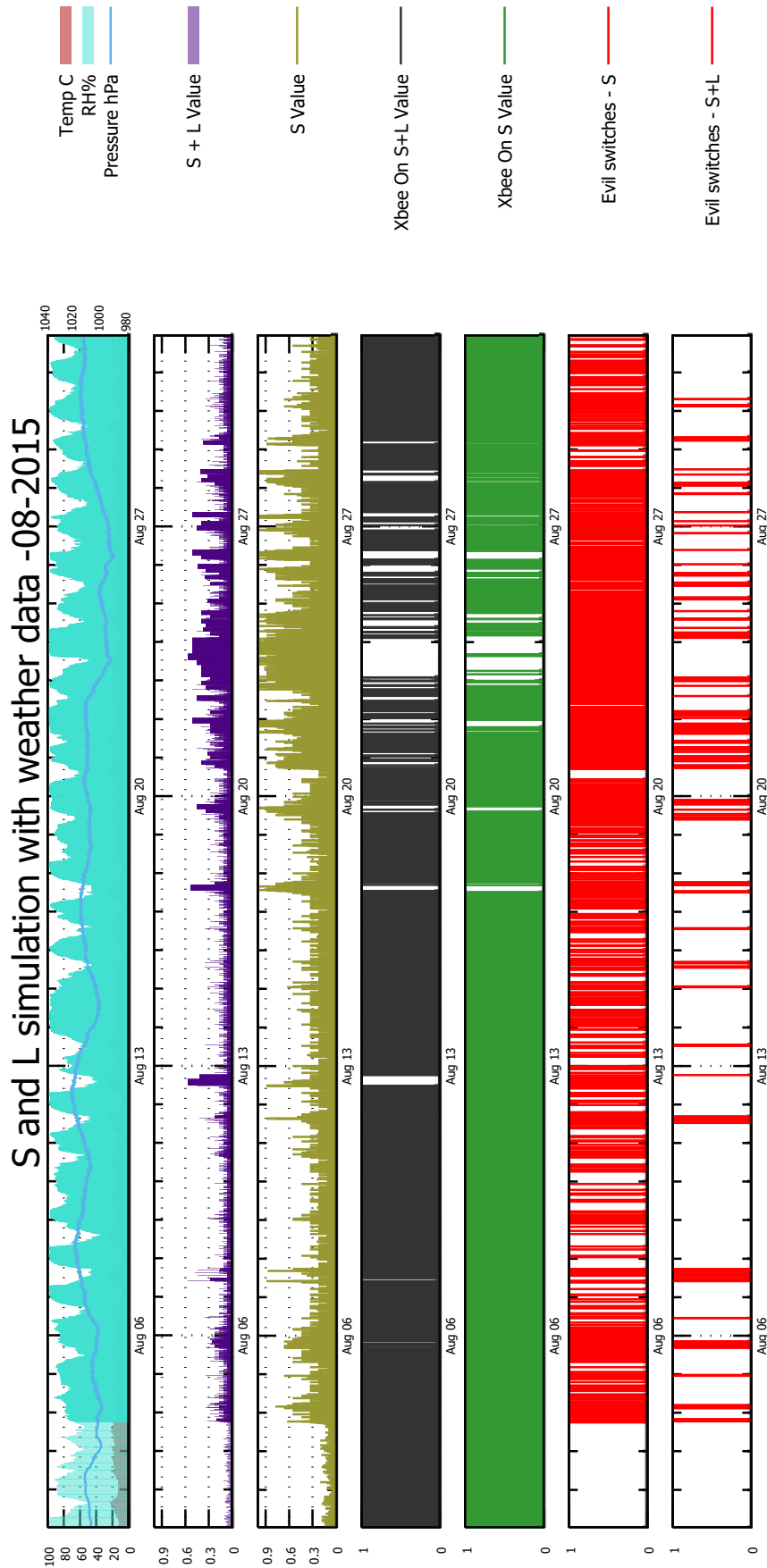
Fig. 4.4 Simulation run during August 2015 data using values that causes S+L evil switching
- table showing details on table 4.12

Table 4.13 August 2015 sub optimal Parameters

| August 2015 | Value |
|---|---|
| Total Traversed Readings: | 80392 |
| Usable Traversed Readings: | 62739 |
| Evil Switches on S: | 830 |
| Evil Switches on S+L: | 73 |
| Time spent with S 868 Mhz: | 2626839 |
| Time spent with S+L 868 Mhz: | 92096 |
| Score Threshold: | 0.3 |
| Temp Threshold: | 6,4 |
| Humidity Threshold: | 32.0 |
| Pressure Threshold: | 1022 |
| Temp Ratio: | 0.95 |
| Humidity Ratio: | 0.95 |
| Pressure Ratio: | 1.07 |
| Temp Weighting | 0.25 |
| Humidity Weighting | 0.25 |
| Pressure Weighting | 0.5 |

made landfall, the ground was too saturated to absorb any further rainfall which caused rivers to swell up. The nearby substation located next to the river Lune was flooded causing one week of electrical disruptions to all neighbouring regions.

We have sufficient data to produce more table results of how our weather based LQE would perform. In this section, we shall describe the storms and how wind speeds are classified as this is essentially a rapid change in air pressure.

For such weather phenomena to be classified as a storm, terrestrial wind speeds should measure higher than 10 (sometimes referred as a whole gale) on the Beaufort wind force scale (an empirical scale measuring wind speeds observed at sea or on land) which is greater than or equal to 89 kph or 55 mph. Wind speeds that is greater than 64 mph is classed as a Violent Storm and winds greater than 73 mph is classed as a Hurricane (within the Hurricane class, there are 5 further classifications in the Saffir Simpson Hurricane Wind Scale or SSHWS, which determine western Hemisphere tropical cyclones that exceeds that of a tropical storm

Table 4.14 Beaufort Scale

| Scale | Mean Wind Speed (knots) | Max Speed (knots) | Description | Sea Observation |
|---|---|---|---|---|
| 0 | 0 | 1 | Calm | Calm (glassy) |
| 1 | 2 | 1-3 | Light air | Calm (rippled) |
| 2 | 5 | 4-6 | Light Breeze | Smooth (Wavelets) |
| 3 | 9 | 7-10 | Gentle Breeze | Slight |
| 4 | 13 | 11-16 | Moderate Breeze | Slight Moderate |
| 5 | 19 | 17-21 | Fresh Breeze | Moderate |
| 6 | 24 | 22-27 | Strong Breeze | Rough |
| 7 | 30 | 14-17 | Near Gale | Rough - Very Rough |
| 8 | 37 | 34-40 | Gale | Very Rough - High |
| 9 | 44 | 41-47 | Strong Gale | High |
| 10 | 52 | 48-55 | Storm | Very High |
| 11 | 60 | 58-63 | Violent Storm | Very High |
| 12 | - | >64 | Hurricane | Phenomenal |

Table 4.15 2015 UK storms

| Name | Date Named | Date of Impact on UK/Ireland |
|---|---|---|
| Abigail (Data Available) | 10 November | 12 - 13 November |
| Barney (Data Available up to 17th) | 16 November | 17 - 18 November |
| Clodagh (Data Not Available) | 28 November | 29 November |
| Desmond (Data Available on 4th and 5th) | 4 December | 5 - 6 December |

and are formed in the Atlantic Ocean. In the next sub sections, we show the results for the weather based LQE during November and December 2015.

### 4.4.3 Weather Based LQE Results in November and December 2015

In this subsection, we display the sub optimal values and the optimal values for November period when Abigail, Barney and Clodagh impacted the UK. According to the simulation data, we find that because data is missing in both months due to winds affecting the receiver end and the supply of power, it was possible to collect storm data for Abigail, partially on Barney and Desmond which was the storm that severely impacted Lancaster city and the University. We observe that optimal data for both months remain the same with minimal disruption for S+L when the storm was approaching on the 10th of November. On graph 4.5 using parameters

listed in table 4.16, there is a rapid descent in air pressure from approximately 1000 hPa down to approximately 980 hPa and then rising to 1000 hPa within 4 hours. Between the 16th and 17th of November, we see oscillations in air pressure which signals the incoming of another storm (Barney) and we observe very little effect on the S evil switching graph, but none in the S+L evil switching graph.

During the 4th of December, in graph 4.6 with parameters listed on table 4.19, we observe the incoming of storm Desmond as air pressure falls from around 1020hPa down to approximately 991 hPa during the 5th of December. We observe only two outages with S+L, but many are observed during the midnight of the 4th of December 2015.

Table 4.16 November 2015 Sub Optimal Values

| November 2015 | Value |
| --- | --- |
| Total Traversed Readings: | 86156 |
| Usable Traversed Readings: | 82348 |
| Evil Switches on S | 524 |
| Evil Switches on S+L | 65 |
| Time spent with S 868 Mhz: | 2564079 |
| Time spent with S+L 868 Mhz: | 1480533 |
| Score Threshold: | 0.3 |
| Temp Threshold: | -2.4 |
| Humidity Threshold: | 48 |
| Pressure Threshold: | 1024.59 |
| Temp Ratio: | 0.95 |
| Humidity Ratio: | 1.05 |
| Pressure Ratio: | 1.03 |
| Temp Weighting | 0.25 |
| Humidity Weighting | 0.25 |
| Pressure Weighting | 0.5 |

Table 4.17 November 2015 Optimal Values

| November 2015 | Value |
| --- | --- |
| Total Traversed Readings: | 86211 |
| Usable Traversed Readings: | 79312 |
| Evil Switches on S: | 524 |
| Evil Switches on S+L: | 29 |
| Time spent with S 868 Mhz: | 2564079 |
| Time spent with S+L 868 Mhz: | 1876713 |
| Score Threshold: | 0.3 |
| Temp Threshold: | 16.59 |
| Humidity Threshold: | 57.0 |
| Pressure Threshold: | 991.59 |
| Temp Ratio: | 0.95 |
| Humidity Ratio: | 1.05 |
| Pressure Ratio: | 1.03 |
| Temp Weighting | 0.25 |
| Humidity Weighting | 0.25 |
| Pressure Weighting | 0.5 |

Table 4.18 December 2015 Sub optimal Values

| December 2015 | Value |
|---|---|
| Total Traversed Readings: | 21462 |
| Usable Traversed Readings: | 20717 |
| Evil Switches on S | 32 |
| Evil Switches on S+L | 14 |
| Time spent with S 868 Mhz: | 744230 |
| Time spent with S+L 868 Mhz: | 698488 |
| Score Threshold: | 0.3 |
| Temp Threshold: | -1.6 |
| Humidity Threshold: | 48 |
| Pressure Threshold: | 1021.9 |
| Temp Ratio: | 0.95 |
| Humidity Ratio: | 0.95 |
| Pressure Ratio: | 1.03 |
| Temp Weighting | 0.25 |
| Humidity Weighting | 0.25 |
| Pressure Weighting | 0.5 |

Table 4.19 December 2015 Optimal Values

| November 2015 | Value |
|---|---|
| Total Traversed Readings: | 25432 |
| Usable Traversed Readings: | 24701 |
| Evil Switches on S: | 32 |
| Evil Switches on S+L: | 2 |
| Time spent with S 868 Mhz: | 744230 |
| Time spent with S+L 868 Mhz: | 737148 |
| Score Threshold: | 0.3 |
| Temp Threshold: | 16.59 |
| Humidity Threshold: | 57.0 |
| Pressure Threshold: | 991.59 |
| Temp Ratio: | 0.95 |
| Humidity Ratio: | 1.05 |
| Pressure Ratio: | 1.03 |
| Temp Weighting | 0.25 |
| Humidity Weighting | 0.25 |
| Pressure Weighting | 0.5 |
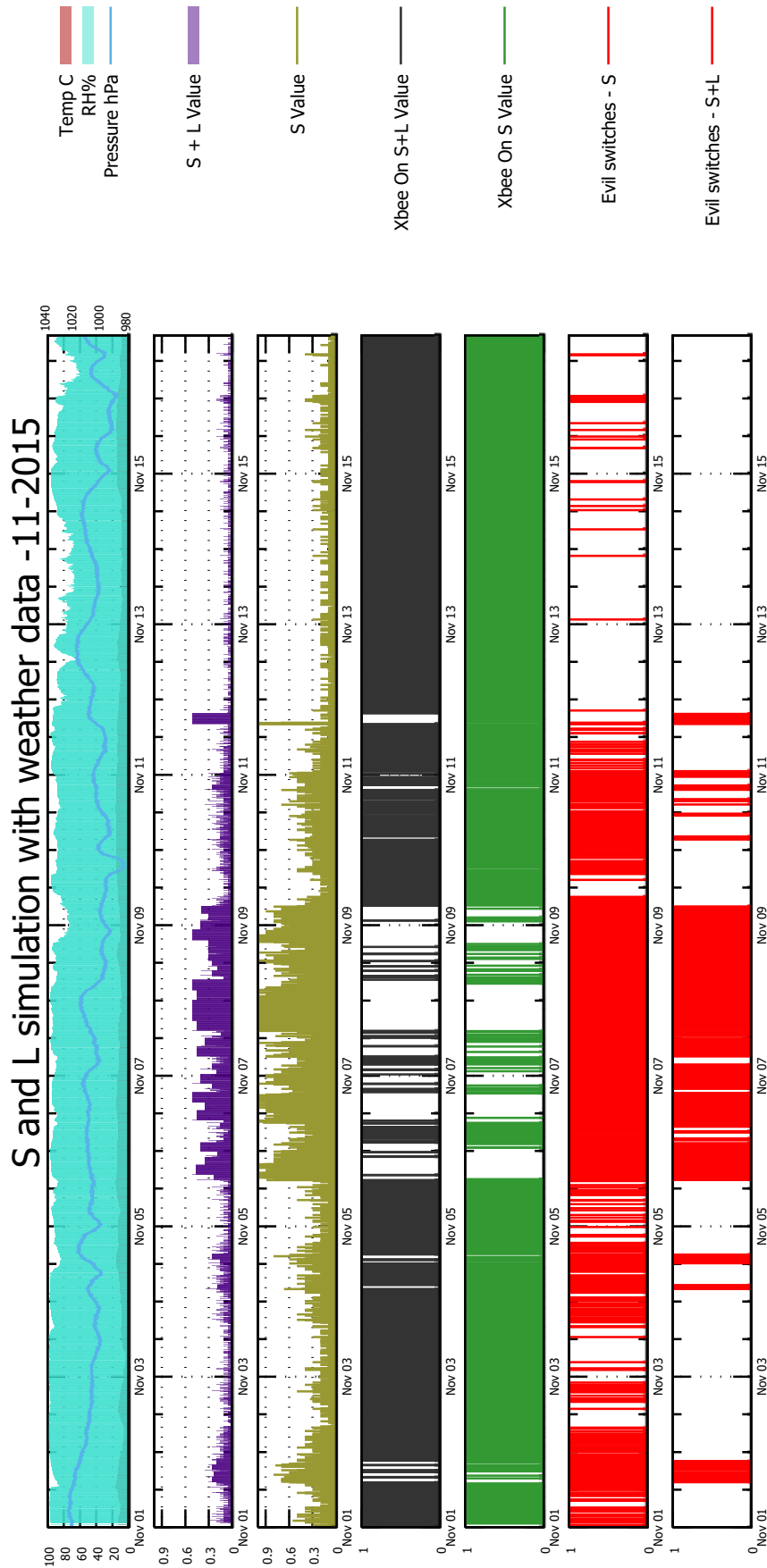
Fig. 4.5 November 2015 period from the 1st to the 17th November
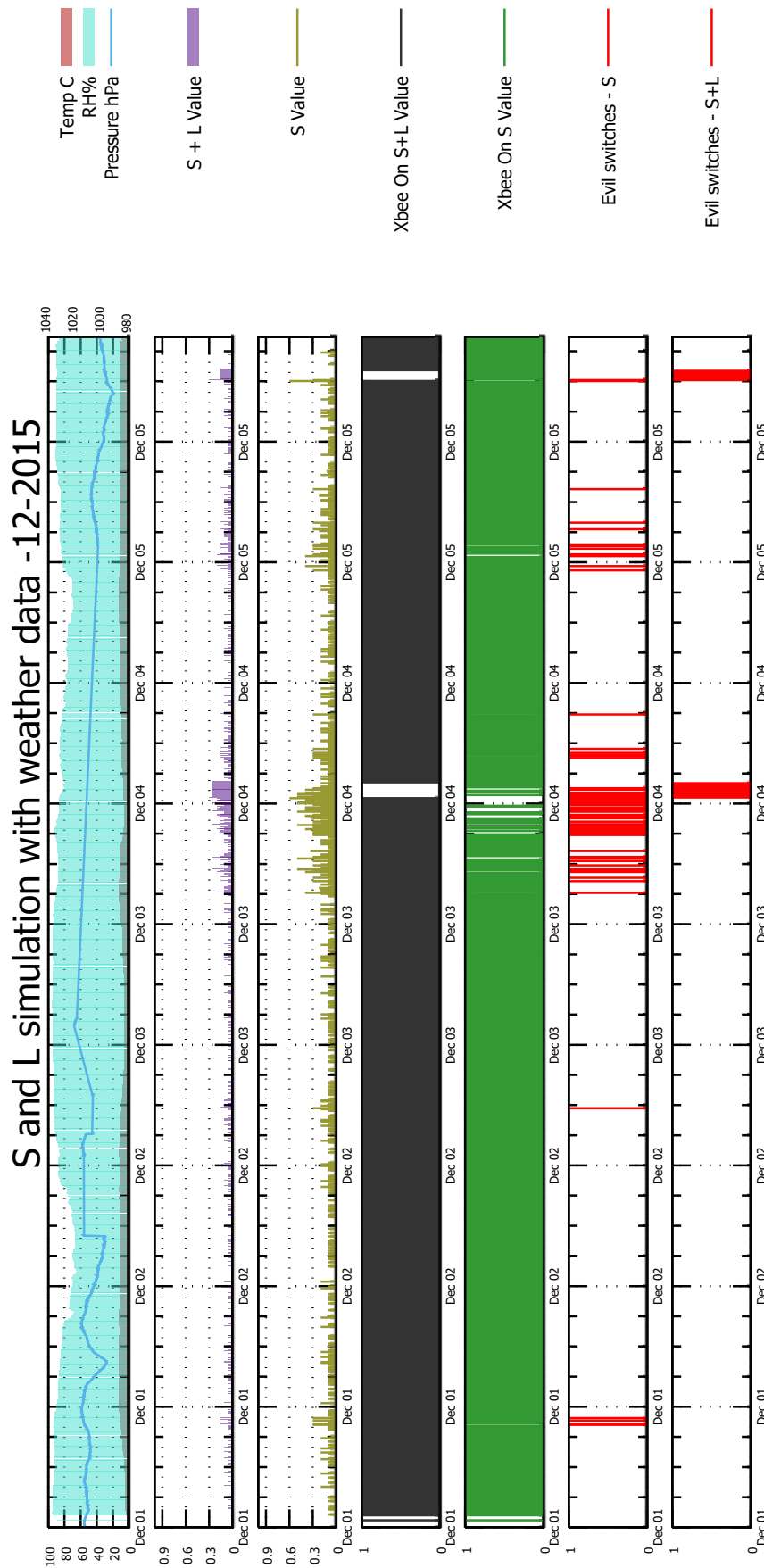
Fig. 4.6 December 2015 period from the 1st to the 5th December

## 4.5   Chapter Summary

In this chapter, we looked at what short and long term LQE's accomplish and highlight that long term LQE's can be useful to reduce network switching which short term LQE's fail to accomplish. We then looked into detail how the weather based link selection scheme works in deciding when to best select which radio transceiver based on predefined rules and weather data previously collected. We also define a blocking decision algorithm that blocks the node to check for new data based on how the weather is which has certain advantages for small nodes where energy is a constraint. An evaluation as to how the link selection scheme performed was given demonstrating that it does eliminate more than 98% of evil switching at the cost of utilizing a cheaper radio. However it should be noted that fetching parameters from one month to the next needs to be profiled beforehand to get values close to the optimal values in order to achieve optimal efficiency in switching although a full month of data is not required as per our results obtained during the 2015 storms.

In our tests, we find that in some months, it can significantly reduce switches taking place - in May 2015, we noticed a reduction from 1407 switches to just 34 in table 4.11 which is a reduction of 98.23% switches potentially taking place in May, by using values as shown in table 4.3. We conducted experiments to show that it is possible to profile the next month by running results on the previous month which will yield results that is close to optimal values. We also ran similar tests using different weights in 2014 and 2015 and we found that changing weights can affect the effectiveness on how effectively switching occur.

One optimization problem we have encountered is that certain value combinations can yield a different efficiency result; for example, changing any parameter will either increase or decrease 868 Mhz switching efficiency. Another problem we face is that we cannot use the same values throughout the year, although it may be possible to find best values for certain types of weather conditions. We also observe that by altering weight values, we can limit the amount of S+L switching taking place as seen in figures 4.2 and 4.3. To improve the

Fig. 4.7 Storm Desmond - Lancaster Flooded

reliability of the algorithm, we have run the algorithm to test two months in 2015 which are May and June. It is possible to use the values from the previous month and use them on the next month with a small penalty of 75600 seconds as can be seen in tables 4.2, 4.9 and 4.11.

An evaluation was given as to how the radio link selection scheme performed and then highlighted an optimization problem which can be solved by mapping the previous month to fetch parameters for the next month of usage with minor penalties.
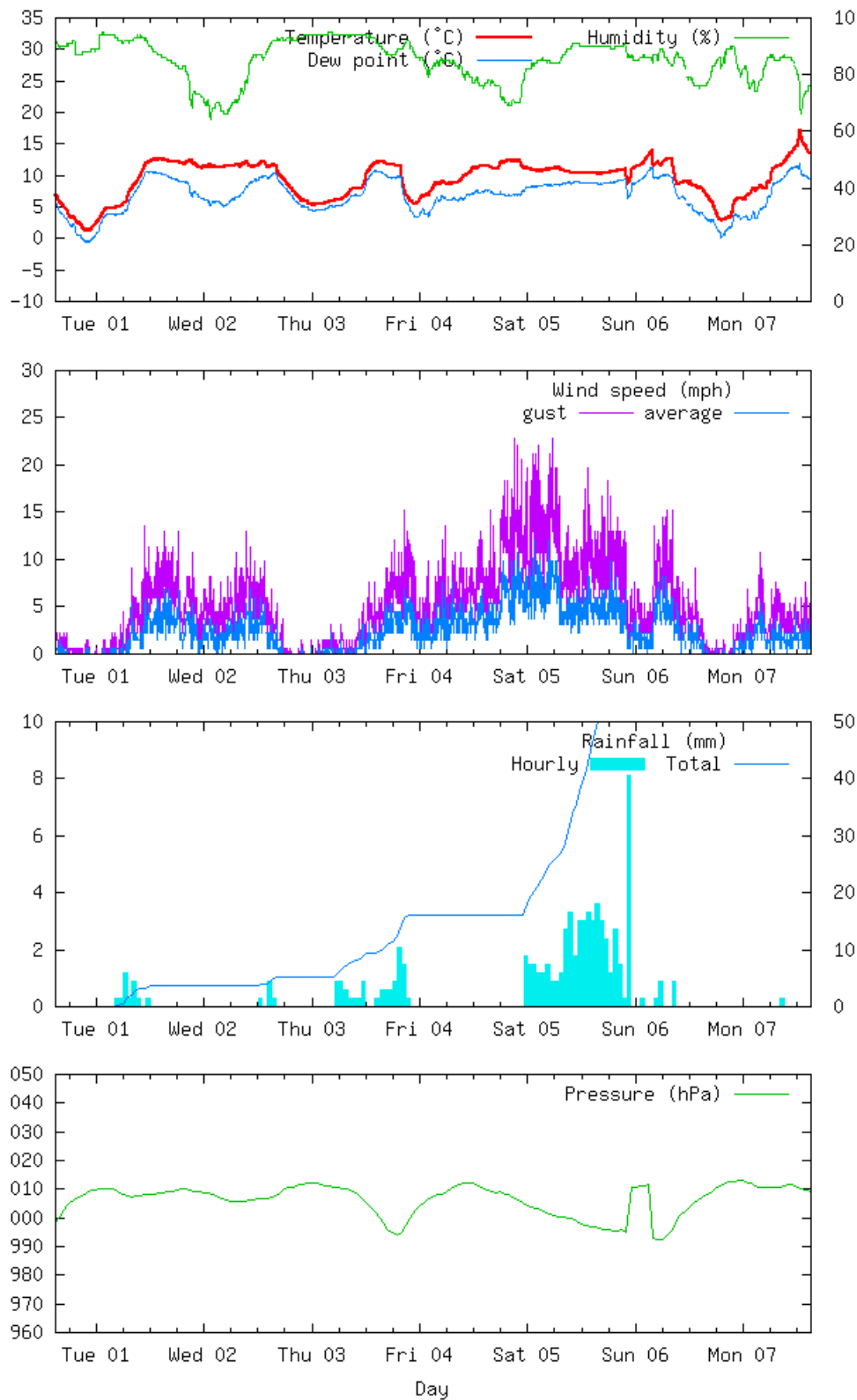
Fig. 4.8 Weather chart of Storm Desmond's approach and impact as seen on the sudden jump and decline of air pressure during late Saturday evening and Sunday morning. Total rainfall was off the charts as it exceeded normal rainfall expectations.

# Chapter 5

# Prototyping, deploying and evaluating open architecture RTU

## 5.1   Chapter Overview

In the first chapter, we gave a brief overview of an RTU that would be part of our contribution in order to develop the technologies required to develop our weather based link quality estimator. In this chapter, we shall give an over view of the prototype that was built for the project, the hardware components used and what software was used to be able to make a working 5 volt RTU prototype a reality.

## 5.2   Implementation Of RTU

In this section, we shall give an overview of how the prototype Remote Terminal Unit (RTU) was built using off the shelf components available in electronic specialist stores. We will split this section into three sub sections; requirements, hardware and software.

### 5.2.1  Requirements

The Remote Terminal Unit's primary goal was to be able to be run on a pumping station that are remotely located from one another and be able to communicate between each other if failure should occur on one of the neighbouring sub stations. This is a complete different outlook as to what the water company currently has which is a centralised SCADA approach with one point of failure. The unit should ideally be easy to replicate and inexpensive to replace with off-the-shelf (OTS) components that are ideally not closed architectures as these tend to lock in the buyer with specialist software. On the field with respect to security (RTU's in sub stations do not require to be connected to the Internet which unnecessarily opens up to security threats which are more costly to manage), these units will not be networked to the Internet and thus, they should be able to have their own time keeping hardware, such as a real time clock and are accessed by a an experienced operator who would visually inspect if the RTU is operating or not. There should also be a power switch or reset button that the operator can use if the RTU should require a restart or power up/down. The device should also have some capability to allow manual control over the pumps if there is a need by the operator.

The inputs for the RTU will be via an ultrasonic sensor that senses water levels in the wet well. When this level alters, this will cause the software to either activate, or deactivate the switch, causing the actuator to either turn on or off respectively.

### 5.2.2  Hardware Components

**Ultrasonic Sensor**

The model used was an OsiSense xx918a3c2m12 ultrasonic sensor cylindrical M18 - Sn 0.5 m - 4..20mA with a M12 connector. The sensor itself required its own power source as the operating range range is between 10V and 28V. It has 4 wires which two of them were used

for power and the remaining third was to provide an input sensing water levels. The fourth wire was not used as it is used for training the sensor. See figure A.5 for data sheet and figure 5.1 for the actual sensor.



Fig. 5.1 OsiSense Analog Ultrasonic sensor.

**Communications**

In communicating with other RTU's and the main central computer, a GSM modem (Huawei E220) and a cheap radio transceiver (such as the XBee series 5 in figure 5.2) would interface with the software communication module. These radio nodes would be connected to the RTU and use the communication module called FIS COM which is later explained in this section. In order to correctly interface an xbee radio, it was necessary to use a USB xbee explorer which is a separately purchased device which allows the user to plug in the xbee to a USB controlled interface which then API commands can be sent to the modem for user configuration. For Xbee 868 Mhz pro series 5 data sheet, see figure A.4 and [6] for the manual.
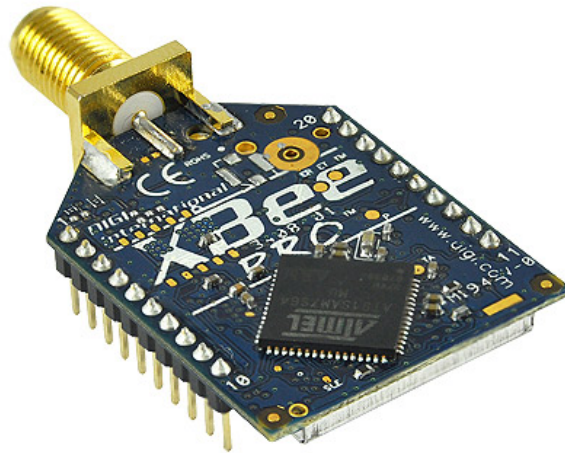
Fig. 5.2 Xbee Pro 868 Mhz series 5.

**Raspberry Pi Model B**

Since 2012, the Raspberry Pi has undergone several revisions and has a bare bone stripped version which is cheaper to run. The one acquired at the time was the Raspberry model B R2 as seen in figure 5.3. The R2 had a more reliable USB power line than the fist revision hence the xbee transceiver could not be used to its full power of 500mA with a transmit power of 315mW which was needed for the test bed experiments.



Fig. 5.3 Raspberry Pi model B Rev 2.

**Gertboard**

The Gertboard is an IO electronic multi-purpose board that attaches onto the Raspberry Pi via the GPIO pins and uses all 26 pin outs. It has 12 buffered outputs which are from 0V to 3.3V as seen on figure 5.4.
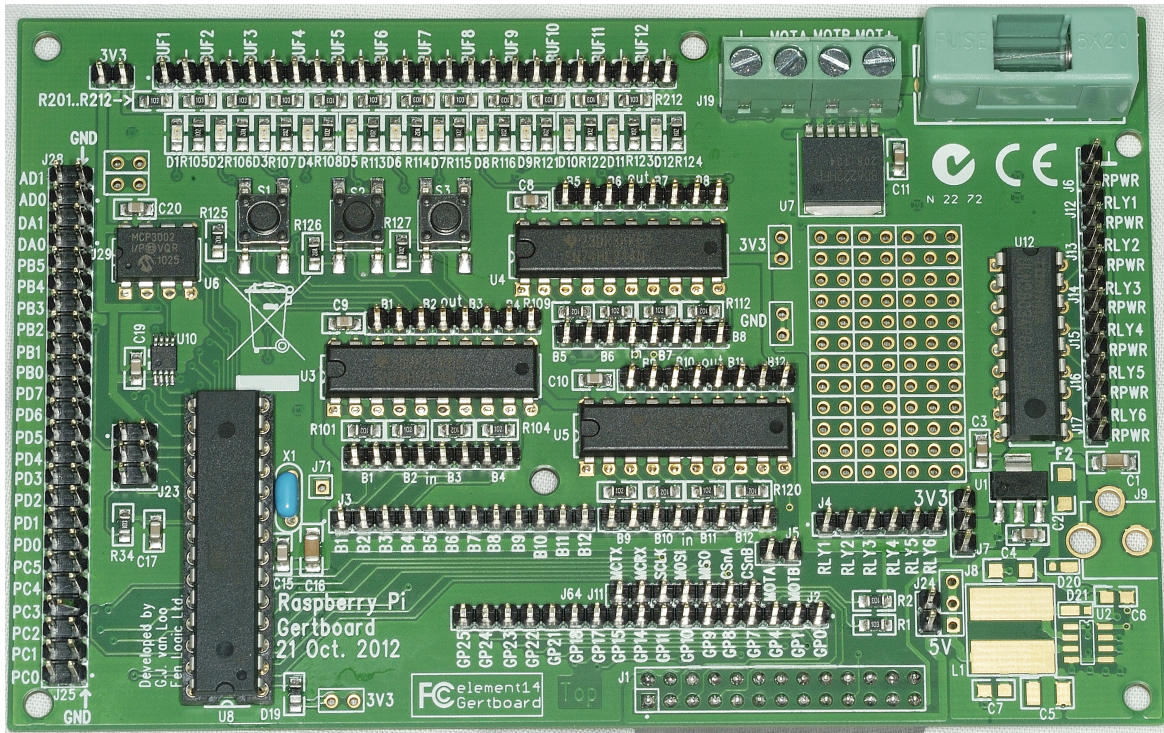


Fig. 5.4 Gertboard.

**Euro Card**

A standard euro card (see figure 5.5) was used to be able to solder on components required that interfaces the IO channels from the Gertboard to the actual devices such as the real time clock (see figure 5.6), actuators, and LED light status.

**Realtime clock**

The Raspberry Pi does not come with a real time clock and so one was attached to the Euro Card to be able to provide accurate time stamps as these units will not be connected to
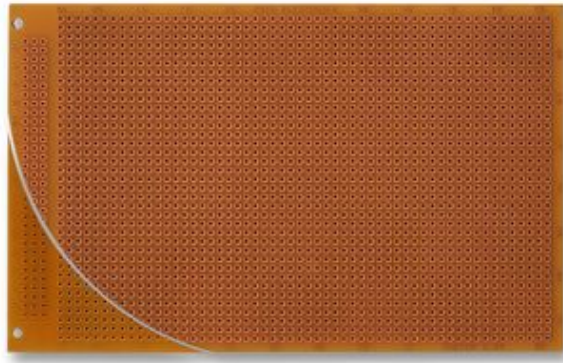
Fig. 5.5 Euro card used to interface with the gertboard and external devices.
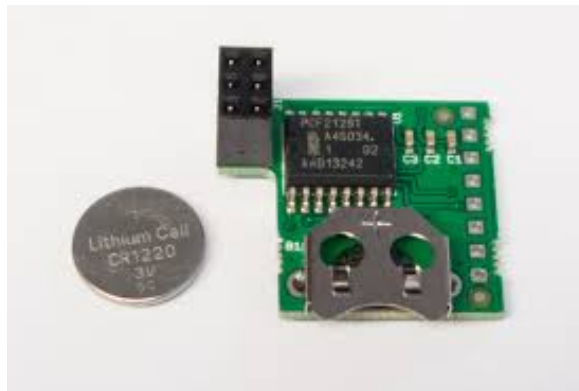


Fig. 5.6 RAS clock.

the Internet. We used a RASclock from Afterthought which uses a 3.3V power line and communications were linked by plugging it on to the euro card and making connections to the gertboard. Since this uses I2C communications with the raspberry pi, at boot time, it would fetch the time and then switch back to Serial Peripheral Interface (SPI) required for other IO operations.

**LED And Power Switch**

These are standard LED lights that are placed on pre drilled holes to give the operator some indication if there is an error. These give the status on whether a software module is on/off such as the AI aspect and the communication core and which pumps are on/off.

**DC to DC Booster**

A boost to the signal from the Gertboard which is a 3.3V line to a 15V line was needed to turn the switch on or off. This enabled the software AI module to send a digital signal that was converted via the DAC chip onboard the Gertboard which was then boosted from a 3.3V signal to 15V signal. A transistor (metal–oxide–semiconductor field-effect transistor) was used to activate the relay via the DC to DC booster whenever it detected a high signal. These can be seen in figure 5.7.
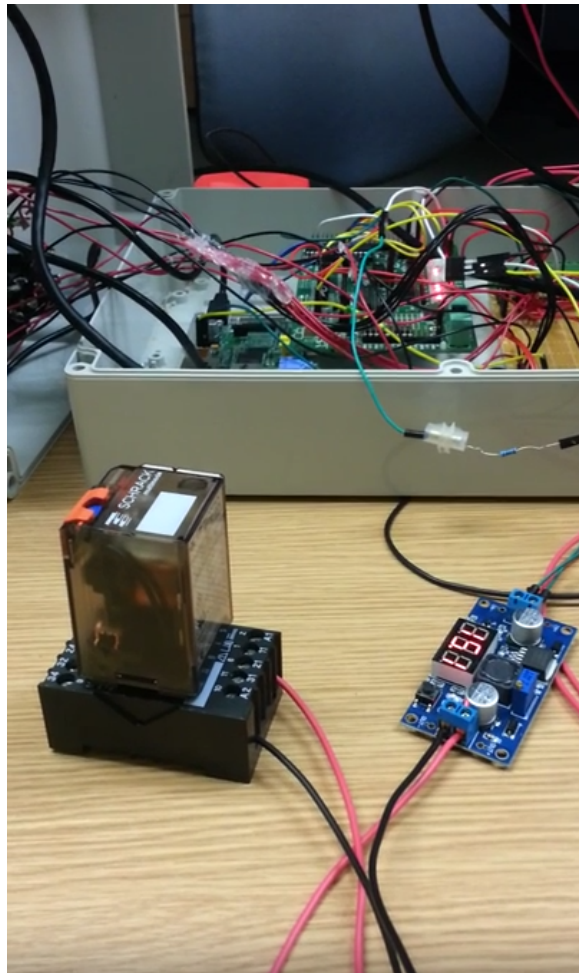


Fig. 5.7 A photo of the switch bottom left, DC to DC booster on the right and the RTU.

**Actuator Switch**

These switches are required to turn the pumps on or off. These require a high voltage of 12V to 15V to activate/deactivate. A series of experimental processes were conducted to use the ADC lines located on the left side of the board labelled AD0 for the ultrasonic sensor, DA0, DA1 for the pump switching but current was very limited. After many tests, it was found that opting for the buffered lines was the best option.

### 5.2.3   Assembly Of RTU

In this subsection, we will piece together the aforementioned components and visually present them how they were assembled together within Lancaster University's Infolab21 premises.

**Front Panel**

The front panel has two toggle switches and two push switches. Feedback is given on four LED lights which are for Pump1 (duty pump), Pump2 (storm pump), FISIO and FISALG which can be seen in figure 5.8. The two push buttons implemented are to reset the Raspberry pi (Rev2 has two pins which can be used as reset where as the first Raspberry pi lacked this feature). The functionality to allow an operator to change the AI algorithm on the RTU (Change AI function) was not implemented as there was only one algorithm available using the Mamdani FRB system and more thought was required in how to scale the design - perhaps by recompiling a different FISALG algorithm or integrating all algorithms into one single C file. Ultimately, the water utility company would use only one algorithm that is tried and tested. The remaining toggle buttons are for WatchDog and Power. WatchDog is an inbuilt algorithm in FISIO that detects when the toggle is either ON or OFF. If it is ON, it will not execute commands issued by FISALG. When it is OFF, it will resume normal FISALG operations. The power toggle feeds power to the RTU from the power source.

Fig. 5.8 RTU Front Panel.

The inside front panel connects the interfacing devices to the Eurocard which is placed inside the RTU as seen in figure 5.9. The connections on the side of the RTU is for USB connections, power and an RJ45 to establish SSH communications with the Raspberry Pi if required by an operator or if maintenance or upgrade is required. The grommets (rubber ports to prevent water ingress and allow wiring access to the RTU) on the bottom part of the panel is for output lines; for the ultrasonic sensor and switch wires.

**Inside The RTU**

Viewing the inside of the RTU, we see the eurocard which is brown and the Gertboard that sits on top of a Raspberry Pi as seen in figure 5.10. On the Eurocard, we have interfaces that link the Gertboard (digital signals) and outside of the RTU (Ultrasonic sensor and switch).
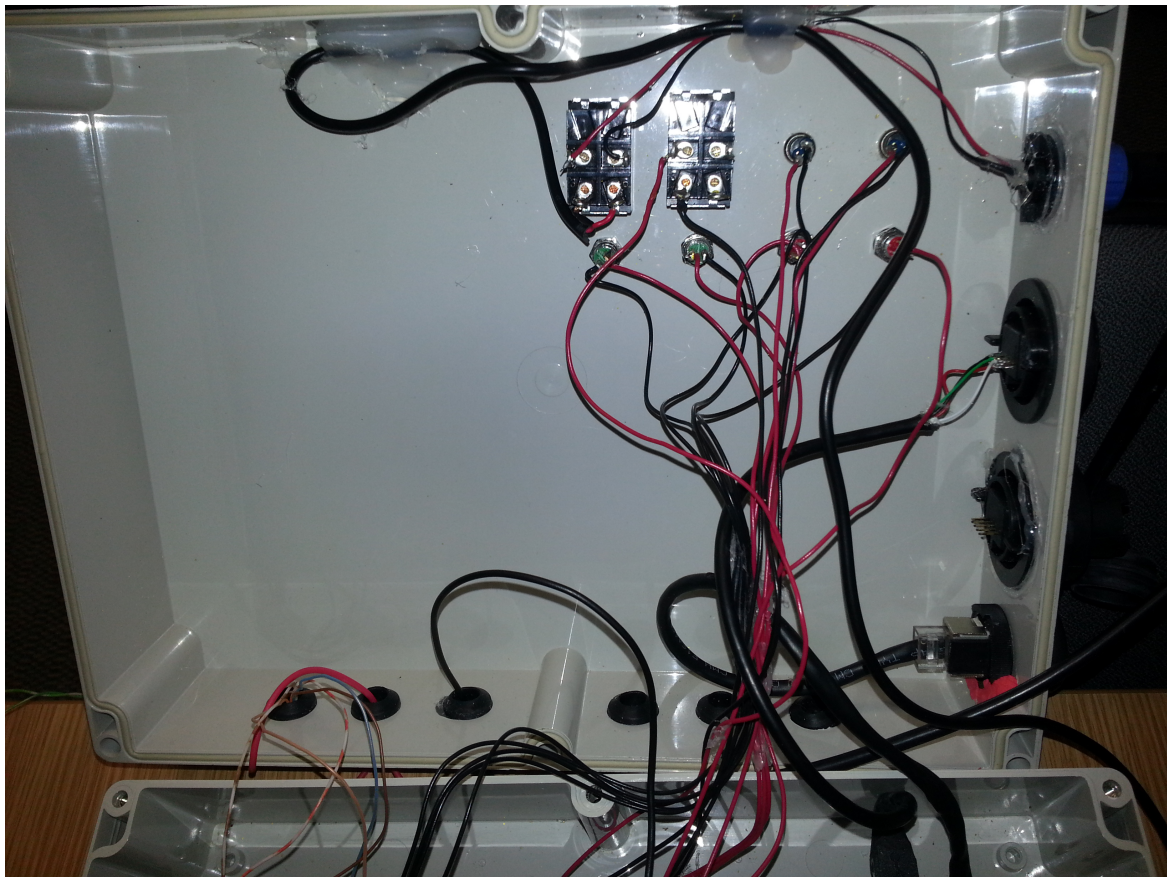
Fig. 5.9 RTU Inside Front Panel.

The DC to DC boosters sit on top of the eurocard which sends a signal to the switches which then activates/deactivates a pump.

## 5.2.4   Test Bed Used For Testing RTU

The test bed was built by another PhD student (Ben Green) who also researches Cyber Physical Systems and security systems in water utilities. We have two tanks which collects water with PVC pipes and valves; the left tank is a reservoir that simulates the inflow from Combined Sewage Overflows which is controlled separately from an external SCADA software, and the right tank is where it is emptied from simulating our pumping station. When the ultrasonic sensor detects a fast rate of change in rising water, this data is conveyed to the RTU and the algorithm (discussed under FISALG later) will decide if to activate the
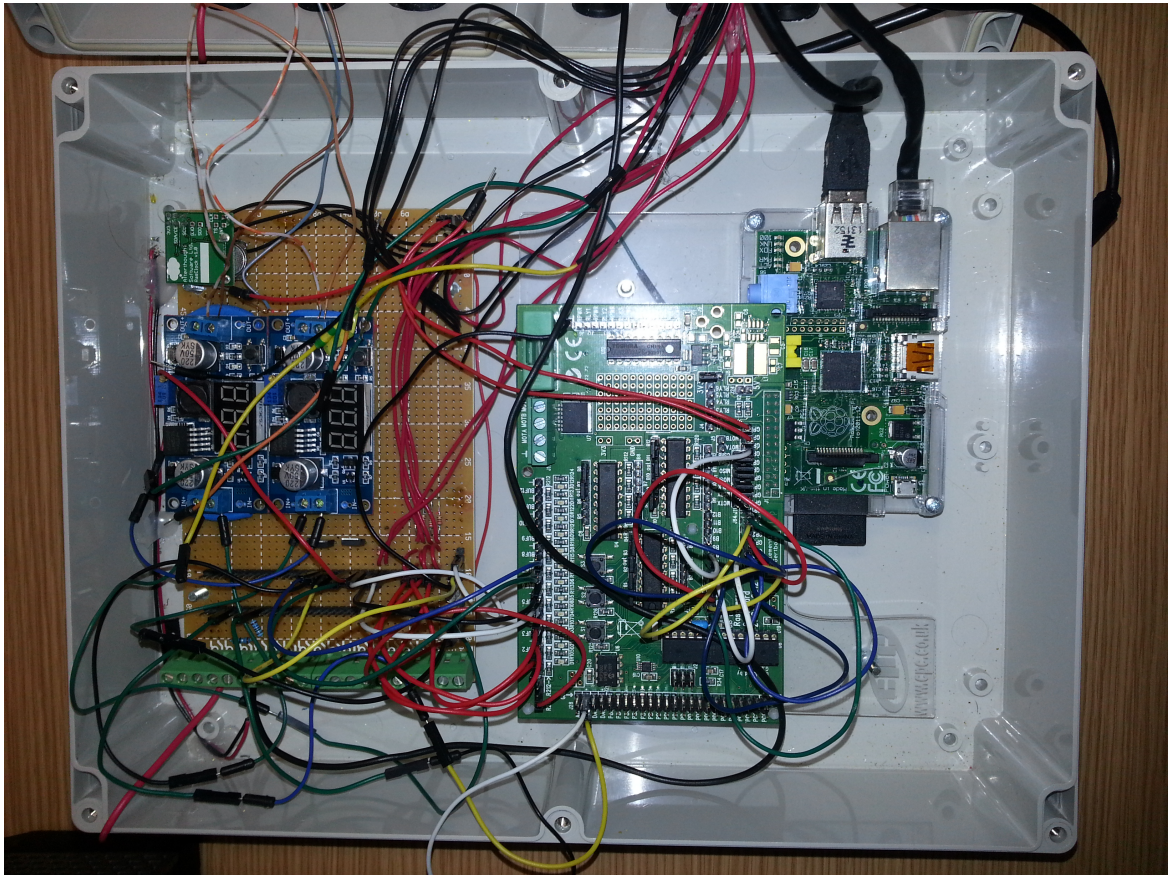
Fig. 5.10 Inside the RTU.

pumps or not. The duty pump which is located on the right will empty the tank, but inflow will keep ongoing until pump2 is activated which will stop all inflow - this has the same behaviour when having a duty pump and an assist storm pump which can pump out water at greater volumes. The RJ45 network socket serves as an interface between the RTU, the switches and ultrasonic sensor.

In figure 5.12, are the two switches which control the activation of the pumps and the left is a 24V Power Supply Unit (PSU) which will power up the ultrasonic sensor located on top of the right tank in figure 5.11.

Fig. 5.11 Test Bed used to test the RTU and algorithm.

### 5.2.5   Software Utilized - FISPI And Other Libraries

The RTU has software known as FISPI, which was written in ANSI C and uses external software libraries that are tried and tested by a community of developers that allow the FISPI modules to interact with the hardware aspect of the RTU.

**FISPI**

FISPI or Fuzzy Inference System PI, is the architecture for the modules responsible for sensing, acting and communicating states with other neighbouring sub station nodes. It is split into four modules mentioned below with the FISPI architecture in diagram 5.13.
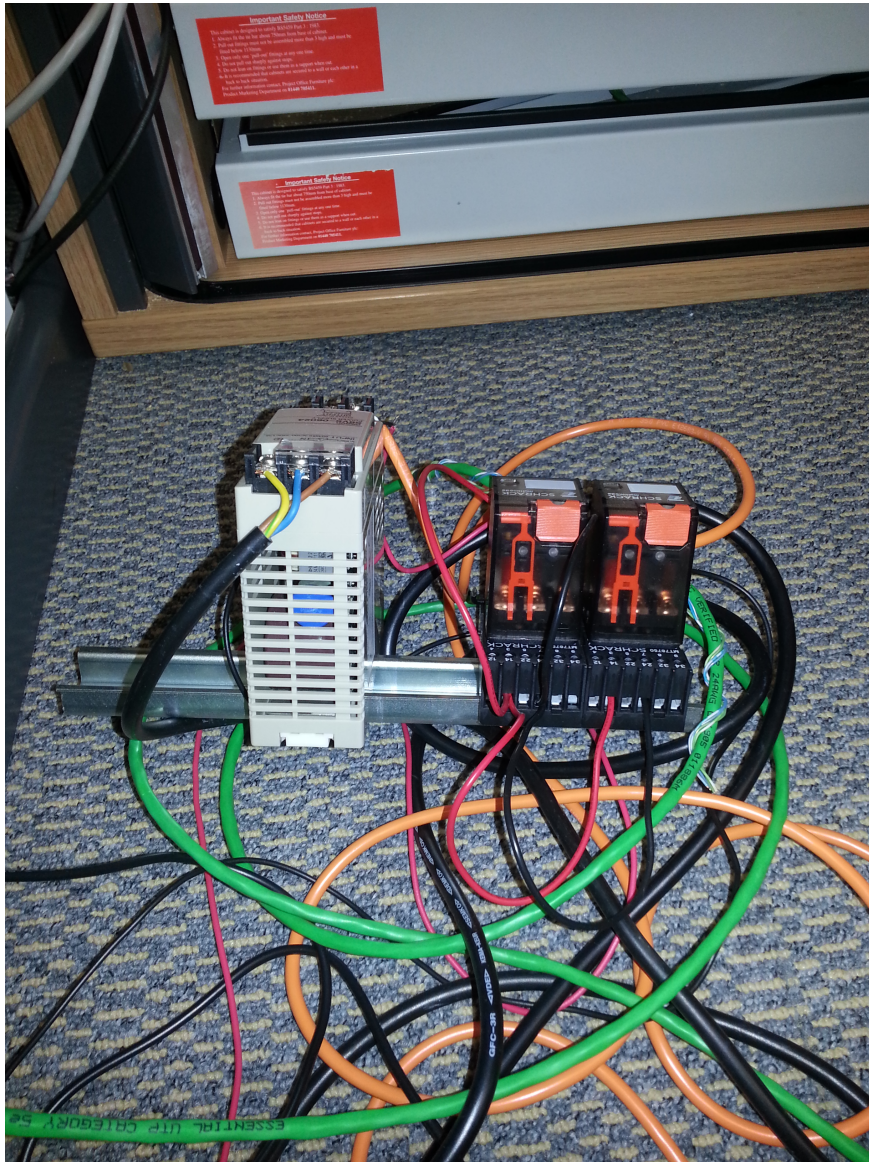
Fig. 5.12 Switches for the pumps and separate power source for ultrasonic sensor.

**FIS CORE**

This module handles all communications between the modules and is the first module to start up. This module opens a TCP port at port 5000 which the below mentioned modules then use to communicate.
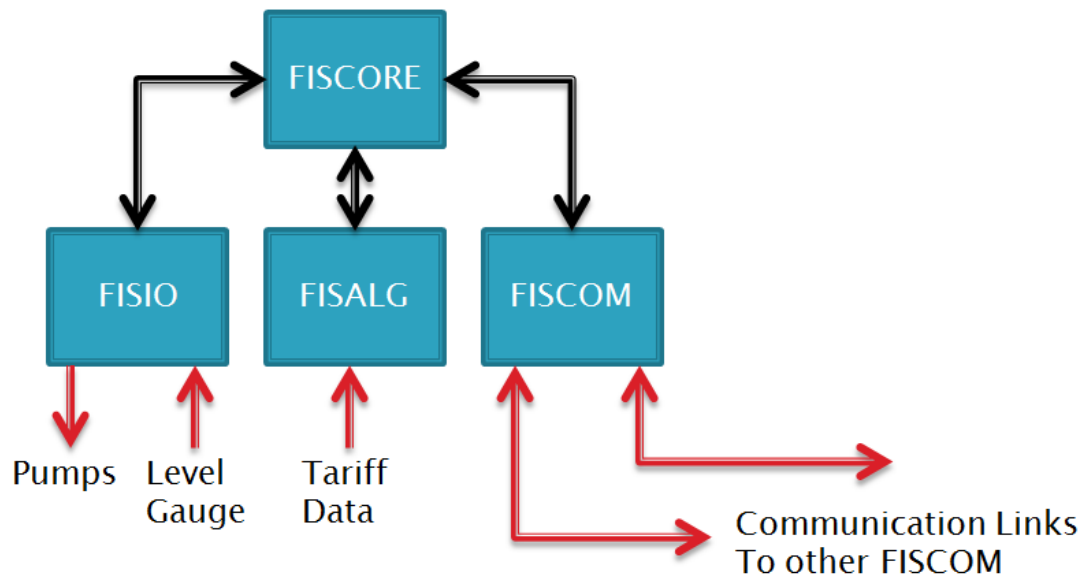
Fig. 5.13 FISPI architecture.

As seen in diagram 5.14, data is encapsulated with its core as the command (by type and ID) which is encapsulated by the header which routes it for processing and the destination component is the module to be addressed. The command is plain text such as:

```
fisio(well0 level 75)
```

Which means that the instruction goes to the local fisio module which is then processed as a WELL instruction to determine the wet well water level and attribute is 75 which means three quarters full. Other instructions exist such as:

```
fisio(LED0 ON/OFF)
fisio(PUMPx ON/OFF)
```
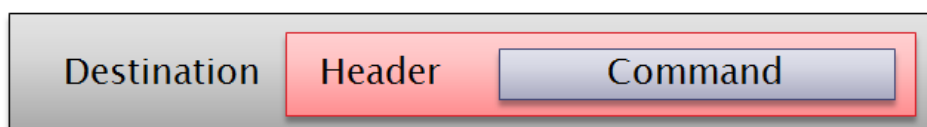


Fig. 5.14 FISPI data encapsulation.

**FIS ALG**

This is the Artificial Intelligent algorithm module that has C code that was translated from MATLAB. The type of AI implemented and tested on a real site is Mamdani. The AI is trained by having a text file which is read by the module and determines when are the best times to operate the pumps when energy tariffs are at it lowest (usually at night).

**FIS IO**

This module handles all aspects of the inputs and outputs that are being sensed by the module. It is responsible for sensing the water levels and activating or deactivating pumps.

**FIS COM**

This module sends and receives radio communications from the GPS and Xbee radio transceivers. The purpose of FIS COM was to predict when the 868 Mhz band is affected by meteorological environments and implement this new body of knowledge to develop the LQE. Its task would be to predict which radio link should be used, dependent on the online weather data received and make smart switching (can be from a local weather station as an example).

**Libraries**

WiringPi is a tested and community supported library which is available for free, that offers a layer of indirection and is readily usable for any developer. The WiringPi library was essential as it has code that makes hardware communications between the Gertboard IO channels and the actuators possible.

At the time of coding in 2013, the company Digi did not have available any software libraries that could be used by developers. At that time, a reliable library was libxbee which

provided function calls to be able to communicate with the xbee radio. After 2015, Digi released several software libraries written for C++, python and Java users.

## 5.3   Communication Component FIS COM

The remaining module which was not completed due to the sponsor company having no contact with us in 2014 hence this module was not implemented but envisaged as part of what ideally should be and unfortunately. In a future implementation, the module should contain the LQE that has been devised in section 4 and be able to predict which interface should be used by using online weather data. A routing layer should also be required to be implemented so that it can have a record of other neighbouring RTU's within a table. Since the LQE is reliant on weather data, an outdoor weather station can be used to feed information to the FIS COM module or fetch weather data via a weather cloud based service.

## 5.4   Evaluation Testbed

The RTU was tested in a small test bed that control water levels in small tanks (cereal size boxes sold in kitchen wear shops). One tank pumped water in which represents the wet well and the other tank is the reservoir of water which is reused to pump water into the wet well. Under normal conditions, the RTU reacts to changes once every minute although this can be changed to be much frequent or less frequent. Further calibrating of sensor input levels was needed so that values represented could be detected so that the RTU could start pumping out water.

During tests, we did observe the RTU pumping water out successfully and maintaining a level of water if the tariff level was too high indicating that some energy saving features of the RTU was present. However, we did not test how much energy we could save as this was part of another KTP project which the creator of this algorithm was doing at that time. We

have learned at a later date that the KTP's conclusion was that the algorithm did not deliver the energy efficiency that was promised.

## 5.4.1 Performance Of The RTU

Ben Green, who owns the test bed used for use in other projects, in his view, the RTU serves as a decentralised node to control and relay data to a central point supervisory control and data acquisition (SCADA) but at the moment, does not relay data to a central point (This was to be implemented in FISCOM). The prototype developed does not have the SCADA component as this was to be later developed and tested within Anglian Waters facilities. The RTU as it stands, measures and controls water levels in the tank (simulated wet well) and as far as it is known, this RTU is novel in terms that it only draws 5V current whereas other RTU's draw 24V to power up the RTU which would have advantages if a power outage would occur and required battery power instead.

## 5.4.2 Challenges In Developing The RTU

Developing the RTU was very challenging in trying to find reliable libraries that can be used for lower level communications. Building the hardware components together was also a challenge since experience in electronics was limited and it is recommended that any researcher taking this path should have a basic understanding in electronics if time is a constraint. Due to these limitations, the hardware aspect took longer to build as several difficulties were encountered, one being how to boost a digital signal from 3.3v to 15V. The the simplest and effective solution was taken and whilst conducting tests in a test bed laboratory setting, it emptied the tanks when they were at a particular level. We also noted that the tariff code also had an effect as it would not activate pumps as regularly during the day and it would activate more often during the night which is when the tariff is cheaper. The tariff list is a line of text which is used to train the AI system. Unfortunately due to

unforeseen circumstances, it was not possible to build and develop several more units and use the sponsor company's test bed to evaluate how the FISCOM module would work in a real setting.

## 5.5   Chapter Summary

In this chapter, we discussed how the RTU was built and assembled from electronic components and then discussed how the hardware aspect would communicate with the software modules. We highlighted that external libraries were used to communicate with the hardware components as time was an issue. We also discussed the FISPI architecture and went through each module outlining their roles with the RTU. The only module that was not completed was FISCOM due to resources not being made available and thus only one prototype was developed. The novelty in this prototype is mainly on the low voltage as RTU's use a higher voltage.

# Chapter 6

# Conclusions

## 6.1   Chapter Overview

In this chapter, we conclude the thesis in presenting the problems that we looked at, the hypothesis and how we validated our hypothesis. We then present our recommendations for future work that could be done in this area.

## 6.2   The Problem Presented In This Thesis

In the UK, water utility companies face challenges when wet wells are remotely located. These wet wells are important to mitigate flooding by pumping out excess water that are derived from rain, domestic and industrial waste water. These pumping stations require successful communications to send and receive basic instructions via remote terminal units. Today, efficient and reliable communications is a challenge due to long distances involved, geographical areas and environmental factors that affect radio propagation. Water utility project managers have recognized that a centralised communications model will have pitfalls and realise that communications should be a distributed model where each pumping station can make its own decisions to 1) mitigate flooding and 2) save pumping activations to

save on pump maintenance and energy costs. If communications were to be lost with the central computer from a SCADA network, the pumping stations should act on a smart algorithm that was pre-programmed, as the standard way of operating these pumping stations; sending a trained human operator to geographically remote locations to activate or deactivate pump switching. In the context of this thesis, we describe a problem which addresses the communications aspect; when a an RTU changes radio interfaces from a cheap radio to a more expensive and reliable GSM radio, it should do so in a smart way for the following reasons. Firstly, it should know when a network switch will happen because of incoming bad weather and secondly, to know when to switch itself back from the expensive to cheap radio link when conditions permits it. Thirdly, there are switching costs in terms of time taken; when doing frequent unnecessary switching, time is lost in updating the addresses of the neighbouring nodes and then switching back to the previous radio link within a very short time frame (within a 5 minute period as an example) and these switches should be kept to a minimum - we refer to this event as an evil switch.

In this thesis, we presented our three contributions as explained in section 1.

We summarise these as the following:

1) To better understand how meteorological aspects affect link quality - we looked on the 868 Mhz ISM band and GSM band.

2) Design a Link Quality Estimator based on what we learned from our first contribution to mitigate network switches between a cheaper and expensive radio link.

3) Use the LQE designed to make smart switches.

## 6.3   The Proposed Hypothesis

Traditional Link Quality Estimators are mostly short term LQE's and if these were to be used in this context, we would have a network that would be constantly switching within a short time frame. Hence, we proposed that if we understood how the weather affects the

868 Mhz band, we can understand when the cheaper 868 Mhz band will be likely to fail. The weather based Link Quality Estimator would be designed from real weather data and signal strength/packet losses and see if there are correlations between signal strength/packet losses with air pressure, air temperature and relative humidity. We then give a mathematical model of our LQE that describes when switching should take place and save switching costs. We proposed a mathematical model with the use of S which is for the short term link quality estimator that examines signal strength and S+L would be our weather based LQE that evaluates all three weather factors. If we see that there are packet drops exceeding a pre-defined threshold with S as our short term warning mechanism, we would then allow the algorithm to process S+L.

In section 3.3.1 that we saw a moderate to strong correlation in most days when there was activity in all three weather factors and we stated that the mathematical model would be based on the general premise that: If there is a significant change to air pressure or exceeds a pre-defined threshold AND there is a temperature increase or exceeds a threshold AND humidity is within a pre-defined threshold OR if there is a significant change to humidity. If these conditions evaluate to true, then we would apply a temporary time block to the cheap radio link and focus our use on the more expensive link.

By using the weather link quality estimator, we foresee that there would be less network switching from occurring and the novelty in this LQE is that it uses RSSI as a short term warning predictor which if there is a risk of radio link loss, the long term LQE would run to make a decision on weather the node should carry on using the cheaper or more expensive GSM radio link by examining current weather patterns.

## 6.4   Work Done To Validate Our Hypothesis

In this section, we give an overview on how we validated our hypothesis by summarising our test bed set up and our results.

### 6.4.1  Test Bed Platforms Developed

In section 3.3, we describe our test bed layout where we have two nodes located in the Infolab21 building, one was elevated and powered, and the other was outside and powered by batteries within the Infolab21 grounds. The elevated radio receives packets from Galgate and records the RSSI received or if a time out happens, record it as a dropped packet. The ground level only responds to AT commands and sends the RSSI result back to Galgate. We also had a local weather station installed which we then collect data and amalgamate this data with the signal strength and packet losses occurred.

These radio transceivers are about 1.25Km apart which is a realistic distance for our domain problem in the water utility sector. We collected data from the elevated and ground level to see if there were any marked difference between the two radio nodes located at the Infolab21 building. We saw from the graphs in section 3.3.1 that both nodes operated within the same RSSI levels and there was no need to carry on with the ground level investigations.

### 6.4.2  Experiments Carried Out

During 2014 and 2015, we collected data from the weather station and the elevated radio transceiver which has a raspberry pi connected to it that saves signal strength and packet drops. We analysed the hottest month which was June since we have high temperatures during the day and rapid cooling during the night causing humidity levels to fluctuate more than in the winter. During July 2014 period, we analysed signal strength and packet drops from the elevated radio transceiver and we correlated air pressure, temperature and humidity with packet losses and signal strength.

During July 2014, April 2015, May 2015, June 2015, November 2015 and December 2015, we ran our LQE weather based simulator based on the data captured and observe how our weather based LQE would perform. We looked into July period as we already stated it is the warmest period and November and December was the period where we had storms in

the UK. We did not look into other forms of measurements such as radio interference from nearby sources as an example and focussed solely on the three weather factors; air pressure, temperature and relative humidity.

We used a brute force algorithm to determine the best thresholds by analysing weather data, radio signal strength and packet drops so that we can use optimal thresholds to carry out our link switches. We then used these values on our simulator to determine how our weather based LQE would perform.

### 6.4.3   Results Obtained

During July 2014, we obtained weather data and signal strength data as well as packet drop data. We correlated the data with the three weather factors in July 2014 and we found that in most days when the weather was variable, we had a moderate to strong correlation in one, two or all weather factors. When the weather was stable, correlation was weak. On other days, the results were mixed and variable and thus, did not match what we expected. We then used this correlation to derive a general mathematical model that would be our weather based LQE which aims to predict when a switch should occur. We summarise the result tables with data that was used in this thesis.

During the warmest months in the summer period.

During July 2014, in table 4.8, we have a saving of 419 switches and time spent on the S+L LQE was 1729538 seconds and time spent on S LQE was 2303637 seconds.

During June 2015, in table 4.11, we have a saving of 1373 switches and time spent on the S+L LQE was 2171897 seconds and time spent on S LQE was 2505430 seconds.

We also included the stormiest months in 2015.

During November 2015, in table 4.17, we have a saving of 495 switches and time spent on the S+L LQE was 1876713 seconds and time spent on S LQE was 2564079 seconds.

During December 2015, in table 4.19, we have a saving of 30 switches and time spent on the S+L LQE was 737148 seconds and time spent on S LQE was 744230 seconds.

### 6.4.4  Analysis Of Results

In analysing the results of July 2014, we obtained a moderate to strong correlation when the days were variable indicating that changes in weather correlates with the three weather factors we analysed. If we were right in assuming that changes in air pressure, temperature and humidity caused a weaker signal, then we should be able to see this evidence on our simulations being run, otherwise, we would not be able to observe the link switching savings that this LQE should yield.

During our simulations, we modelled the LQE based on our observations during July 2014 and carrying out simulations on other months during the winter season and summer season. We observed in our experiments that the xbee 868 Mhz band suffered from signal strength degradation whereas a GSM modem was stronger due to a mast located nearby although the GSM was not impervious to extreme stormy weather. We did observe a reduction in link switching, but more importantly, a reduction in evil switching which we highlighted earlier was a factor we wanted to avoid as much as possible due to costs involved when performing constant link switching.

With this analysis, it would be recommended for any future wireless sensor industrial deployment using two or more radio interfaces (at least with a cheaper radio link and a GSM modem) located within a rural setting, to make use of an LQE that utilises frequently available weather data to be able to predict when outages might occur.

# 6.5    Future Work Recommendations

We will highlight some investigations required to properly assess the viability of this project which were not completed in time due to unforeseen circumstances relating to the sponsor water utility company.

## 6.5.1    Evaluating the Hardware Energy Efficiency of the RTU Build

We highlighted earlier that the RTU unit built is powered via a 5V line. Typically, all proprietary RTU's use 24V power as it needs a sufficient voltage line to be able to activate/deactivate the switches. It would be of benefit to know how much time and power this RTU can operate with emergency batteries when there is no power available to the sub station.

## 6.5.2    FIS COM Performance With Weather Based LQE

We also highlighted the FIS COM module that requires to be implemented within the FISPI architecture and evaluate how the weather based LQE performs in a real environment bearing in mind that data used for our simulations is real.

## 6.5.3    Simpler And Efficient FISALG Module

We learned that the algorithm that was developed by a partner University failed to deliver the energy savings that were promised to the sponsor company and thus have looked at working with another University in Lincoln. It would be possible to research an algorithm that may be simpler and more streamlined that does deliver the energy savings that the water utility company requires. This can be as simple as several IF statements or be more complex in AI such as fuzzy logic or Genetic Algorithms (which the attempt in Fuzzy Logic has already failed). The task would be to rewrite a new FISALG component that accept inputs and outputs from a new algorithm.

### 6.5.4   Using Parameters From Previous Months For LQE

We suggested a way of using data that is not arbritary to be able to predict when the LQE should decide which radio transceiver should be used. We did argue that it was possible to use previous data (ideally from previous month) as a way of training the system and then be able to use n-1 months of data to be used on the following month. How practical would this approach be in the real world?

# References

[1] Bbc - weather bomb hits power and travel in northern uk. http://www.bbc.co.uk/news/uk-30407295. [Online: accessed 01-05-2015].

[2] Ieee 802.11 standard. http://standards.ieee.org/getieee802/download/802.11-2012.pdf. [Online: accessed 13-09-2016].

[3] Texas instruments calculation and usage of lqi and rssi. https://e2e.ti.com/support/wireless_connectivity/w/design_notes/calculation-and-usage-of-lqi-and-rssi. [Online: accessed 13-September-2016].

[4] Ti cc2400 datasheet. http://www.ti.com/lit/gpn/cc2400. [Online: accessed 13-September-2016].

[5] Ti cc2420 datasheet. http://www.ti.com/lit/gpn/cc2420. [Online: accessed 13-September-2016].

[6] Xbee 868 series manual. http://ftp1.digi.com/support/documentation/90001020_F.pdf. [Online: accessed 13-September-2016.

[7] Zigbee technology. http://www.smkusa.com/usa/technologies/zb. [Online: accessed 01/10/2015].

[8] Daniel Aguayo, John Bicket, Sanjit Biswas, Glenn Judd, and Robert Morris. Link-level measurements from an 802.11b mesh network. *ACM SIGCOMM Computer Communication Review*, 34(4):121, 2004.

[9] Giuseppe Anastasi, a. Falchi, a. Passarella, M. Conti, and E. Gregori. Performance measurements of motes sensor networks. *Proceedings of the 7th ACM international symposium on Modeling, analysis and simulation of wireless and mobile systems - MSWiM '04*, page 174, 2004.

[10] Nouha Baccour, Anis Koubâa, Luca Mottola, Marco Antonio Zúñiga, Habib Youssef, Carlo Alberto Boano, and Mário Alves. Radio link quality estimation in wireless sensor networks. *ACM Transactions on Sensor Networks*, 8(4):1–33, September 2012.

[11] Nouha Baccour, Anis Koubâa, Habib Youssef, Maissa Ben Jamâa, Denis Do Rosário, Mário Alves, and Leandro B. Becker. F-LQE: A fuzzy link quality estimator for wireless sensor networks. *Lecture Notes in Computer Science (including subseries Lecture Notes in Artificial Intelligence and Lecture Notes in Bioinformatics)*, 5970 LNCS:240–255, 2010.

[12] Kenneth Bannister, Gianni Giorgetti, and S K Gupta. Wireless sensor networking for hot applications: Effects of temperature on signal strength, data collection and localization. *Proceedings of the 5th Workshop on Embedded Networked Sensors (HotEmNets 2008)*, pages 1 – 5, 2008.

[13] Carlo Alberto Boano, Kay Römer, and Nicolas Tsiftes. Mitigating the adverse effects of temperature on low-power wireless protocols. In *Proceedings - 11th IEEE International Conference on Mobile Ad Hoc and Sensor Systems, MASS 2014*, pages 336–344. IEEE, oct 2015.

[14] Carlo Alberto Boano, Nicolas Tsiftes, Thiemo Voigt, James Brown, and Utz Roedig. The impact of temperature on outdoor industrial sensornet applications. *IEEE Transactions on Industrial Informatics*, 6(3):451–459, 2010.

[15] K. Bullington. Radio Propagation at Frequencies above 30 Megacycles. *Proceedings of the IRE*, 35(10):128–136, 1947.

[16] Douglas SJ De Couto, Daniel Aguayo, John Bicket, and Robert Morris. A high-throughput path metric for multi-hop wireless routing. *Wireless Networks*, 11(4):419–434, 2005.

[17] Rohit Dube, Cynthia D Rais, Kuang-yeh Wang, and Satish K. Tripathi. Signal Stability based Adaptive Routing (SSA) for Ad-Hoc Mobile Networks. *Personal Communications, IEEE*, 4(1):36—-45, 1997.

[18] L. Montestruque et al. Csonet: a metropolitan scale wireless sensor-actuator network. In *Int Workshop on Mobile Device and Urban Sensing (MODUS)*, 2008.

[19] R Fonseca, O Gnawali, K Jamieson, and P Levis. Four-Bit Wireless Link Estimation. *HotNets*, pages 0–5, 2007.

[20] M. Gerharz, C. de Waal, M. Frank, and P. Martini. Link stability in mobile wireless ad hoc networks. In *Local Computer Networks, 2002. Proceedings. LCN 2002. 27th Annual IEEE Conference on*, pages 30–39, Nov 2002.

[21] V. C. Gungor and M. K. Korkmaz. Wireless link-quality estimation in smart grid environments. *International Journal of Distributed Sensor Networks*, 2012, 2012.

[22] M.P.M. Hall and C.M. Comer. Changes in radio field strength at v.h.f. and u.h.f. due to disintegration of reflecting layers in the troposphere. *Proceedings of the Institution of Electrical Engineers*, 117(10):1925.

[23] Reza Langari J Yen. *Fuzzy Logic: Intelligence, Control, And Information.* Pearson Education, 1999.

[24] S M Jiang, D J He, and J Q Rao. A prediction-based link availability estimation for mobile ad hoc networks. *in Proc. IEEE INFOCOM, vol. 3, Anchorage, AK, Apr*, pages 1745–1752, 2001.

[25] Woochul Kang, John a Stankovic, and Sang H Son. On Using Weather Information for Efficient Remote Data Collection in WSN. *Weather*, pages 1–5, 2008.

[26] Noble B Kim M. Mobile network estimation. *Proceedings of the Annual International Conference on Mobile Computing and Networking, MOBICOM*, pages 298–309, 2001.

[27] Dhananjay LaI Dhananjay LaI, A. Manjeshwar, F. Herrmann, E. Uysal-Biyikoglu, and A. Keshavarzian. Measurement and characterization of link quality metrics in energy constrained wireless sensor networks. *GLOBECOM '03. IEEE Global Telecommunications Conference (IEEE Cat. No.03CH37489)*, 1:446–452, 2003.

[28] KSAP Levis. Rssi is under appreciated. In *Proceedings of the Third Workshop on Embedded Networked Sensors, Cambridge, MA, USA*, volume 3031, page 239242, 2006.

[29] Gough Lui, Thomas Gallagher, Binghao Li, Andrew G. Dempster, and Chris Rizos. Differences in RSSI readings made by different Wi-Fi chipsets: A limitation of WLAN localization. *2011 International Conference on Localization and GNSS, ICL-GNSS 2011*, pages 53–57, 2011.

[30] Yunqian Ma. Improving wireless link delivery ratio classification with packet SNR. *2005 IEEE International Conference on Electro Information Technology*, pages 6 pp.–6, 2005.

[31] a B McDonald and T Znati. A path availability model for wireless ad-hoc networks. *WCNC 1999 IEEE Wireless Communications and Networking Conference Cat No99TH8466*, 1:35–40, 1999.

[32] J.M. Mendel. Fuzzy logic systems for engineering: a tutorial. *Proceedings of the IEEE*, 83(3):345 –377, mar 1995.

[33] Yu Song Meng, Yee Hui Lee, Boon Chong Ng, and Shao Ying Huang. Wind and rain influences on forested radiowave propagation. In *2007 IEEE Antennas and Propagation Society International Symposium*, pages 3748–3751. IEEE, 2007.

[34] Cesar Ortega-Corral, Luis E Palafox, J Antonio Garcia-Macias, Jaime Sanchez Garcia, Leocundo Aguilar, and Juan Ivan Nieto Hipolito. Transmission power control based on temperature and relative humidity. In *Intelligent Sensors, Sensor Networks and Information Processing (ISSNIP), 2014 IEEE Ninth International Conference on*, pages 1–6. IEEE, 2014.

[35] S. Ostojin, SR Mounce, and JB Boxall. An artificial intelligence approach for optimizing pumping in sewer systems. *Journal of hydroinformatics*, 13(3):295–306, 2011.

[36] Athanasios D. Panagopoulos, Pantelis-Daniel M. Arapoglou, and Panayotis G. Cottis. Satellite communications at KU, KA, and V bands: Propagation impairments and mitigation techniques. *IEEE Communications Surveys & Tutorials*, 6(3):2–14, 2004.

[37] Vidyasagar Potdar, Atif Sharif, and Elizabeth Chang. Wireless sensor networks: a survey. *2009 International Conference on Advanced Information Networking and Applications Workshops*, pages 636–641, 2009.

[38] Daniele Puccinelli and Martin Haenggi. Arbutus: Network-Layer Load Balancing for Wireless Sensor Networks. *2008 IEEE Wireless Communications and Networking Conference*, pages 2063–2068, 2008.

[39] Daniele Puccinelli and Martin Haenggi. Duchy: Double Cost Field Hybrid Link Estimation for Low-Power Wireless Sensor Networks. *Proceedings of the 5th Workshop on Embedded Networked Sensors (HotEmNets'08)*, pages 1–5, 2008.

[40] N Braithwaite S Ross, S Lewis. *Understanding The Weather - S189*. Open University Press, 2009.

[41] Pouria Sadeghi-Tehran, Ana Belen Cara, Plamen Angelov, Hector Pomares, Ignacio Rojas, and Alberto Prieto. Self-evolving parameter-free rule-based controller. In *Fuzzy Systems (FUZZ-IEEE), 2012 IEEE Int Conference on*, pages 1 –8, june 2012.

[42] Manfred Schütze, Alberto Campisano, Hubert Colas, Wolfgang Schilling, and Peter a. Vanrolleghem. Real time control of urban wastewater systems, where do we stand today? *Journal of Hydrology*, 299(3-4):335–348, December 2004.

[43] M. Senel, K. Chintalapudi, Dhananjay Lal Dhananjay Lal, a. Keshavarzian, and E.J. Coyle. A Kalman Filter Based Link Quality Estimation Scheme for Wireless Sensor Networks. *IEEE GLOBECOM 2007 - IEEE Global Telecommunications Conference*, pages 875–880, 2007.

[44] Kannan Srinivasan, Mayank Jain, Jung Il Choi, Tahir Azim, Edward S. Kim, Philip Levis, and Bhaskar Krishnamachari. The $\kappa$ factor. *Proceedings of the sixteenth annual international conference on Mobile computing and networking - MobiCom '10*, pages 317–329, 2010.

[45] John Thelen. Radio Wave Propagation in Potato Fields. *In Proceedings of the First Workshop on Wireless Network Measurements - WiNMee 2005*, 2:5, 2004.

[46] Alec Woo and David Culler. Evaluation of Efficient Link Reliability Estimators for Low-Power Wireless Networks. *Time*, pages 1–20, 2003.

[47] Yue Wu, Chunlei Shi, Mohammed Ismail, and Hakan Olsson. Temperature compensation design for a 2.4 GHz CMOS low noise amplifier. In *2000 IEEE International Symposium on Circuits and Systems. Emerging Technologies for the 21st Century. Proceedings (IEEE Cat No.00CH36353)*, volume 1, pages 323–326. Presses Polytech. Univ. Romandes, 2000.

[48] Akira Yamaguchi and Misato Sasaki. Evaluation of radio link selection with Analytic Hierarchy Process algorithm in heterogeneous radio networks. *Radio and Wireless ...*, pages 279–282, 2012.

[49] Shunzo Yamashita, Takanori Shimura, Kiyoshi Aiki, Koji Ara, Yuji Ogata, Isamu Shimokawa, Takeshi Tanaka, Hiroyuki Kuriyama, Kazuyuki Shimada, and Kazuo Yano. A 15/spl times/15 mm, 1 /spl mu/A, reliable sensor-net module: enabling application-specific nodes. In *2006 5th International Conference on Information Processing in Sensor Networks*, pages 383–390. IEEE, 2006.

[50] Jerry Zhao and Ramesh Govindan. Understanding packet delivery performance in dense wireless sensor networks. In *Proceedings of the 1st international conference on Embedded networked sensor systems*, pages 1–13. ACM, 2003.

# Appendix A

# Data Sheets
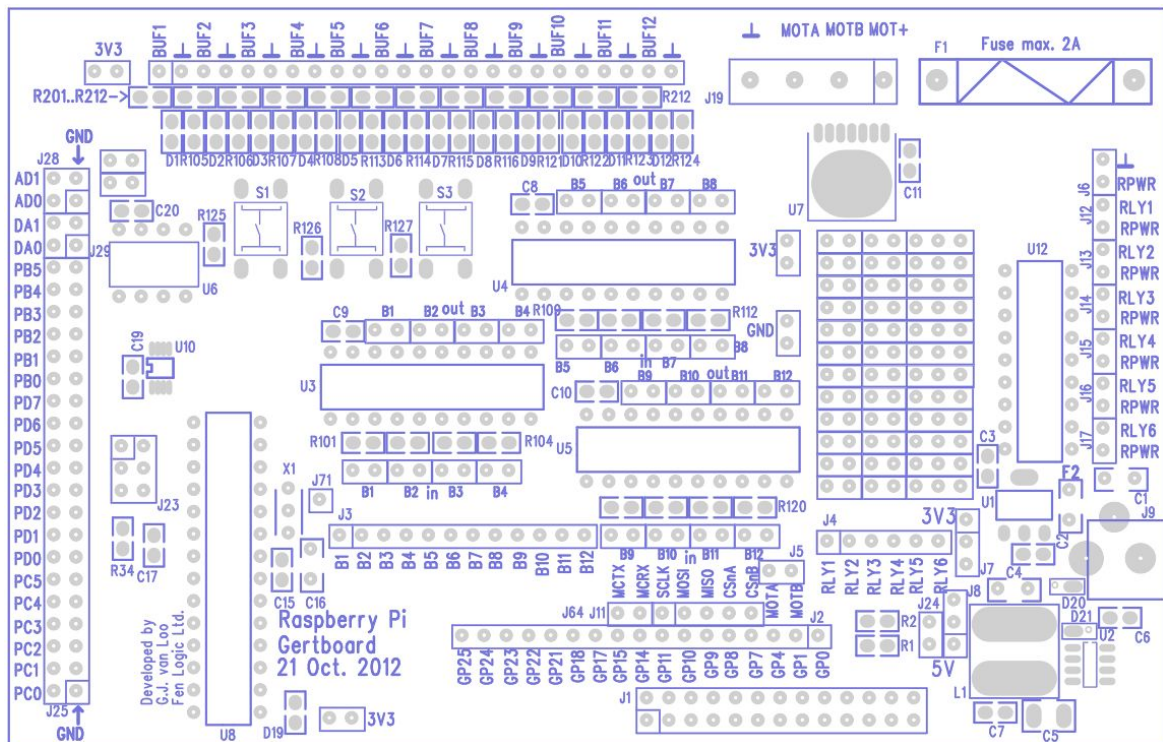


Fig. A.1 Gertboard schematic diagram.

| | | | |
|---|---|---|---|
| 3.3V | 1 | 2 | 5V |
| I2C0 SDA | 3 | 4 | DNC |
| I2C0 SCL | 5 | 6 | GROUND |
| GPIO4 | 7 | 8 | UART TXD |
| DNC | 9 | 10 | UART RXD |
| GPIO 17 | 11 | 12 | GPIO 18 |
| GPIO 21 | 13 | 14 | DNC |
| GPIO 22 | 15 | 16 | GPIO 23 |
| DNC | 17 | 18 | GPIO 24 |
| SP10 MOSI | 19 | 20 | DNC |
| SP10 MISO | 21 | 22 | GPIO 25 |
| SP10 SCLK | 23 | 24 | SP10 CE0 N |
| DNC | 25 | 26 | SP10 CE1 N |

Fig. A.2 Raspberry Pi R2 GPIO pinouts.

## Mechanical Drawings

Mechanical drawings of the XBee-PRO®RF Modules (antenna opstions not shown)
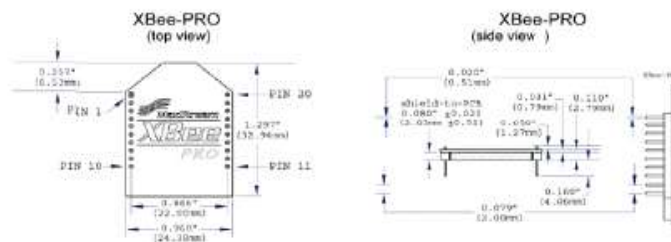


Mechanical Drawings for the RPSMA Variant
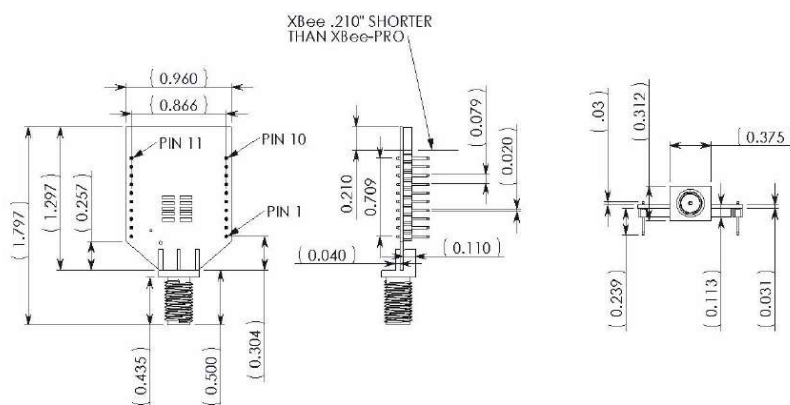


## Mounting Considerations

The XBee/XBee-PRO® RF Module (through-hole) was designed to mount into a receptacle (socket) and therefore does not require any soldering when mounting it to a board. The Development Kits contain RS-232 and USB interface boards which use two 20-pin receptacles to receive modules.

Fig. A.3 Xbee Pro 868 Mhz series radio transceiver used in our test bed experiments.

## Specifications

**Specifications of the XBee-PRO® 868RF Module**

| Specification | XBee-PRO® |
|---|---|
| **Performance** | |
| Indoor/Urban Range | up to 1800 ft (550 m) |
| Outdoor RF line-of-sight Range | up to25 miles (40 km) w/2.0 dB dipole antenna up to 50 miles (80 km) w/high gain antenna |
| Transmit Power Output | 85-500 mA, depending on power level setting |
| RF Data Rate | 24 kbps |
| Data Throughput | 2.4 kbps |
| Duty Cycle | 10% |
| Receiver Sensitivity | -112 dBm |
| **Serial Interface** | |
| UART | 3.3V CMOS (5V tolerant) |
| Data Rate (software selectable) | 1200 - 230400 bps (non-standard baud rates also supported) |
| **Power Requirements** | |
| Supply Voltage | 3.0 to 3.6 VDC |
| Operating Current | 500 mA typical (800 mA max) |
| Operating Current (receive) | 65 mA typical |
| Sleep Current | 55 μA typical @3.3 V |
| **General** | |
| Operating Frequency Band | SRD g3 Band (869.525 MHz) |
| Dimensions | 0.960" x 1.297" (2.438 cm x 3.294 cm) |
| Operating Temperature | -40 to 85 C (Industrial), 0 to 95% non-condensing |
| Antenna Options | 1/4 wave wire antenna, RPSMA RF connector, U.FI RF connector |
| **Networking & Security** | |
| Supported Network Topologies | Point-to-point, point-to-multipoint, peer-to-peer |
| Number of Channels | Single Channel |
| Addressing Options | Network ID, 64-bit addresses |
| Encryption | 128 bit AES |
| **Agency Approvals** | |
| Europe (CE) | Yes Italy 25 mW max (+14 dBm) Slovak Republic 10 mW max (+10 dBm) |
| RoHS | Lead-free and RoHS compliant |

Fig. A.4 Xbee Pro 868 Mhz series 5 data sheet.

*Product datasheet*
*Characteristics*

**xx918a3c2m12**

ultrasonic sensor cylindrical M18 - Sn 0.5 m - 4..20 mA - M12 connector

### Main

| | |
|---|---|
| Range of product | OsiSense XX |
| Sensor type | Ultrasonic sensor |
| Series name | General purpose |
| Sensor name | XX9 |
| Sensor design | Cylindrical M18 |
| Detection system | Diffuse |
| [Sn] nominal sensing distance | 0.5 m adjustable with remote teach push-button |
| Material | Plastic |
| Type of output signal | Analogue |
| Wiring technique | 4-wire |
| Analogue output function | 4...20 mA |
| [Us] rated supply voltage | 12...24 V DC with reverse polarity protection |
| Electrical connection | Male connector M12 4 pins |
| [Sd] sensing range | 0.051...0.508 m |
| Beam angle | 6 ° |
| IP degree of protection | IP67 conforming to IEC 60529 |

### Complementary

| | |
|---|---|
| Enclosure material | Valox |
| Front material | Epoxy |
| ISO thread | M18 x 1 |
| Supply voltage limits | 10...28 V DC |
| [Sa] assured operating distance | 0.051...0.508 m (teach mode) |
| Blind zone | 0...51 mm |
| Transmission frequency | 300 kHz |
| Repeat accuracy | 1.27 % |
| Deviation angle from 90° of object to be detected | -7...7 ° |
| Minimum size of detected object | Cylinder diameter 1.6 mm |
| Status LED | 1 LED (dual colour) for setting-up assistance<br>1 LED (green) for supply on<br>1 LED (yellow) for output state |
| Current consumption | 40 mA |
| Maximum switching capacity | 10...500 Ohm with overload and short-circuit protection |
| Voltage drop | < 1 V |
| Setting-up | Slope selection using teach button |
| Delay first up | 100 ms |
| Delay response | 25 ms |
| Delay recovery | 25 ms |
| Marking | CE |
| Threaded length | 43 mm |
| Height | 18 mm |
| Width | 18 mm |
| Depth | 79 mm |
| Product weight | 0.033 kg |

### Environment

| | |
|---|---|
| Standards | IEC 60947-5-2 |

**Telemecanique**
**Sensors**

Fig. A.5 Ultrasonic sensor data sheet used to test the RTU in a small scale test bed.

# Appendix B

# Table results and simulation graphs

Table B.1 September 2014 parameters

| Output for September 2014 | Value |
| --- | --- |
| Total Traversed Readings: | 66927 |
| Usable Traversed Readings: | 32318 |
| Evil Switches on S | 26 |
| Evil Switches on S+L | 9 |
| Time spent with S 868 Mhz | 2589945 seconds |
| Time spent with S+L 868 Mhz | 1415383 seconds |
| Score Threshold: | 0.3 |
| Temp Threshold: | 5.4 |
| Humidity Threshold: | 37.0 |
| Pressure Threshold: | 1025.19 |
| Temp Ratio: | 0.95 |
| Humidity Ratio: | 1.05 |
| Pressure Ratio: | 1.03 |
| Temp Weighting | 0.25 |
| Humidity Weighting | 0.25 |
| Pressure Weighting | 0.5 |

Table B.2 November 2014 parameters

| Output for November 2014 | Value |
|---|---|
| Total Traversed Readings: | 77178 |
| Usable Traversed Readings: | 71308 |
| Evil Switches on S | 106 |
| Evil Switches on S+L | 9 |
| Time spent with S 868 Mhz | 2585075 seconds |
| Time spent with S+L 868 Mhz | 2471734 seconds |
| Score Threshold: | 0.3 |
| Temp Threshold: | 13.89 |
| Humidity Threshold: | 49.0 |
| Pressure Threshold: | 980.29 |
| Temp Ratio: | 0.95 |
| Humidity Ratio: | 1.05 |
| Pressure Ratio: | 1.03 |
| Temp Weighting | 0.25 |
| Humidity Weighting | 0.25 |
| Pressure Weighting | 0.5 |

Table B.3 December 2014 parameters

| Output for December 2014 | Value |
|---|---|
| Total Traversed Readings: | 45850 |
| Usable Traversed Readings: | 40846 |
| Evil Switches on S | 255 |
| Evil Switches on S+L | 42 |
| Time spent with S 868 Mhz | 1522336 seconds |
| Time spent with S+L 868 Mhz | 1341236 seconds |
| Score Threshold: | 0.3 |
| Temp Threshold: | 11.09 |
| Humidity Threshold: | 46.0 |
| Pressure Threshold: | 984.4 |
| Temp Ratio: | 0.95 |
| Humidity Ratio: | 1.04 |
| Pressure Ratio: | 1.03 |
| Temp Weighting | 0.25 |
| Humidity Weighting | 0.25 |
| Pressure Weighting | 0.5 |

Table B.4 March 2015 parameters

| Output for March 2015 | Value |
|---|---|
| Total Traversed Readings: | 78926 |
| Usable Traversed Readings: | 61593 |
| Evil Switches on S | 745 |
| Evil Switches on S+L | 31 |
| Time spent with S 868 Mhz | 2626862 seconds |
| Time spent with S+L 868 Mhz | 2271603 seconds |
| Score Threshold: | 0.3 |
| Temp Threshold: | -2.09 |
| Humidity Threshold: | 47.0 |
| Pressure Threshold: | 985.59 |
| Temp Ratio: | 0.95 |
| Humidity Ratio: | 1.04 |
| Pressure Ratio: | 1.07 |
| Temp Weighting | 0.25 |
| Humidity Weighting | 0.25 |
| Pressure Weighting | 0.5 |

Table B.5 April 2015 parameters

| Output for April 2015 | Value |
|---|---|
| Total Traversed Readings: | 85991 |
| Usable Traversed Readings: | 71487 |
| Evil Switches on S | 717 |
| Evil Switches on S+L | 27 |
| Time spent with S 868 Mhz | 2118894 seconds |
| Time spent with S+L 868 Mhz | 1743605 seconds |
| Score Threshold: | 0.3 |
| Temp Threshold: | 24 |
| Humidity Threshold: | 26.0 |
| Pressure Threshold: | 1027.5 |
| Temp Ratio: | 0.95 |
| Humidity Ratio: | 0.95 |
| Pressure Ratio: | 1.03 |
| Temp Weighting | 0.25 |
| Humidity Weighting | 0.25 |
| Pressure Weighting | 0.5 |

Table B.6 May 2015 experiment

| Output for May 2015 | Value |
| --- | --- |
| Total Traversed Readings: | 88877 |
| Usable Traversed Readings: | 63863 |
| Evil Switches on S: | 1297 |
| Evil Switches on S+L: | 36 |
| Time spent with S 868 Mhz: | 2606420 |
| Time spent with S+L 868 Mhz: | 2089671 |
| Score Threshold: | 0.3 |
| Temp Threshold: | 20.0 |
| Humidity Threshold: | 65.0 |
| Pressure Threshold: | 988.0 |
| Temp Ratio: | 0.65 |
| Humidity Ratio: | 1 |
| Pressure Ratio: | 0.65 |
| Temp Weighting | 0.25 |
| Humidity Weighting | 0.25 |
| Pressure Weighting | 0.5 |

Table B.7 May 2015 - with higher weighting on pressure and lower weights on temperature and humidity

| Output for May 2015 | Value |
| --- | --- |
| Total Traversed Readings: | 88877 |
| Usable Traversed Readings: | 63863 |
| Evil Switches on S | 1297 |
| Evil Switches on L | 30 |
| Time spent with S 868 Mhz: | 2606420 |
| Time spent with S+L 868 Mhz: | 2132872 |
| Score Threshold: | 0.3 |
| Temp Threshold: | 20.0 |
| Humidity Threshold: | 66.0 |
| Pressure Threshold: | 988.0 |
| Temp Ratio: | 0.65 |
| Humidity Ratio: | 1 |
| Pressure Ratio: | 1.03 |
| Temp Weighting | 0.2 |
| Humidity Weighting | 0.2 |
| Pressure Weighting | 0.6 |

Table B.8 June 2015

| Output for June 2015 | Value |
| --- | --- |
| Total Traversed Readings: | 85999 |
| Usable Traversed Readings: | 57301 |
| Evil Switches on S | 1407 |
| Evil Switches on S+L | 39 |
| Time spent with S 868 Mhz: | 2505430 |
| Time spent with S+L 868 Mhz: | 1903698 |
| Score Threshold: | 0.3 |
| Temp Threshold: | 26.0 |
| Humidity Threshold: | 66.0 |
| Pressure Threshold: | 1005.0 |
| Temp Ratio: | 0.65 |
| Humidity Ratio: | 1.02 |
| Pressure Ratio: | 1.03 |
| Temp Weighting | 0.25 |
| Humidity Weighting | 0.25 |
| Pressure Weighting | 0.5 |

Table B.9 June 2015 - with higher weighting on pressure and lower weights on temperature and humidity

| Output for June 2015 | Value |
| --- | --- |
| Total Traversed Readings: | 85999 |
| Usable Traversed Readings: | 57301 |
| Evil Switches on S | 1407 |
| Evil Switches on L | 31 |
| Time spent with S 868 Mhz: | 2505430 |
| Time spent with S+L 868 Mhz: | 1946898 |
| Score Threshold: | 0.3 |
| Temp Threshold: | 26.0 |
| Humidity Threshold: | 66.0 |
| Pressure Threshold: | 1005.0 |
| Temp Ratio: | 0.65 |
| Humidity Ratio: | 1.02 |
| Pressure Ratio: | 1.03 |
| Temp Weighting | 0.2 |
| Humidity Weighting | 0.2 |
| Pressure Weighting | 0.6 |

Table B.10 June 2015 - with equal weights

| Output for June 2015 | Value |
|---|---|
| Total Traversed Readings: | 85999 |
| Usable Traversed Readings: | 57293 |
| Evil Switches on S | 1407 |
| Evil Switches on L | 39 |
| Time spent with S 868 Mhz: | 2505430 |
| Time spent with S+L 868 Mhz: | 1833495 |
| Score Threshold: | 0.3 |
| Temp Threshold: | 26.0 |
| Humidity Threshold: | 66.0 |
| Pressure Threshold: | 1005.0 |
| Temp Ratio: | 0.66 |
| Humidity Ratio: | 1.02 |
| Pressure Ratio: | 1.03 |
| Temp Weighting | 0.333 |
| Humidity Weighting | 0.333 |
| Pressure Weighting | 0.333 |

Table B.11 September 2015 parameters

| Output for September 2015 | Value |
|---|---|
| Total Traversed Readings: | 77380 |
| Usable Traversed Readings: | 60147 |
| Evil Switches on S | 757 |
| Evil Switches on S+L | 109 |
| Time spent with S 868 Mhz | 2546749 seconds |
| Time spent with S+L 868 Mhz | 2265064 seconds |
| Score Threshold: | 0.3 |
| Temp Threshold: | 9.9 |
| Humidity Threshold: | 33.0 |
| Pressure Threshold: | 985.9 |
| Temp Ratio: | 0.95 |
| Humidity Ratio: | 1.04 |
| Pressure Ratio: | 1.07 |
| Temp Weighting | 0.25 |
| Humidity Weighting | 0.25 |
| Pressure Weighting | 0.5 |

Table B.12 October 2015 parameters

| Output for October 2015 | Value |
|---|---|
| Total Traversed Readings: | 79887 |
| Usable Traversed Readings: | 63023 |
| Evil Switches on S | 823 |
| Evil Switches on S+L | 111 |
| Time spent with S 868 Mhz | 2632454 seconds |
| Time spent with S+L 868 Mhz | 1800003 seconds |
| Score Threshold: | 0.3 |
| Temp Threshold: | 5.6 |
| Humidity Threshold: | 95 |
| Pressure Threshold: | 992.19 |
| Temp Ratio: | 0.95 |
| Humidity Ratio: | 1.04 |
| Pressure Ratio: | 1.07 |
| Temp Weighting | 0.25 |
| Humidity Weighting | 0.25 |
| Pressure Weighting | 0.5 |
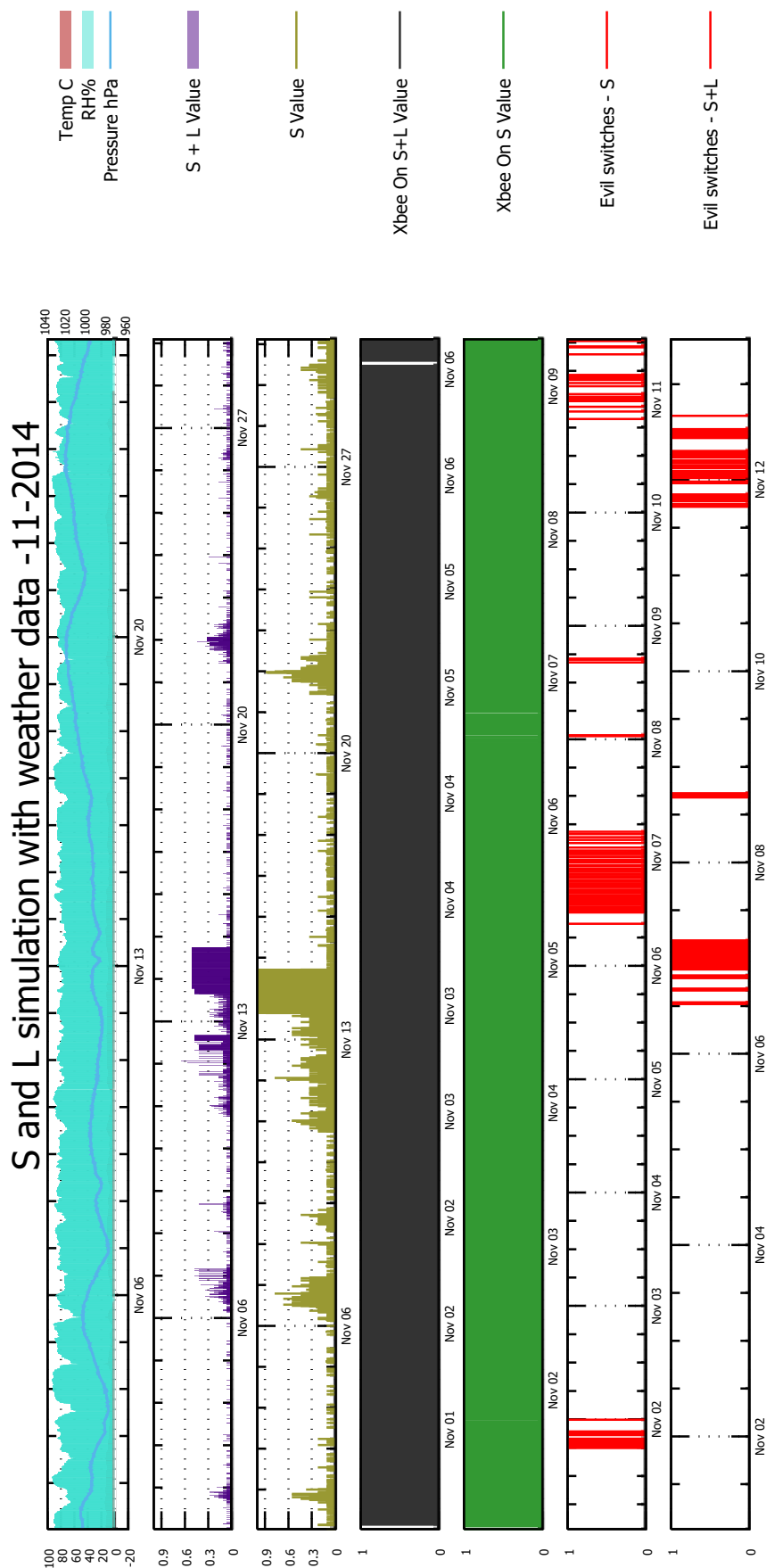
Fig. B.1 Simulation run during November 2014 data using values that causes S+L evil switching
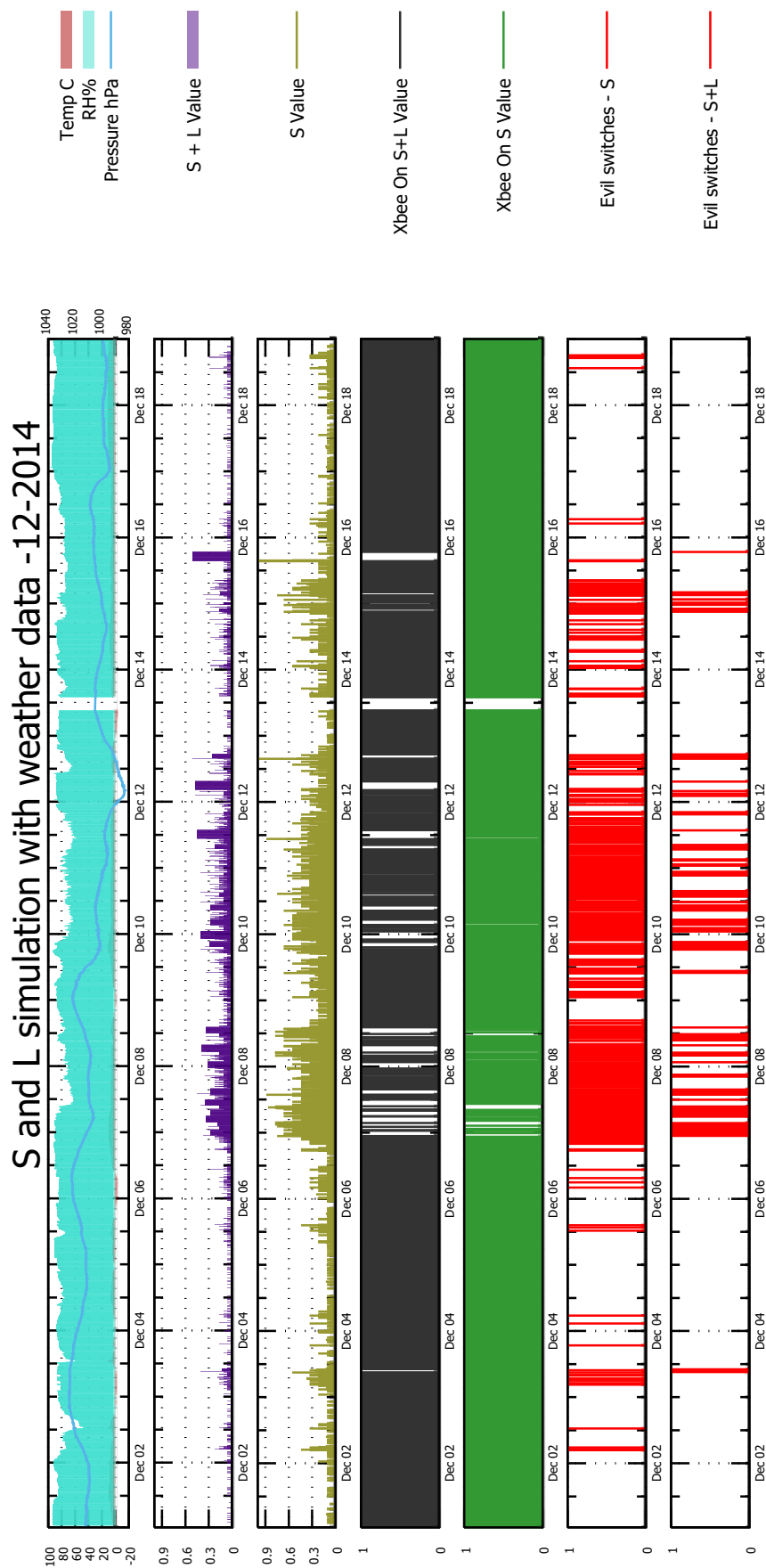
Fig. B.2 Simulation run during December 2014 data using values that causes S+L evil switching
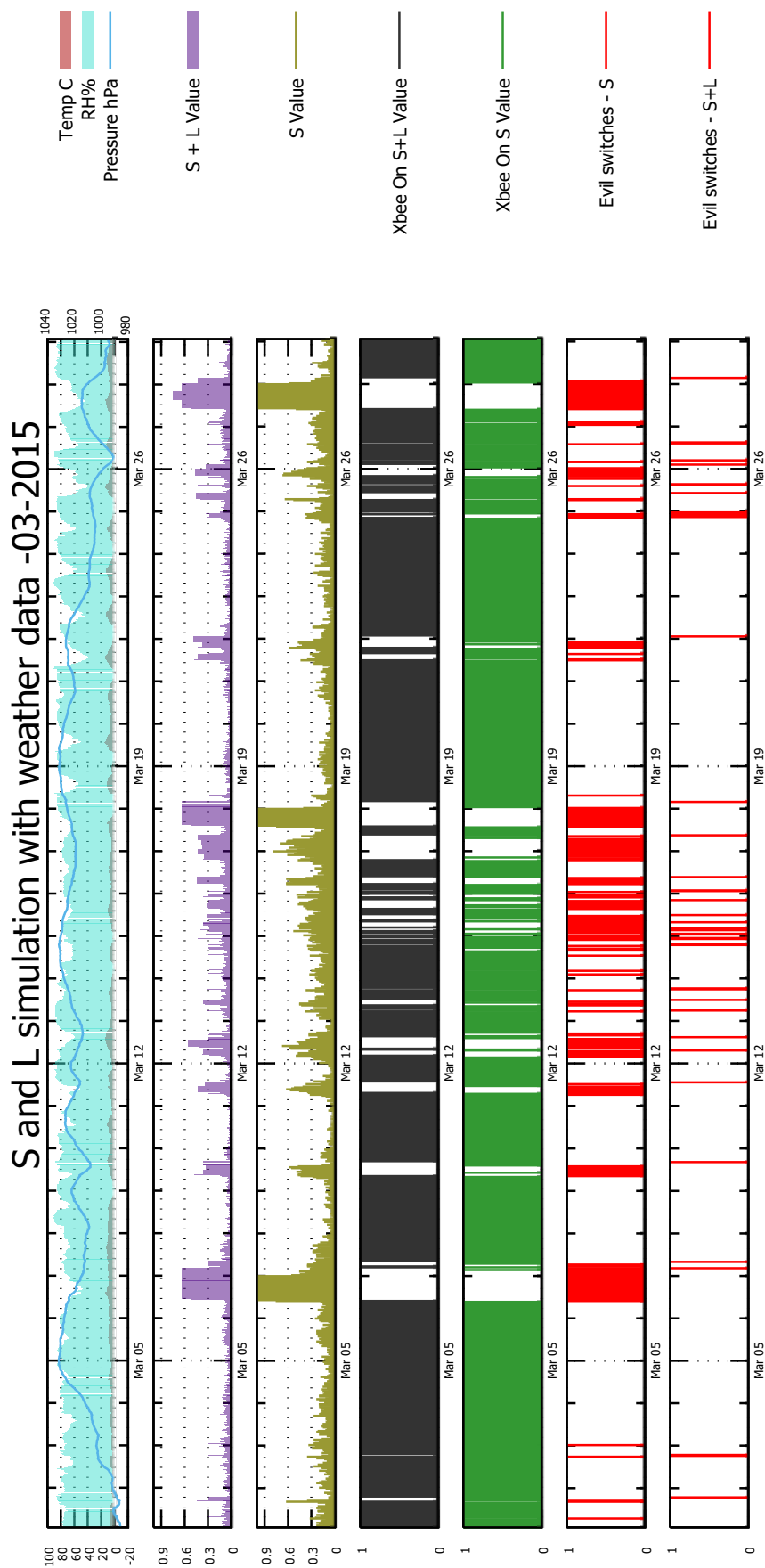
Fig. B.3 Simulation run during March 2015 data using values that causes S+L evil switching
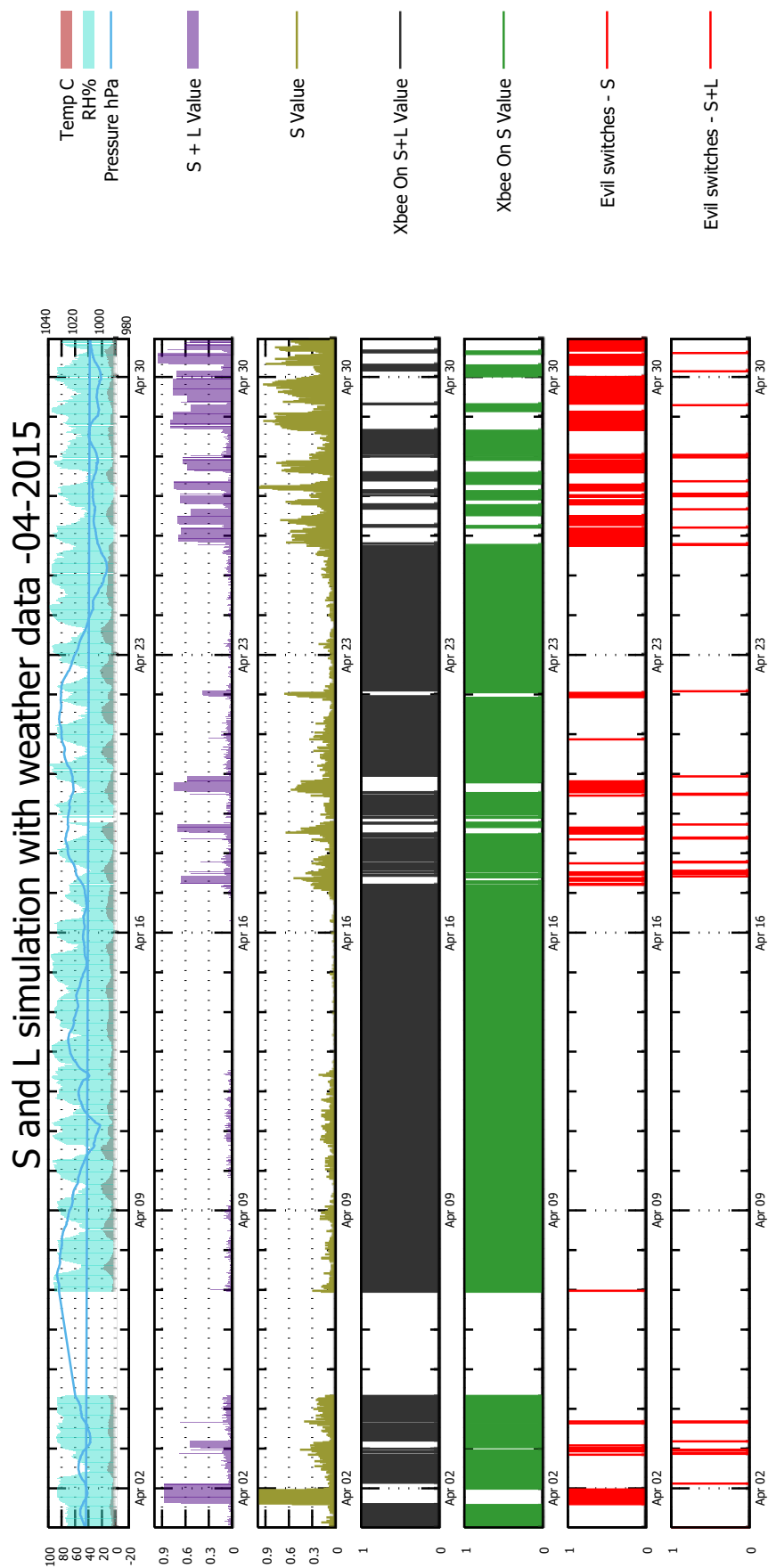
Fig. B.4 Simulation run during April 2015 data using values that causes S+L evil switching - Note: Data is missing from 4th to the 6th.
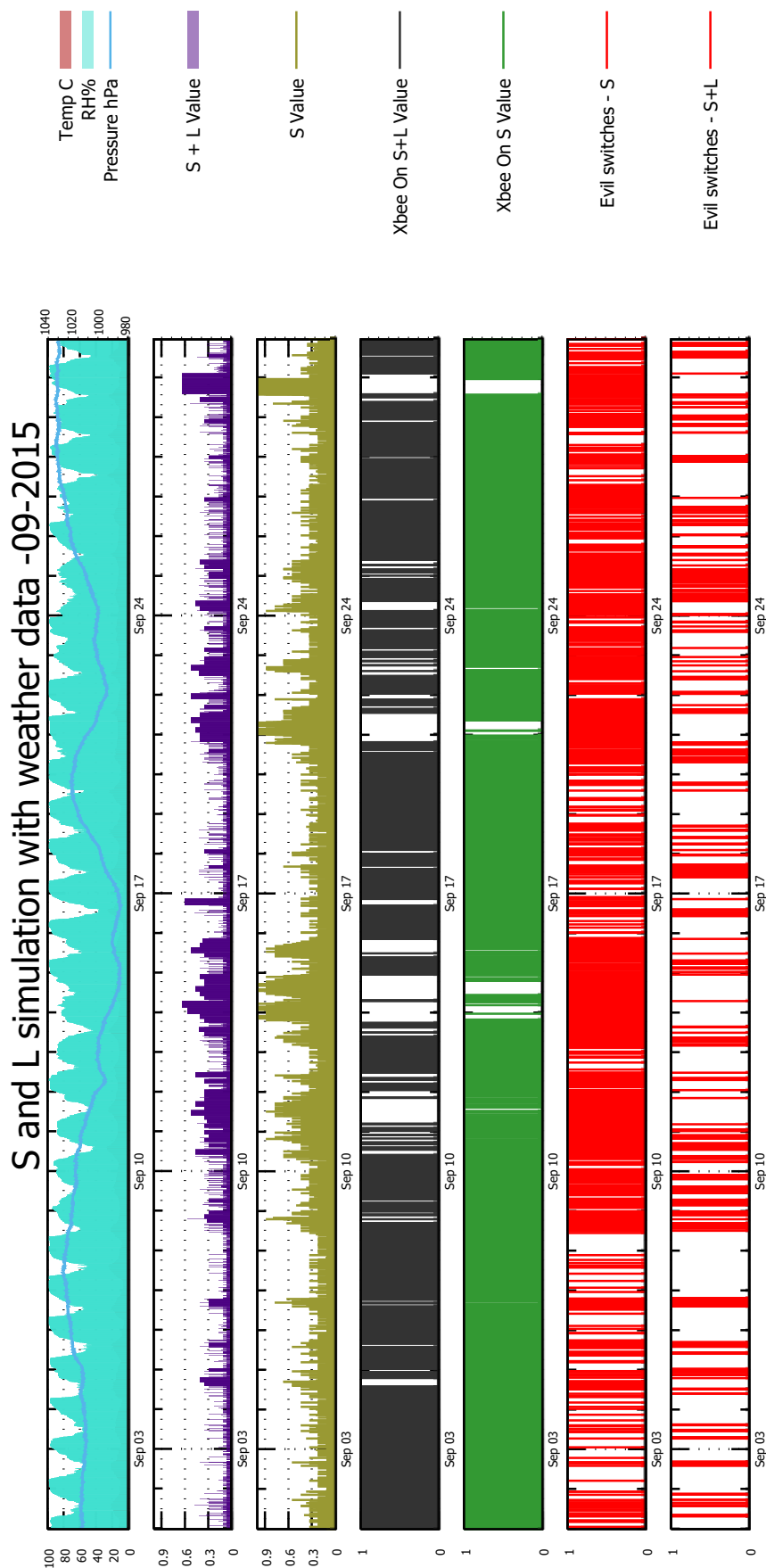
Fig. B.5 Simulation run during September 2015 data using values that causes S+L evil switching.
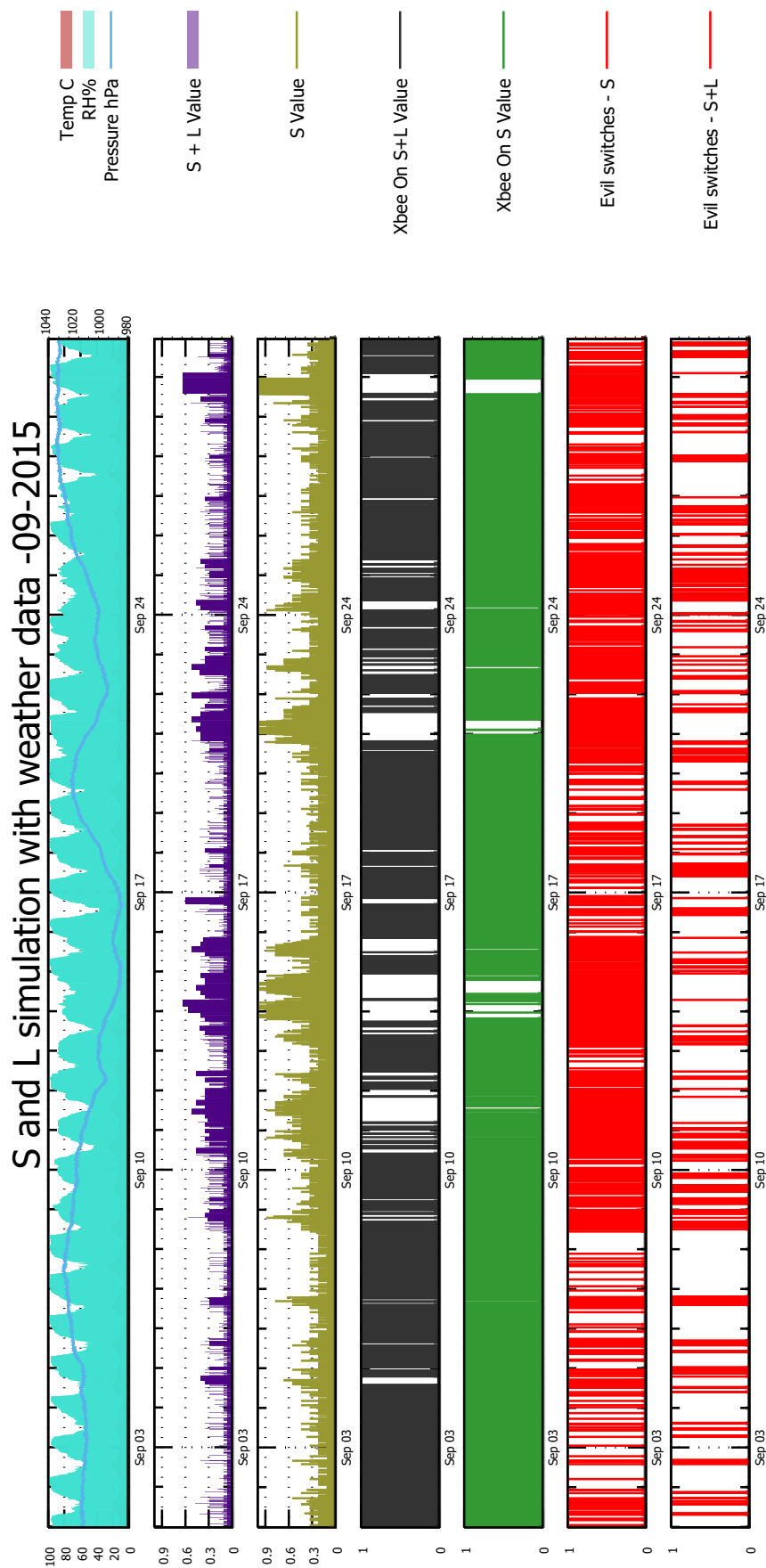
Fig. B.6 Simulation run during October 2015 data using values that causes S+L evil switching.